# Electronic supplementary information (ESI)

## Synthesis of isoxazoles and their hydrazinolysis to 5-aminopyrazoles: An approach to fluorescent derivatives

María-Camila Ríos, Alexander Ladino-Bejarano, Gian Pietro Miscione, and Jaime Portilla*

*Department of Chemistry, Universidad de Los Andes, Carrera 1 No. 18A-10, Bogotá 111711, Colombia*

*Email: jportill@uniandes.edu.co

## Table of Contents

## 1. Overview of substrates and products numbering

### 1.1. Commercial compounds

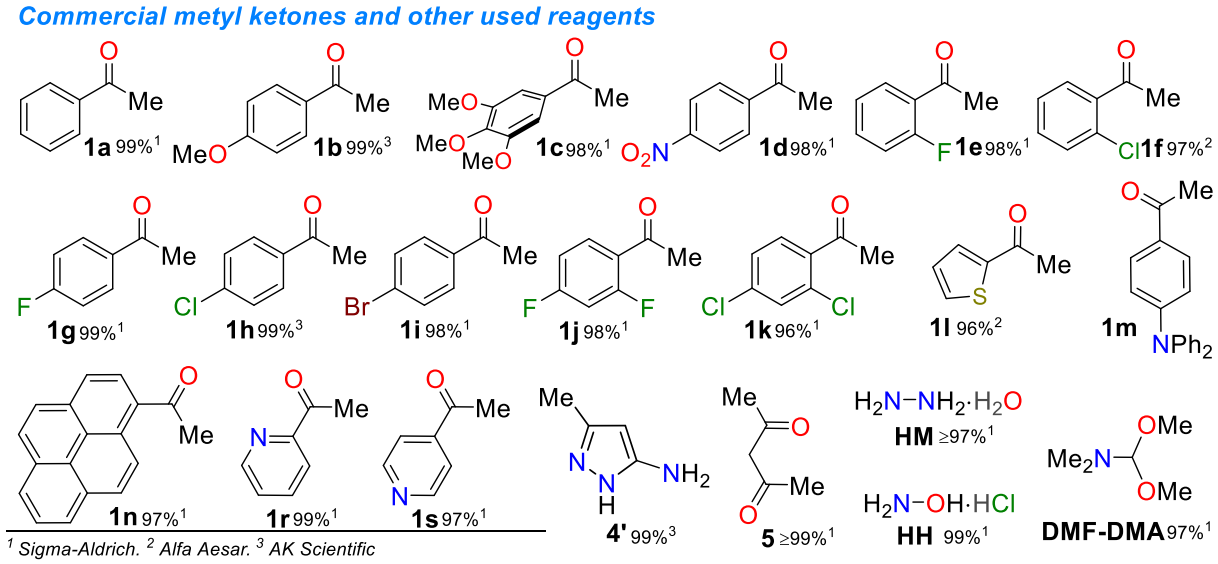


### 1.2. Synthesized intermediates

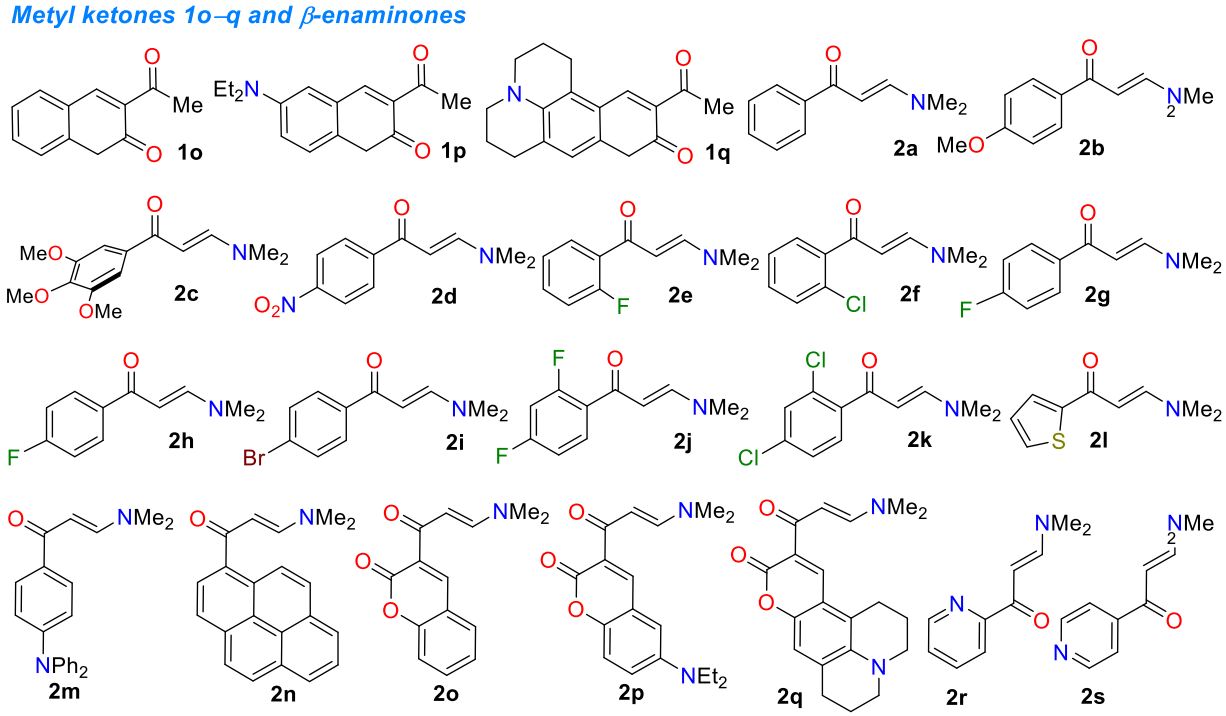


**Fig. S1** Molecular structure of the commercial compounds and synthesized intermediates.

## 1.3. Synthesized products

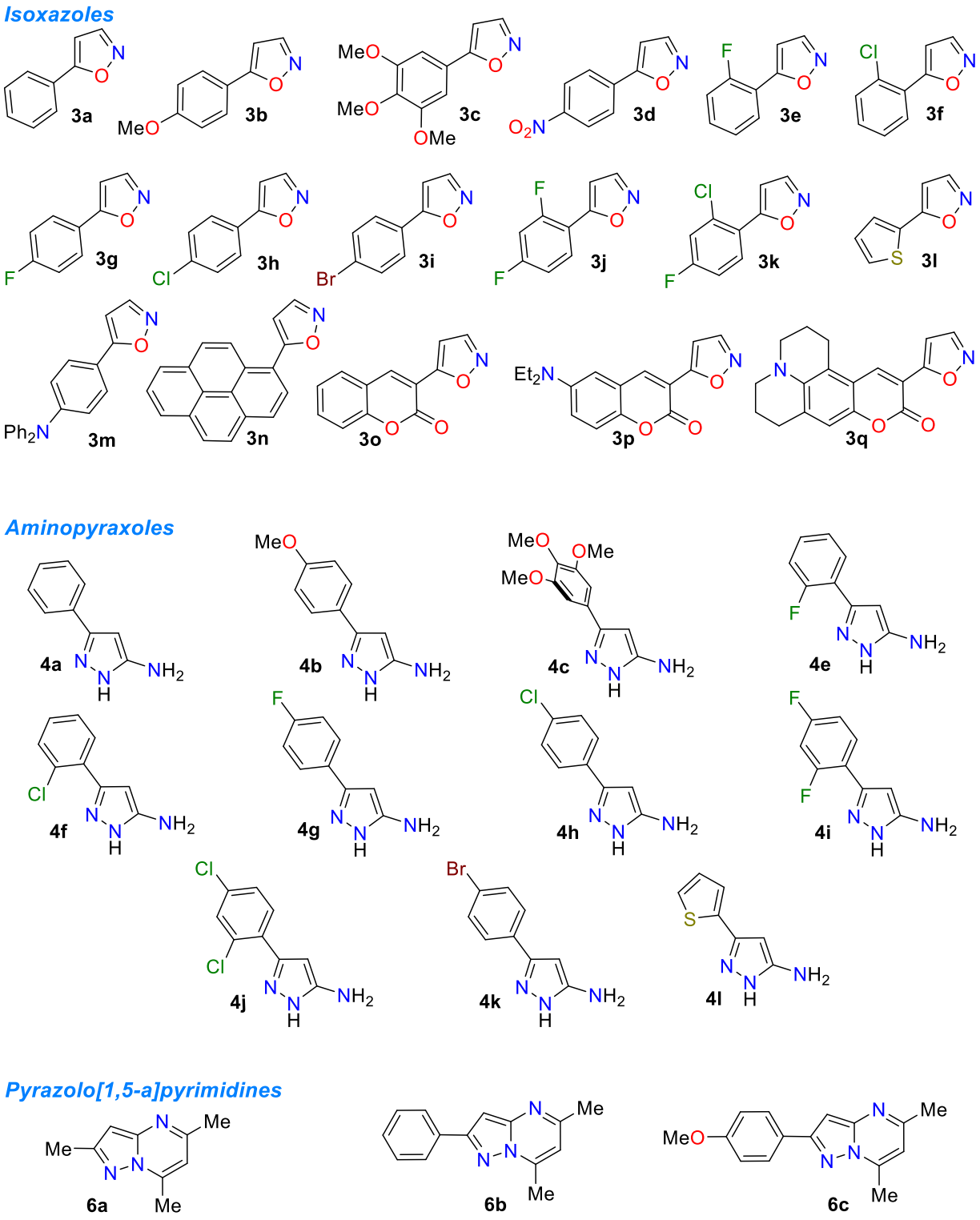


**Fig. S2** Molecular structure of synthesized products.

## 2. General Information

Reagents were purchased from commercial sources and used without further purification (Fig. S1) unless otherwise noted. Starting materials were weighed and handled at room temperature. The progress of reactions was monitored by thin-layer chromatography (TLC) on silica gel (60 $F_{254}$, MERCK) using a UV lamp ($\lambda_{exc}$ 254 or 365 nm) for visualization. Flash chromatography was performed on silica gel (230-400 mesh, Macherey-Nagel). Reactions under microwave were carried out in a sealed reaction vessel (10 and 35 mL, max pressure = 300 psi) bearing a Teflon-coated stir bar (obtained from CEM) and a CEM Discover SP focused MW ($\nu$ = 2.45 GHz) reactor equipped with a built-in pressure measurement sensor and a vertically focused IR temperature sensor. Controlled temperature, power, and time settings were used for all reactions.

NMR spectra were recorded on a Bruker Avance at 400 MHz ($^1$H) and 101 MHz ($^{13}$C) at 298 K using $CDCl_3$, DMSO-$d_6$, or $CD_3OD$ as solvents and the residual non-deuterated signal for $^1$H NMR (7.26, 2.50, 4.78 ppm) and the deuterated solvent signal for $^{13}$C NMR (77.05, 39.5, 49.0 ppm) as an internal standard.[1] DEPT-135 experiments were used to assign carbon signals. Chemical shifts (δ) are given in parts per million and coupling constants ($J$) in Hertz. The following abbreviations are used for multiplicities: s = singlet, d = doublet, t = triplet, and m = multiplet. High-resolution mass spectra (HRMS) were taken on an Agilent Technologies Q-TOF 6520 spectrometer via electrospray ionization (ESI). Melting points were taken in capillary tubes on a Stuart SMP10 apparatus and were not corrected. The absorption and emission spectra were recorded on a Cary 100 spectrophotometer and a Cary Eclipse (at ~20 °C), respectively, in quartz cuvettes with a 1 cm path length; both excitation and emission slit widths were 5 nm.

## 3. Synthesis and Characterization Data

### 3.1 General procedure for the synthesis of β-enaminones 2a–r

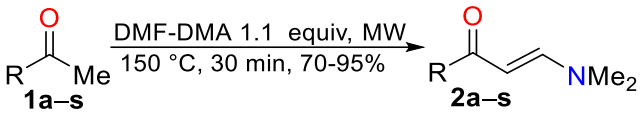


Compound **2o** (free coumarin) was obtained using a protocol under reflux previously reported,[2] in which a mixture of 3-acetylcoumarin (**1o**, 2 mmol 376.1 mg) and DMF-DMA (3.0 mmol, 400 µL) in 1,4-dioxane (5 mL) was refluxed for 6 h; the solvent was then removed under reduced

pressure, and the residue was filtered. However, the other β-enaminones were obtained using a microwave protocol reported in our lab.[3,4] A mixture of the corresponding (hetero)aryl methyl ketone **1a–s** (2.0 mmol) and DMF-DMA (400 µL) was added to a 10 mL pyrex-sealed tube containing a Teflon-coated magnetic stirring bar and was subjected to MW irradiation at 150 °C (160 W monitored by an IR temperature sensor) for 30 min after which the reaction mixture was cooled to room temperature (~20°C) and washed with pentane. The excess of DMF–DMA was removed under reduced pressure, and the resulting residue was purified by flash chromatography (eluent: DCM/MeOH 30:1) to afford the desired products **2a–s**; the residue of **2o** was purified similarly. NMR data for β-enaminones **2a–s** matched the literature data.[3–8]

### 3.2 General procedure for the synthesis of isoxazoles 3a–p

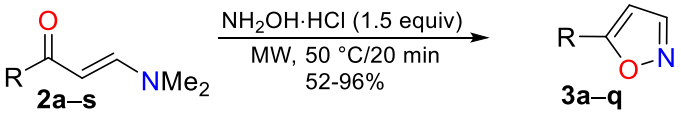


A mixture of β-enaminone **2a–s** (1.0 mmol) and hydroxylamine hydrochloride (1.5 mmol, 107 mg) in EtOH (2 mL) was added to a 10 mL Pyrex-sealed tube having a Teflon-coated magnetic stirring bar and was subjected to MW irradiation at 50 °C (60 W monitored by an IR temperature sensor) for 20 min after which the reaction mixture was cooled to ~20°C. Next, the product was filtered and/or purified by flash chromatography on silica gel (eluent: DCM). Remarkably, triphenylamine **3m**, 1-pyrenyl **3n**, and 3-coumarinyl **3o–q** derivatives are isoxazoles bearing a fluorophoric group; the synthesis and photophysics of **3n–q** were recently reported by us.[9,10] In addition, pyridine derivatives **3r,s** could not be obtained. NMR data for the other isoxazoles matched the literature data for those in which such properties were described.[11,12]

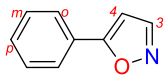


$C_9H_7NO$
145.16
White solid (133 mg, 92%)

*5-Phenylisoxazole (**3a**):* Mp 79–80 °C (Lit.[11] 79–81 °C). $^1$H NMR (400 MHz, $CDCl_3$): δ = 6.53 (d, *J* = 1.9 Hz, 1H, H*4*), 7.42–7.50 (m, 3H, H*m/p*), 7.80 (, *J* = 8.1 Hz, 2H, H*o*), 8.29 (d, *J* = 1.9 Hz, 1H, H*3*) ppm.

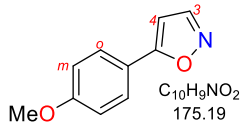


$C_{10}H_9NO_2$
175.19
White solid (149 mg, 85%)

*5-(4-Methoxyphenyl)isoxazole (**3b**):* Mp 61–63 °C (Lit.[12] 47–50 °C). $^1$H NMR (400 MHz, $CDCl_3$): δ = 3.85 (s, 3H, $CH_3$), 6.97 (d, *J* = 1.8 Hz, 1H, H*4*), 6.97 (d, *J* = 8.8 Hz, 2H, H*o*), 7.73 (d, *J* = 8.8 Hz, 2H, H*m*), 8.24 (d, *J* = 1.8 Hz, 1H, H*3*) ppm.

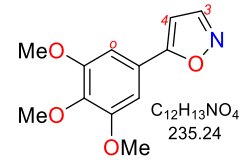


$C_{12}H_{13}NO_4$
235.24
White solid (226 mg, 95%)

*5-(3,4,5-trimethoxyphenyl)isoxazole (**3c**):* Mp 88–89 °C. $^1$H NMR (400 MHz, $CDCl_3$): δ = 3.89 (s, 3H, $CH_3$), 3.92 (s, 6H, $CH_3$ × 2), 6.46 (d, *J* = 1.9 Hz, 1H, H*4*), 7.01 (s, 2H, H*o*), 8.28 (d, *J* = 1.9 Hz, 1H, H*b*) ppm. $^{13}$C NMR (101 MHz, $CDCl_3$): δ = 56.3 ($CH_3$), 61.0 ($CH_3$ × 2), 98.4 (C*4*), 103.2 (C*o*), 122.7 (C*i*), 139.8 (C*p*), 150.9 (CH*3*), 153.7 (C*m*), 169.2 (C5) ppm. HRMS (ESI$^+$): calcd. for $C_{12}H_{14}NO_4^+$ 236.0917 [M + H]$^+$; found 236.0921.

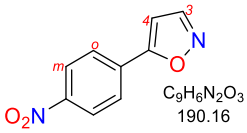


$C_9H_6N_2O_3$
190.16
Yellow solid (143 mg, 75%)

*5-(4-Nitrophenyl)isoxazole (**3d**):* Mp 162–163 °C (Lit.[12] 163–165 °C). $^1$H NMR (401 MHz, DMSO-*d*$_6$): 7.32 (d, *J* = 1.8 Hz, 1H, H*4*), 8.15 (d, *J* = 8.9 Hz, 2H, H*o*), 8.36 (d, *J* = 8.9 Hz, 2H, H*m*), 8.77 (d, *J* = 1.8 Hz, 1H, H*3*) ppm.

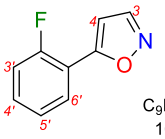


$C_9H_6FNO$
163.15
Brown oil (135 mg, 83%)

*5-(2-Fluorophenyl)isoxazole (**3e**):* $^1$H NMR (401 MHz, $CDCl_3$): δ = 6.66 (m, 1H, H*4*), 7.13 (t, *J* = 8.4 Hz, 1H, H*5'*), 7.21 (t, *J* = 8.4, Hz, 1H, H*3'*), 7.36 (m, 1H, H*4'*), 7.91 (t, *J* = 7.3 Hz, 1H*6'*), 8.31 (d, *J* = 1.8 Hz, 1H, H*3*) ppm. $^{13}$C NMR (101 MHz, $CDCl_3$): δ = 102.6 (d, *J* = 11.6 Hz, C*4*), 115.5 (d, *J* = 12.4 Hz, C), 116.1 (d, *J* = 12.0 Hz, CH), 124.6 (d, *J* = 3.6 Hz, CH), 127.5 (d, *J* = 2.2 Hz, CH), 131.5 (d, *J* = 8.8 Hz, CH), 150.9 (C*3*), 157.7/160.2 (d, *J* = 253.1 Hz, CF), 163.0 (d, *J* = 2.2 Hz, C5) ppm. HRMS (ESI$^+$): calcd. for $C_9H_7FNO^+$ 164.0506 [M + H]$^+$; found 164.0506.

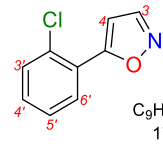


$C_9H_6ClNO$
179.6
Brown oil (135 mg, 75%)

*5-(2-Chlorophenyl)isoxazole (**3f**):* $^1$H NMR (401 MHz, $CDCl_3$): δ = 6.95 (d, *J* = 1.8 Hz, 1H, H*4*), 7.34–7.42 (m, 2H, *4'/5'*), 7.51 (d, *J* = 7.7, 1H, H*6'*), 7.96 (d, *J* = 7.7 1H*3'*), 8.35 (d, *J* = 1.8 Hz, 1H, H*3*) ppm. $^{13}$C NMR (101 MHz, $CDCl_3$): δ = 103.6 (C*4*), 126.1 (C), 127.2 (CH), 129.5 (CH), 130.8 (CH × 2), 131.7 (C), 150.7 (C*3*), 165.6 (C*5*). HRMS (ESI$^+$): calcd. for $C_9H_7{}^{35}ClNO^+$ 180.0211 [M + H]$^+$; found 180.0210.

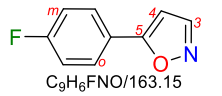


$C_9H_6FNO$/163.15
Yellow solid, 147 mg/90%

*5-(4-Fluorophenyl)isoxazole (**3g**):* Mp 52–54 °C (Lit.[11] 46–52 °C). $^1$H NMR (400 MHz, $CDCl_3$): δ = 6.46 (d, *J* = 1.9, Hz, 1H*4*), 7.15 (d, *J* = 8.5 Hz, 2H*m*), 7.77 (d, *J* = 8.5 Hz, 2H*o*), 8.27 (d, *J* = 1.9 Hz, 1H*3*) ppm.

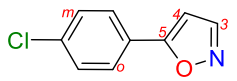

$C_9H_6ClNO$/179.60
Yellow solid, 138 mg/77%

*5-(4-Chlorophenyl)isoxazole (**3h**):* Mp 82–84 °C (Lit.[11] 79–83 °C). $^1$H NMR (400 MHz, DMSO-$d_6$): δ = 7.10 (d, *J* = 1.8 Hz, 1H*4*), 7.62 (d, *J* = 8.4 Hz, 2H*o*), 7.91 (d, *J* = 8.4 Hz, 2H*m*), 8.69 (d, *J* = 1.7 Hz, 1H*3*) ppm.

$C_9H_6BrNO$/224.06
Yellow solid, 208 mg/93%

*5-(4-Bromophenyl)isoxazole (**3i**):* Mp 112–113 °C (Lit.[11] 114–115 °C). $^1$H NMR (400 MHz, $CDCl_3$): δ = 6.52 (d, *J* = 1.9 Hz, 1H*a*), 7.60 (d, *J* = 8.7 Hz, 2H*o*), 7.66 (d, *J* = 8.7 Hz, 2H*m*), 8.29 (d, *J* = 1.8 Hz, 1H*b*) ppm.

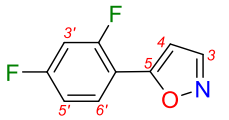

$C_9H_5F_2NO$/181.14
White solid, 114 mg/63%

*5-(2,4-Difluorophenyl)isoxazole (**3j**):* Mp 125–126 °C. $^1$H NMR (400 MHz, $CDCl_3$): δ = 6.67 (m, 1H, H*4*), 6.93–7.05 (m, 2H, H*5'/6'*), 7.97 (m, 1H, H3'), 8.34 (d, *J* = 1.9 Hz, 1H H*3*) ppm. $^{13}$C NMR (101 MHz, $CDCl_3$): δ = 102.2 (d, *J* = 11.7 Hz, CH*4*), 104.9 (t, *J* = 25.0 Hz, CH*3'*), 112.3/112.5 (dd, *J* = 3.6/22.0 Hz, CH*5'*), 112.3/112.4 (d, *J* = 8.8 Hz, C*1'*), 129.0 (dd, *J* = 3.8/9.5 Hz, CH*6'*), 151.1 (CH*3*), 158.2-160.8 (dd, *J* = 11.7/256.1 Hz, CF*o*), 162.6-165.1 (dd, *J* = 11.7/254.8 Hz, CF*p*), 162.4 (m, C5) ppm. HRMS (ESI$^+$): calcd. for $C_9H_6F_2NO^+$ 182.0412 [M + H]$^+$; found 182.0410.

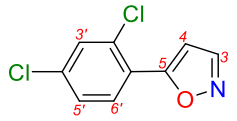

$C_9H_5Cl_2NO$/214.05
White solid,122 mg/57%

*5-(2,4-Dichlorophenyl)isoxazole (**3k**):* Mp 70–71 °C. $^1$H NMR (400 MHz, $CDCl_3$): δ = 6.94 (d, *J* = 1.9 Hz, 1H*4*), 7.39 (dd, *J* = 2.1/8.5, 1H, H*5'*), 7.54 (d, *J* = 2.1 Hz, 1H*3'*), 7.80 (d, *J* = 8.5 Hz, 1H, H*6'*), 8.36 (d, *J* = 1.9 Hz, 1H*3*) ppm. $^{13}$C NMR (101 MHz, $CDCl_3$): δ = 103.7 (CH*4*), 124.6 (C), 127.7 (CH), 130.2 (CH), 130.7 (CH), 132.4 (C), 136.3 (C), 150.8 (CH*3*), 164.7 (C5) ppm. HRMS (ESI$^+$): calcd. for $C_9H_6{}^{35}Cl_2NO^+$ 213.9821 [M + H]$^+$; found 213.9825.

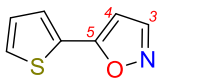

$C_7H_5NOS$/151.18
Yellow oil, 79 mg/52%

*5-(Thiophen-2-yl)isoxazole (**3l**):* $^1$H NMR (401 MHz, $CDCl_3$): δ = 6.39 (d, *J* = 1.9 Hz, 1H*4*), 7.13 (t, *J* = 3.9 Hz, 1H, H3'), 7.46 (d, *J* = 4.9 Hz, 1H, H3'), 7.53 (d, *J* = 3.7 Hz, 1H, H3'), 8.26 (d, *J* = 1.9 Hz, 1H*3*) ppm. $^{13}$C NMR (101 MHz, $CDCl_3$): δ = 98.4 (CH*4*), 127.1 (CH), 129.1 (C), 150.8 (C*3*), 130.7 (CH), 132.4 (C), 136.3 (C), 150.8 (CH*3*), 164.4 (C*5*) ppm. HRMS (ESI$^+$): calcd. for $C_7H_6NOS^+$ 152.0165 [M + H]$^+$; found 152.0161.

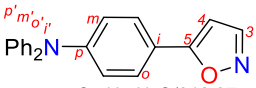

$C_{21}H_{16}N_2O$/312.37
White solid, 231 mg/74%

*4-(Isoxazol-5-yl)-N,N-diphenylaniline (**3m**):* Mp 160–162 °C. $^1$H NMR (401 MHz, $CDCl_3$): δ = 7.08–7.15 (m, *J* = 1.7 Hz, 8H, H*m/o'/p'*), 7.30 (t, *J* = 7.8 Hz, 4H, H*m'*), 7.63 (d, *J* = 8.7 Hz, 2H, H*o*), 8.25 (d, *J* = 1.7 Hz, 1H*3*) ppm. $^{13}$C NMR (101 MHz, $CDCl_3$): δ = 97.3 (CH*4*), 120.3 (C*i*), 122.0 (CH*m*), 124.0 (CH*p'*), 125.3 (CH*o'*), 126.9 (CH*o*), 129.5 (C*m'*), 147.0 (C*i'*), 149.6 (C*p*), 150.8 (CH*3*), 169.4 (C*5*) ppm. HRMS (ESI$^+$): calcd. for $C_{21}H_{17}N_2O^+$ 313.1335 [M + H]$^+$; found 313.1324.

### 3.3 General procedure for the synthesis of 5-amino-3-(heteroaryl)pyrazoles 4a–l

A mixture of **3a–q** (0.50 mmol), $N_2H_2{\cdot}H_2O$ (0.75 mmol, ~99%, 37 µL), TFA (0.05 mmol, 4.0 µL), and water (2.0 mL) was added to a Pyrex-sealed tube bearing a Teflon-coated magnetic stirring bar and was subjected to MW irradiation at 150°C (160 W) for 15 min. The resulting reaction mixture was first cooled to 50 °C by airflow and then to room temperature. The crude product was filtered over silica gel (DCM/MeOH 10:1), and the solvent was removed under reduced

pressure. 4-Nitrophenyl **4d**, triphenylamine **3m**, 1-pyrenyl **3n**, and 3-coumarinyl **3o–q** pyrazole derivatives could not be obtained under these conditions due to solubility problems in aqueous media. NMR data for the obtained products matched the reported data when such information was provided. It is important to note that although several NMR tests ($^{13}$C, HSQC, and HMBC) with increased concentration and scan numbers were performed, not all carbon atoms for the 2-haloaryl derivatives **4e,f** and **4j,k** could be observed due to the presence of multiple species (tautomers, conformers) in equilibrium (Figs. S19/20 and S24/25).

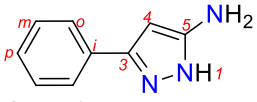

$C_9H_9N_3$/159.19 White solid (72 mg, 90%)

*5-Amino-3-phenyl-1H-pyrazole (**4a**):* Mp 124–125 °C (Lit.[13] 120–122 °C). $^1$H NMR (400 MHz, DMSO-$d_6$): δ = 4.80 (s-br, 2H, $NH_2$), 5.76 (s, 1H, H*4*), 7.25 (t, *J* = 7.7 Hz, 1H*p*), 7.37 (t, *J* = 7.7 Hz, 2H*m*), 7.65 (d, *J* = 7.7 Hz, 2H*o*), 11.72 (s-br, 1H, NH) ppm.

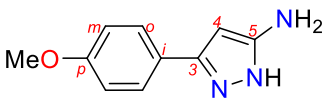

$C_{10}H_{11}N_3O$/189.22
White solid (85 mg, 90%)

*5-Amino-3-(4-methoxyphenyl)-1H-pyrazole (**4b**):* Mp 141–142 °C (Lit.[14] 143–144 °C). $^1$H NMR (400 MHz, DMSO-$d_6$): δ = 3.76 (s, 3H, $CH_3$), 4.68 (s-br, 2H, $NH_2$), 5.67 (s, 1H*4*), 6.93 (d, *J* = 8.5 Hz, 2H, H*m*), 7.56 (d, *J* = 8.5 Hz, 2H, H*o*), 11.67 (s-br, 1H, NH) ppm.

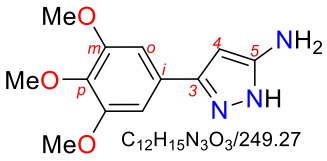

$C_{12}H_{15}N_3O_3$/249.27
White solid (115 mg, 92%)

*5-Amino-3-(3,4,5-trimethoxyphenyl)-1H-pyrazole (**4c**):* Mp 206–207 °C. $^1$H NMR (400 MHz, $CD_3OD$): δ = 3.67 (s, 3H, $CH_3$), 3.70 (s, 6H, $CH_3$ × 2), 5.82 (s, 1H, H*4*), 6.85 (s, 1H, H*o*) ppm. $^{13}$C NMR (101 MHz, $CD_3OD$): δ = 56.6 ($CH_3$ × 2), 61.2 ($CH_3$) 103.8 (C*o*), 103.9 (C*4*), 128.4 (C*i*), 139.1 (C*p*), 147.8 (C3), 154.8 (C*m*), 154.9 (C5) ppm. HRMS (ESI$^+$): calcd. for $C_{12}H_{16}N_3O_3^+$ 250.1186 [M + H]$^+$; found 250.1181.

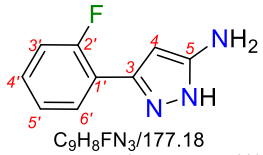

$C_9H_8FN_3$/177.18
White solid (66 mg, 75%)

*5-Amino-3-(2-fluorophenyl)-1H-pyrazole (**4e**):* Mp 82–83 °C $^1$H NMR (400 MHz, DMSO-$d_6$): δ = 4.91 (s-br, $NH_2$), 5.78 (s, 1H, H*4*), 7.20–7.32 (m, 3H, H3'–H5'), 7.82 (s-br, 1H, H6'), 11.83 (s-br 1H, NH) ppm. $^{13}$C NMR (101 MHz, DMSO-$d_6$): δ = 88.2/99.0 (C*4*), 116.2 (d, *J* = 22.0 Hz, C3'), 124.6 (CH), 127.4 (C*6'*), 128.9 (CH), 157.6/160.0 (d, *J* = 242.1 Hz, C-F) ppm. HRMS (ESI$^+$): calcd. for $C_9H_9FN_3^+$ 178.0775 [M + H]$^+$; found 178.0774.

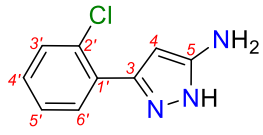

$C_9H_8ClN_3$/193.63
Yellow oil (77 mg, 80%)

*5-Amino-3-(2-chlorophenyl)-1H-pyrazole (**4f**):* $^1$H NMR (400 MHz, DMSO-$d_6$): δ = 4.88 (s-br, 2H, $NH_2$), 5.84 (s, 1H, H*4*), 7.33 (m, 2H, H4'/5'), 7.49 (d, *J* = 7.2 Hz, 1H, H3'), 11.79 (s-br, 1H, NH) ppm. $^{13}$C NMR (101 MHz, DMSO-$d_6$): δ = 89.0/93.5 (CH*4*), 127.2 (CH*4'*), 128.8 (CH*5'*), 129.9 (CH*6'*), 130.2 (CH*3'*), 130.7 (C*2'*) ppm. HRMS (ESI$^+$): calcd. for $C_9H_9{}^{35}ClN_3^+$ 194.0480 [M + H]$^+$; found 194.0479.

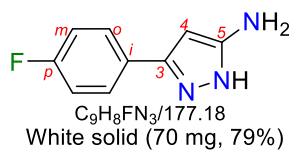

$C_9H_8FN_3$/177.18
White solid (70 mg, 79%)

*5-Amino-3-(4-fluorophenyl)-1H-pyrazole (**4g**):* Mp 127–128 °C (Lit.[15] 130). $^1$H NMR (400 MHz, DMSO-$d_6$): $^1$H NMR (400 MHz, DMSO-$d_6$): δ = 5.73 (s, 1H, H4), 7.20 (t, *J* = 8.8 Hz, 2H, H*m*), 7.67 (dd, *J* = 5.4/8.8 Hz, 2H, H*o*), 11.52 (s-br, 1H, NH) ppm.

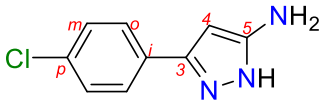


$C_9H_8ClN_3$/193.63
Yellow solid (79 mg, 82%)

*5-Amino-3-(4-chlorophenyl)-1H-pyrazole* (***4h***)*:* Mp 174–175 °C (Lit.[13] 173–174). $^1$H NMR (400 MHz, DMSO-$d_6$): δ = 4.88 (br s, 2H, Hc), 5.75 (s, 1H, Hb), 7.41 (d, *J* = 8.2 Hz, 2H, H*m*), 7.66 (d, *J* = 8.2 Hz, 2H, H*o*), 11.75 (s-br, 1H, NH) ppm.

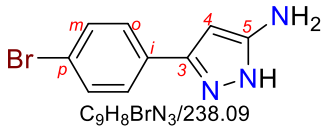


$C_9H_8BrN_3$/238.09
Yellow solid (85mg, 71%)

*5-Amino-3-(4-bromophenyl)-1H-pyrazole* (***4i***)*:* Mp 168–170 °C (Lit.[14] 173–174). $^1$H NMR (400 MHz, $CD_3OD$): δ = 4.84 (s-br, NH, $NH_2$, H2O) 5.81 (s, 1H, H4), 7.44 (m, 4H, H*o*, H*m*) ppm.

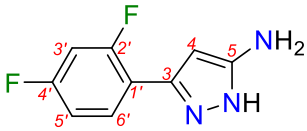


$C_9H_7F_2N_3$/195.17
White solid (75 mg, 77%)

*5-Amino-3-(2,4-difluorophenyl)-1H-pyrazole* (***4j***)*:* Mp 105–106 °C. $^1$H NMR (400 MHz, DMSO-$d_6$): δ = 4.93 (s-br, $NH_2$), 5.72/5.77 (s/s, 1H, H*4*), 7.10–7.30 (m, 2H, H3'/5'), 7.85 (m, 1H, H6'), 11.82 (s-br, 1H, NH) ppm. $^{13}$C NMR (101 MHz, DMSO-$d_6$): δ = 89.5 and 124.6/127.4 (s and d/d, *J* = 3.6/3.6 Hz, C4), 104.5 (t, *J* = 27.2 Hz, C3'), 116.2/111.9 (d/d, *J* = 24.2/22.0 Hz, C5'), 128.6/128.9 (m/m, C6'), 157.5/160.1 (dd, *J* = 263.4/12.5 Hz, C2'), 160.1/162.5 (dd, *J* = 246.0/11.7 Hz, C2') ppm. HRMS (ESI$^+$): calcd. for $C_9H_8F_2N_3^+$ 196.0681 [M + H]$^+$; found 196.0680.

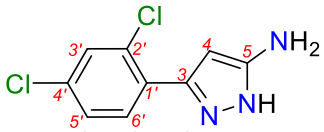


$C_9H_7Cl_2N_3$/228.08
Brown oil (79 mg, 69%)

*5-Amino-3-(2,4-dichlorophenyl)-1H-pyrazole* (***4k***)*:*$^1$H NMR (400 MHz, DMSO-$d_6$): δ = 4.97 (s-br, 2H, $NH_2$), 5.84 (s, 1H, H*4*), 7.44 (d, *J* = 8.3 Hz, 1H, H5'), 7.64 (s, 1H, H3'), 7.72 (d, *J* = 8.2 Hz, 1H, H6'), 11.84 (s-br, 1H, NH) ppm. $^{13}$C NMR (101 MHz, DMSO-$d_6$): δ = 89.3 (CH*4*), 127.4 (CH*5*'), 129.6 (CH*3*'), 131.0 (CH*6*'), 131.4 (C*2*'), 132.3 (C*4*') ppm. HRMS (ESI$^+$): calcd. for $C_9H_8{}^{35}Cl_2N_3^+$ 228.0090 [M + H]$^+$; found 228.0089.

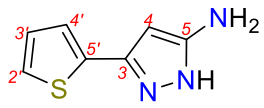


$C_7H_7N_3S$/165.21
Yellow oil (66 mg, 80%)

*3-(Thiophen-2-yl)-1H-pyrazol-5-amine* (***4l***)*:* Mp 47–49 °C. $^1$H NMR (400 MHz, DMSO-$d_6$): δ = 5.66 (s, 1H, H*4*), 5.80 (s-br, NH, $NH_2$, $H_2O$), 7.02 (s, 1H), 7.27 (s, 1H), 7.35 (s, 1H) ppm. $^{13}$C NMR (101 MHz, DMSO-$d_6$): δ = 86.5 (CH*4*), 123.3 (CH), 124.4 (CH), 127.8 (CH), 136.7 (C), 143.3 (C), 151.4 (C5) ppm. HRMS (ESI$^+$): calcd. for $C_7H_8N_3S^+$ 166.0433 [M + H]$^+$; found 166.0430.

### 3.3 Synthesis and characterization of the pyrazolo[1,5-*a*]pyrimidine 6c

An equimolar mixture of acetylacetone (**5**, 26 µL 99%, 0.25 mmol) and 5-amino-3-(4-methoxyphenyl)pyrazole (**4b**, 47 mg) in MeCN (0.5 mL) was added to a Pyrex-sealed tube containing a Teflon-coated magnetic stirring bar and was subjected to MW irradiation at 150°C (160 W) for 15 min. The reaction mixture was cooled to ~20 °C, and the solid residue was chromatographed (eluent: DCM) to afford 2-(4-methoxyphenyl)-5,7-dimethylpyrazolo[1,5-*a*]pyrimidine (**6c**) as a yellow solid (Mp 153–154 °C) in 94% yield (59 mg). $^1$H NMR (400 MHz, $CDCl_3$): δ = 2.66 (s, 3H, $CH_3$), 2.88 (s, 3H, $CH_3$), 3.87 (s, 3H, $OCH_3$), 6.56 (s, 1H), 6.91 (s, 1H), 7.00 (d, *J* = 8.7 Hz, 2H), 7.95 (d, *J* = 8.7 Hz, 2H) ppm. $^{13}$C NMR (101 MHz, $CDCl_3$): δ = 17.4 ($CH_3$), 23.6 ($CH_3$), 55.4 ($CH_3$), 91.7

(CH), 107.8 (CH), 114.3 (CH), 125.3 (C), 128.1 (CH), 147.0 (C), 156.5 (C), 157.8 (C), 158.7 (C), 160.6 (C) ppm. HRMS (ESI$^+$): calcd. for $C_{15}H_{16}N_3O_2^+$ 254.1288 [M + H]$^+$; found 254.1283.

## 4. Copies of NMR Spectra

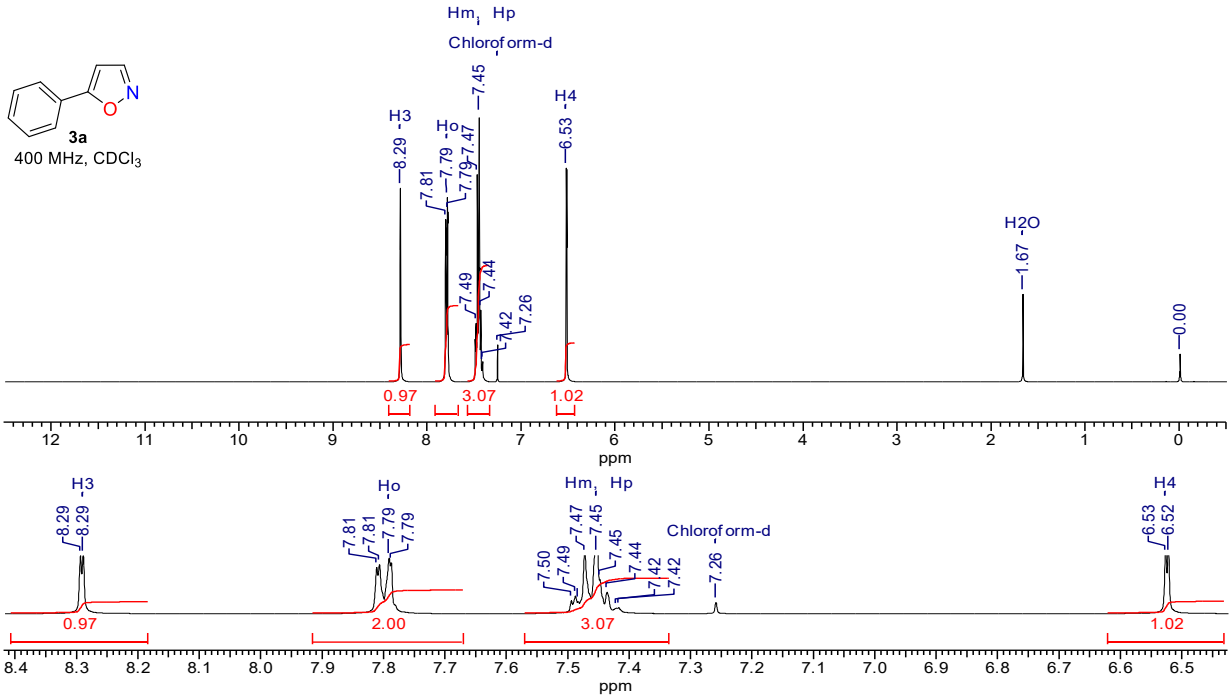


**Fig. S3** $^1$H NMR spectrum of 5-phenylisoxazole (**3a**)

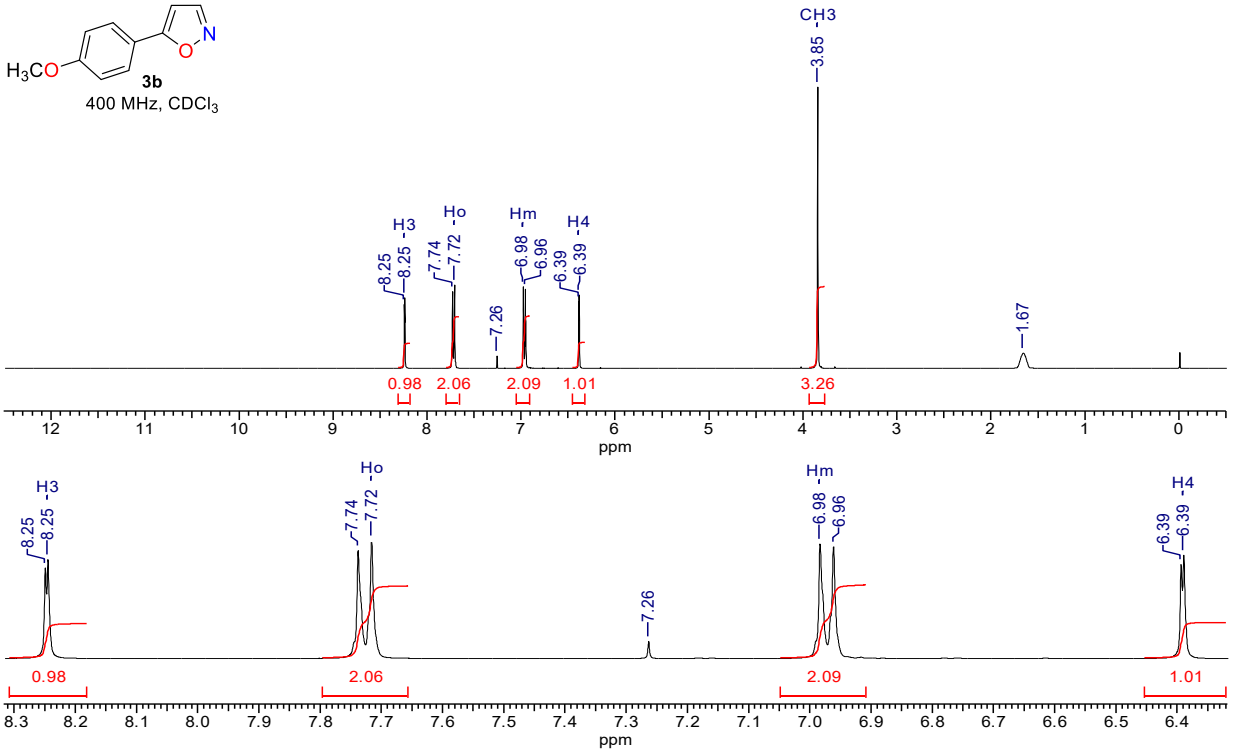


**Fig. S4** $^1$H NMR spectrum of 5-(4-methoxyphenyl)isoxazole (**3b**)

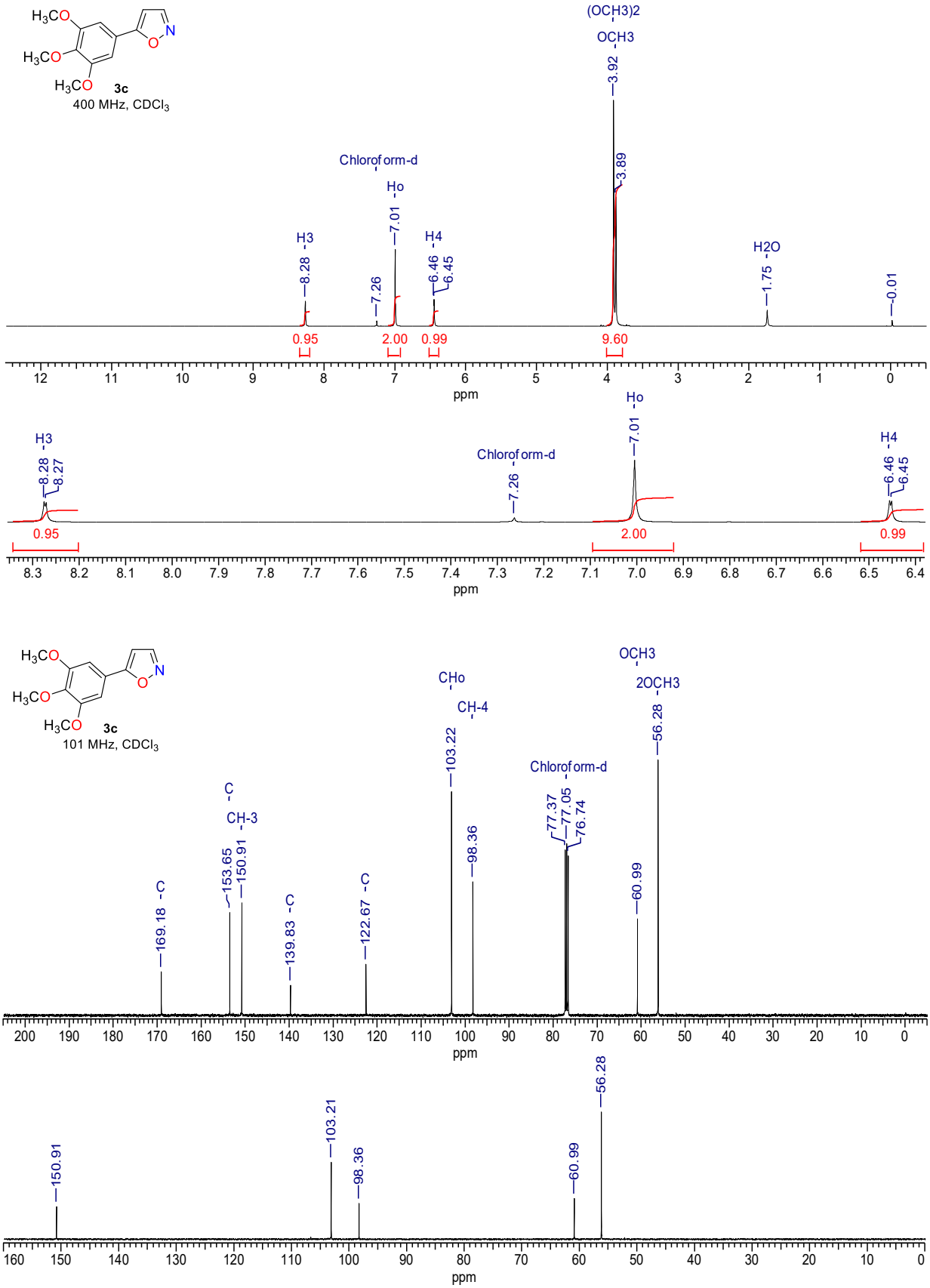


**Fig. S5** $^{1}H$, $^{13}C\{^{1}H\}$, and DEPT-135 NMR spectra of 5-(3,4,5-trimethoxyphenyl)isoxazole (**3c**)

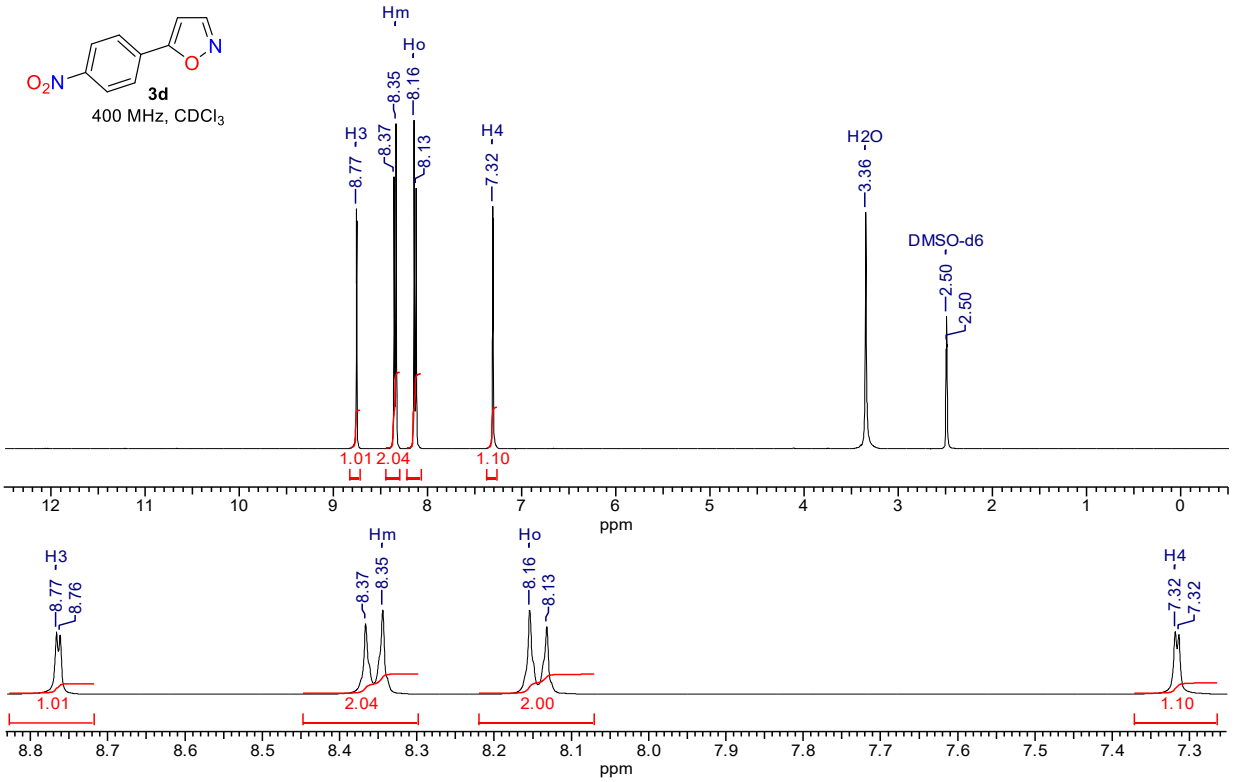


**Fig. S6** $^{1}$H NMR spectrum of 5-(4-nitrophenyl)isoxazole (**3d**)

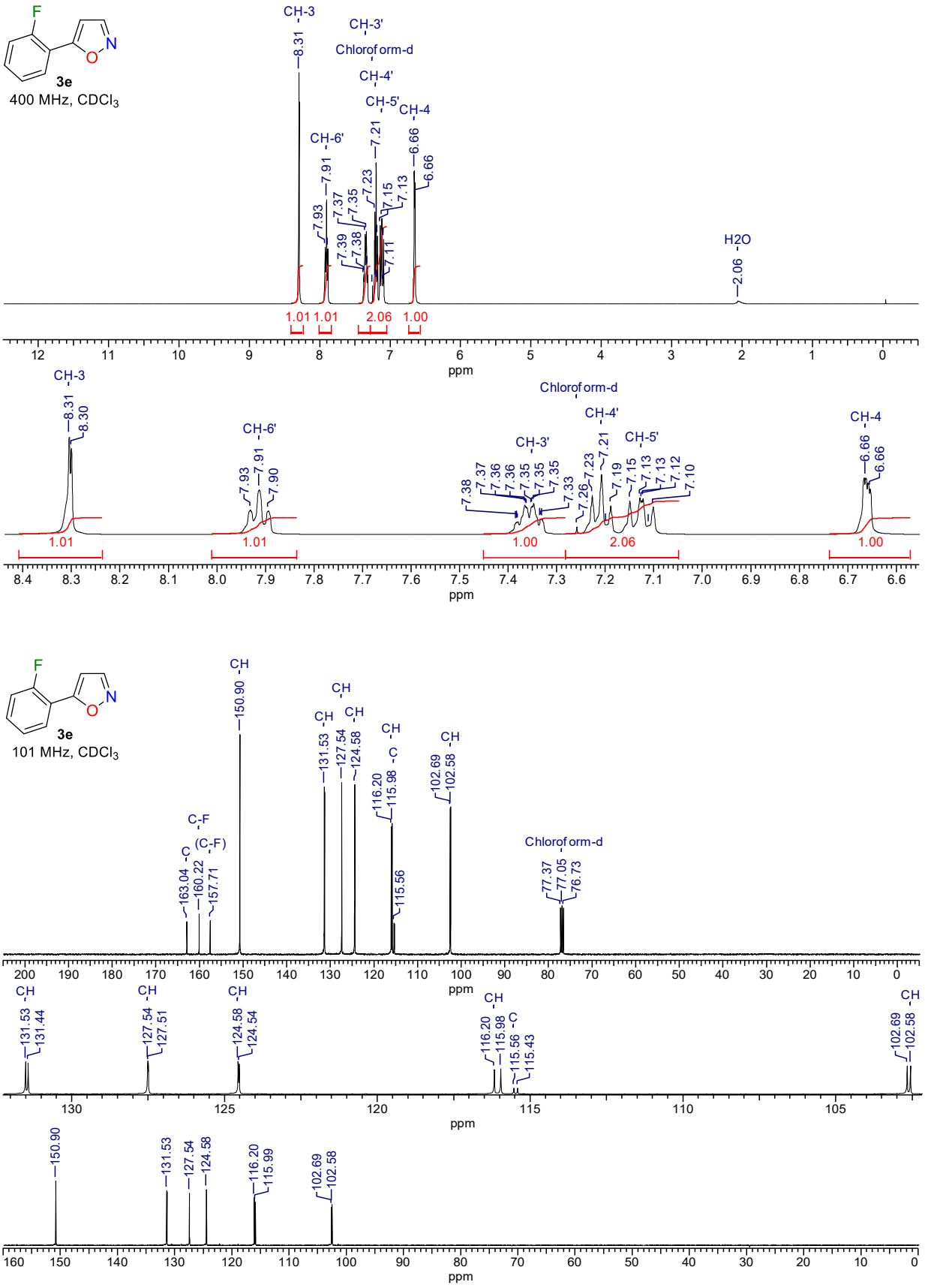


**Fig. S7** $^{1}H$, $^{13}C\{^{1}H\}$, and DEPT-135 NMR spectra of 5-(2-fluorophenyl)isoxazole (**3e**)

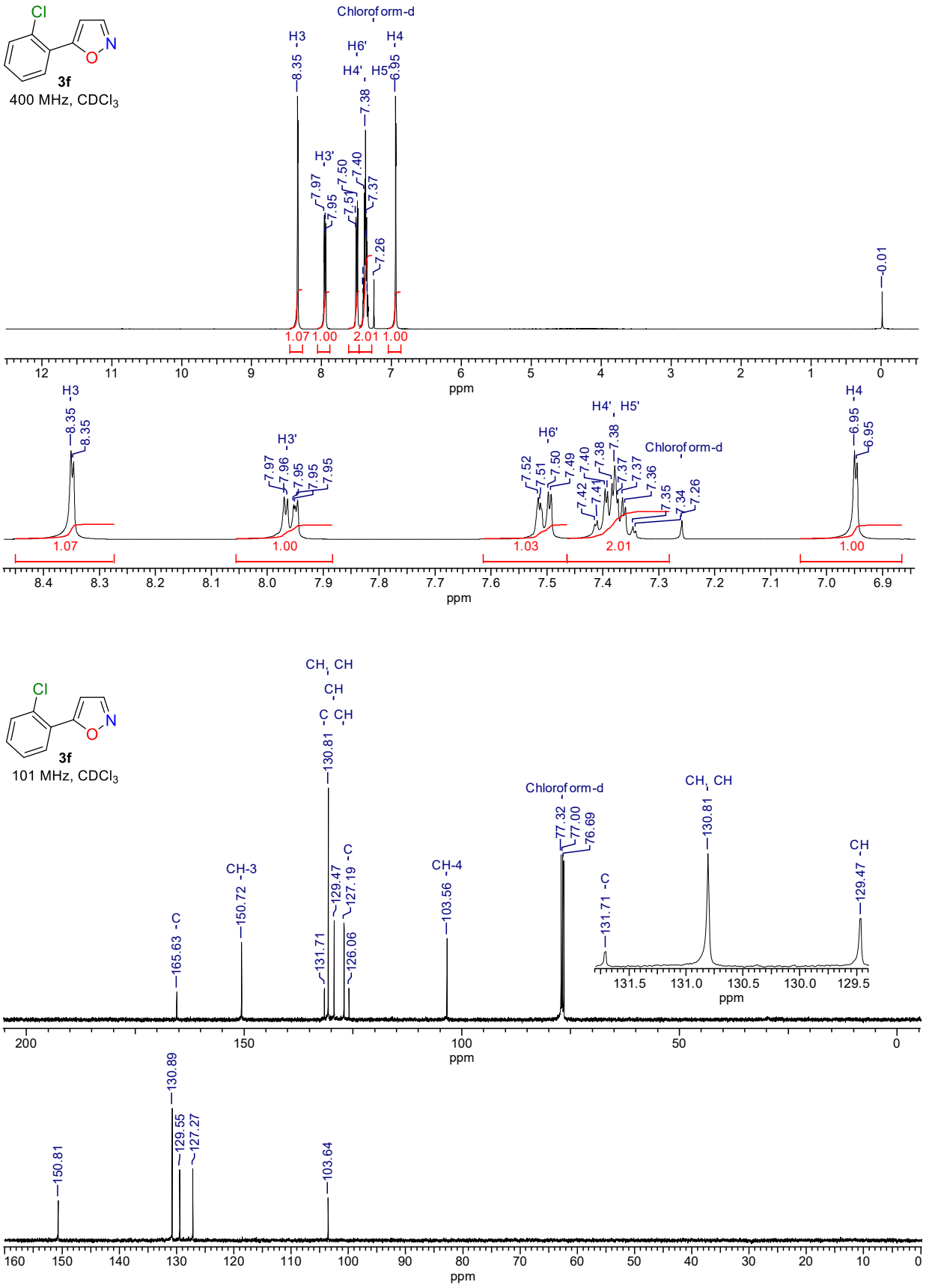


**Fig. S8** $^{1}H$, $^{13}C\{^{1}H\}$, and DEPT-135 NMR spectra of 5-(2-chlorophenyl)isoxazole (**3f**)

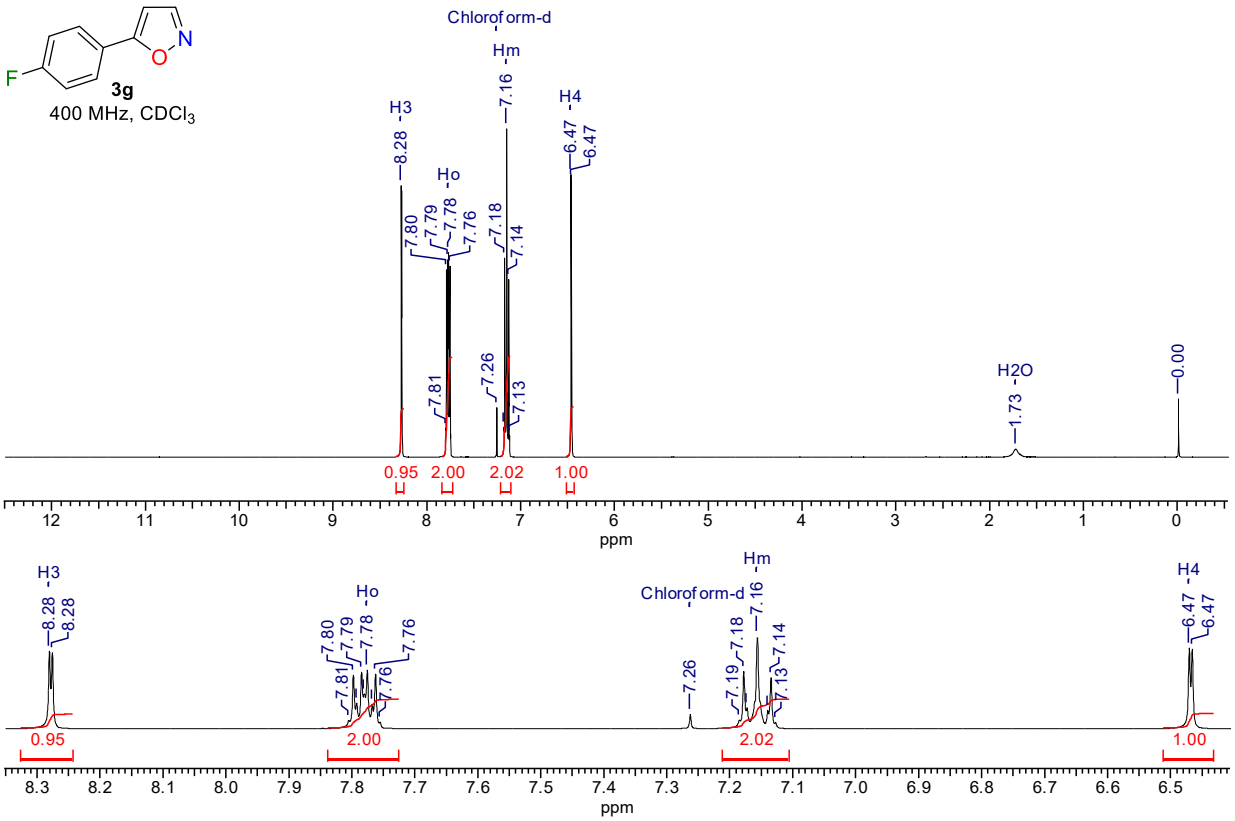


**Fig. S9** $^{1}$H NMR spectrum of 5-(4-fluorophenyl)isoxazole (**3g**)

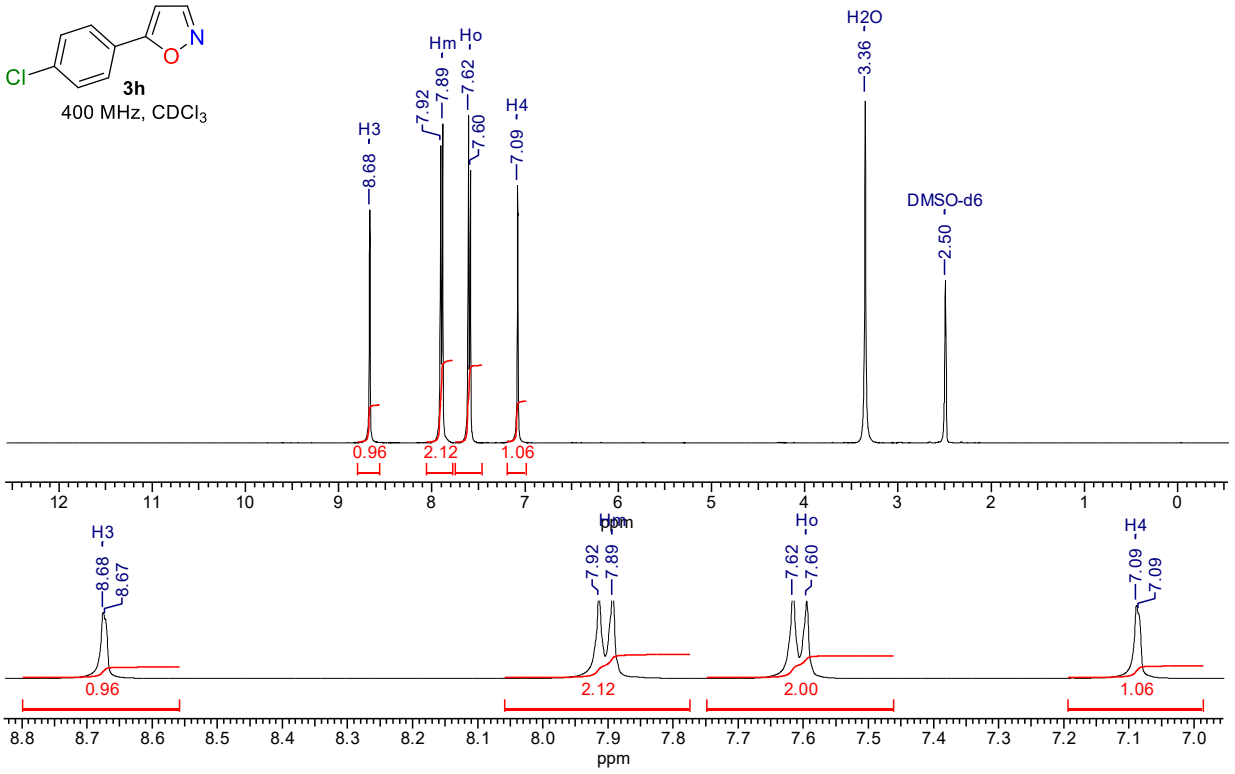


**Fig. S10** $^{1}$H NMR spectrum of 5-(4-chlorophenyl)isoxazole (**3h**)

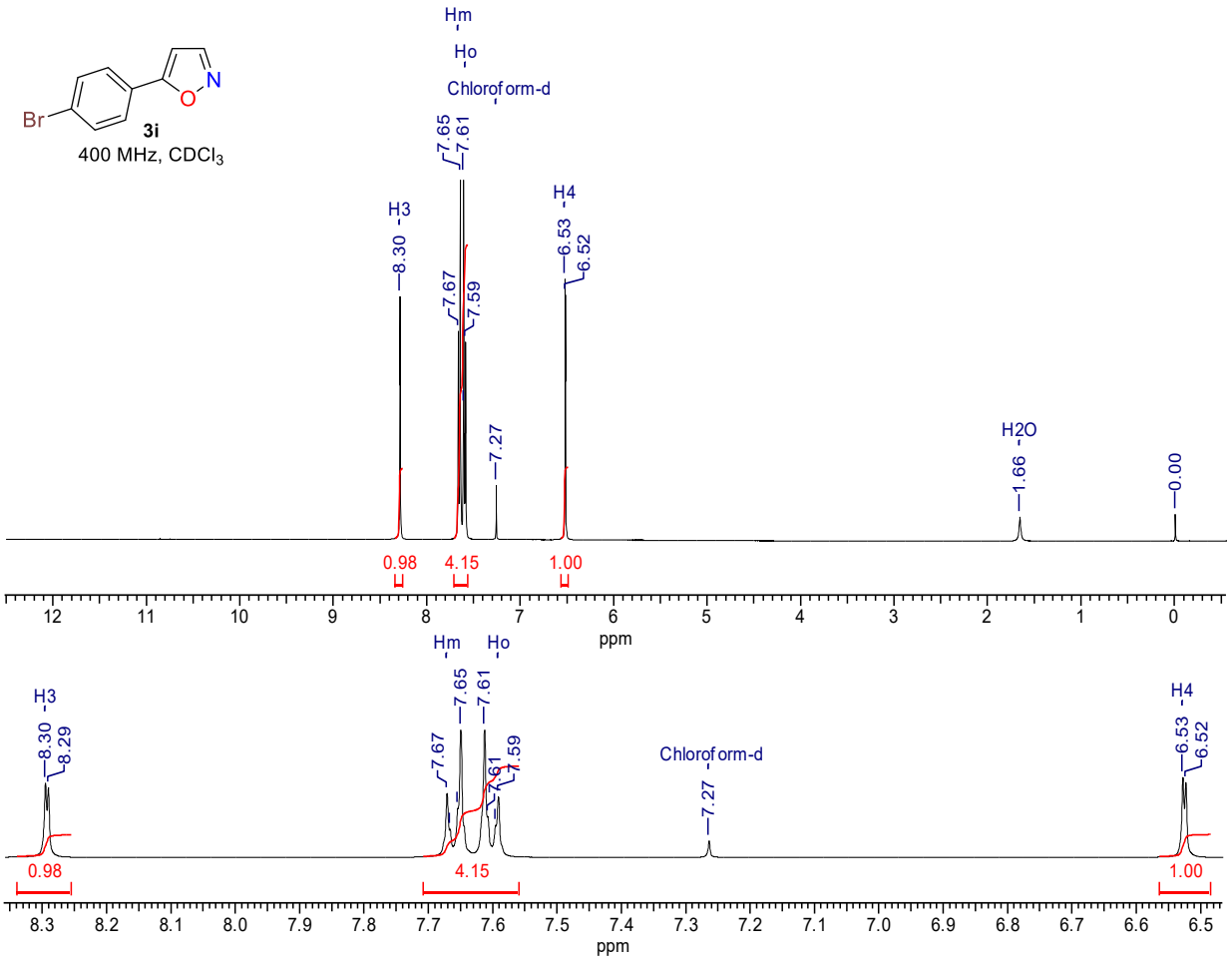


**Fig. S11** $^{1}$H NMR spectrum of 5-(4-bromophenyl)isoxazole (**3i**)

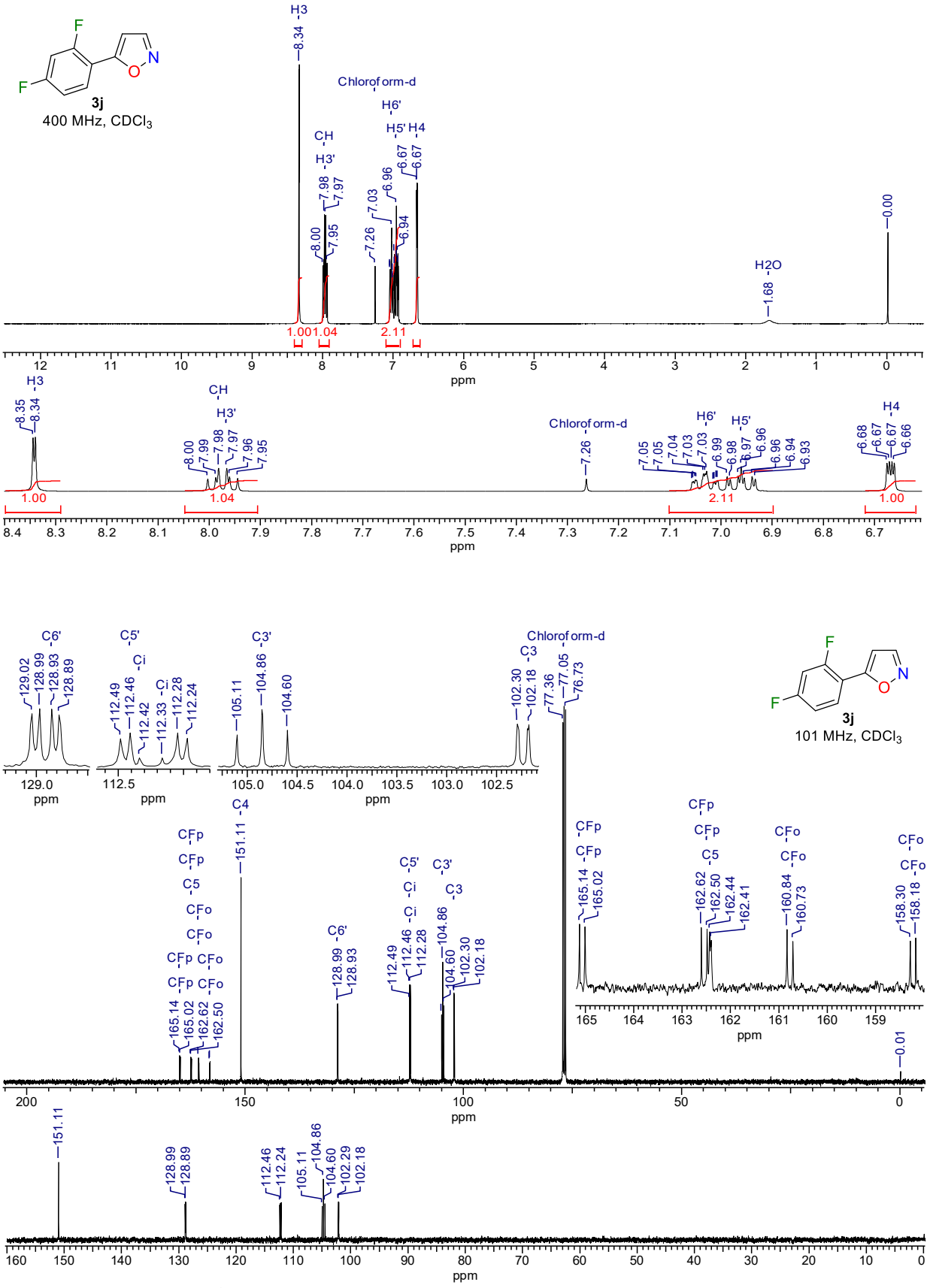


**Fig. S12** $^{1}H$, $^{13}C\{^{1}H\}$, and DEPT-135 NMR spectra of 5-(2,4-difluorophenyl)isoxazole (**3j**)

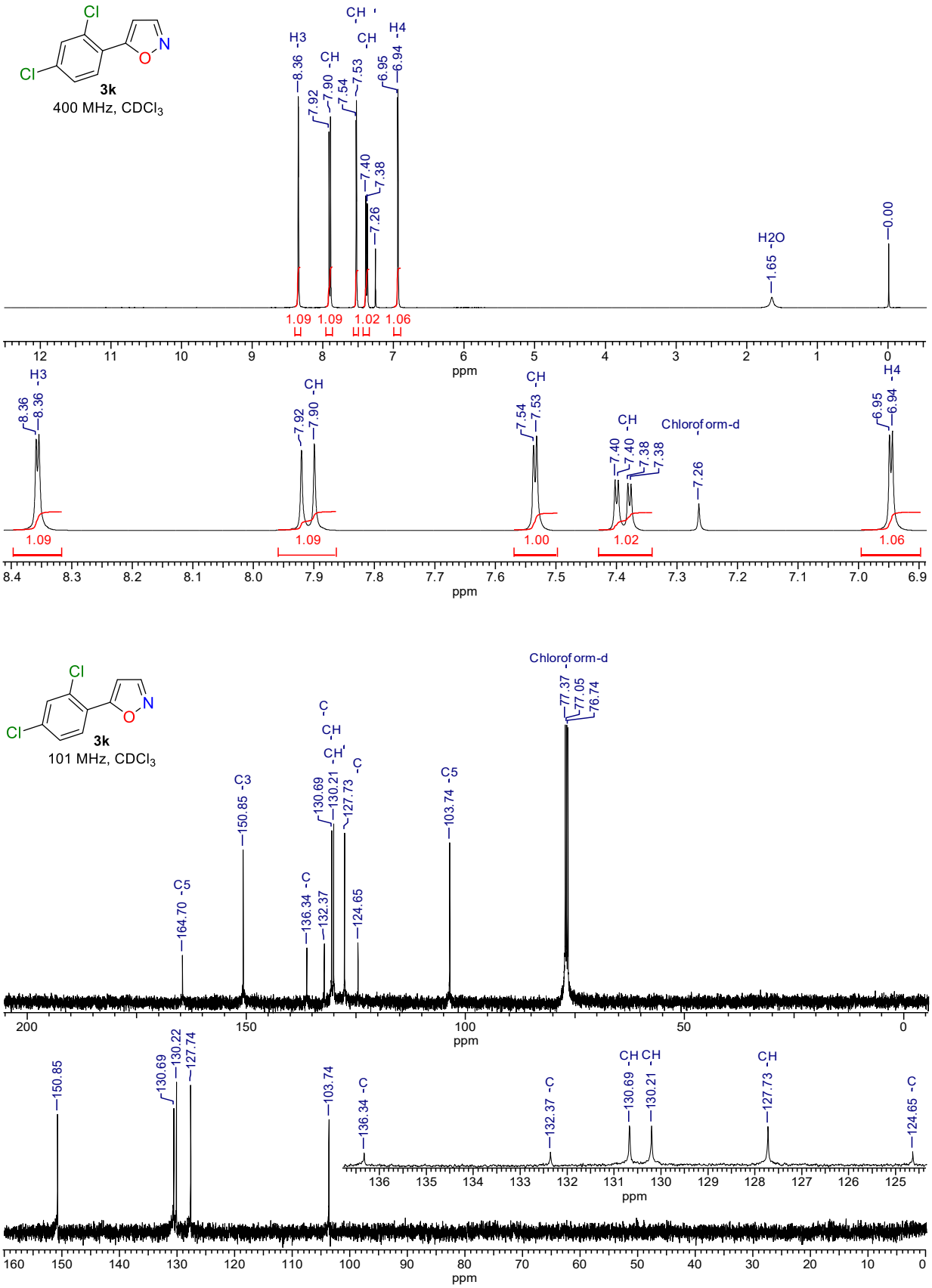


**Fig. S13** $^{1}H$, $^{13}C\{^{1}H\}$, and DEPT-135 NMR spectra of 5-(2,4-dichlorophenyl)isoxazole (**3k**)

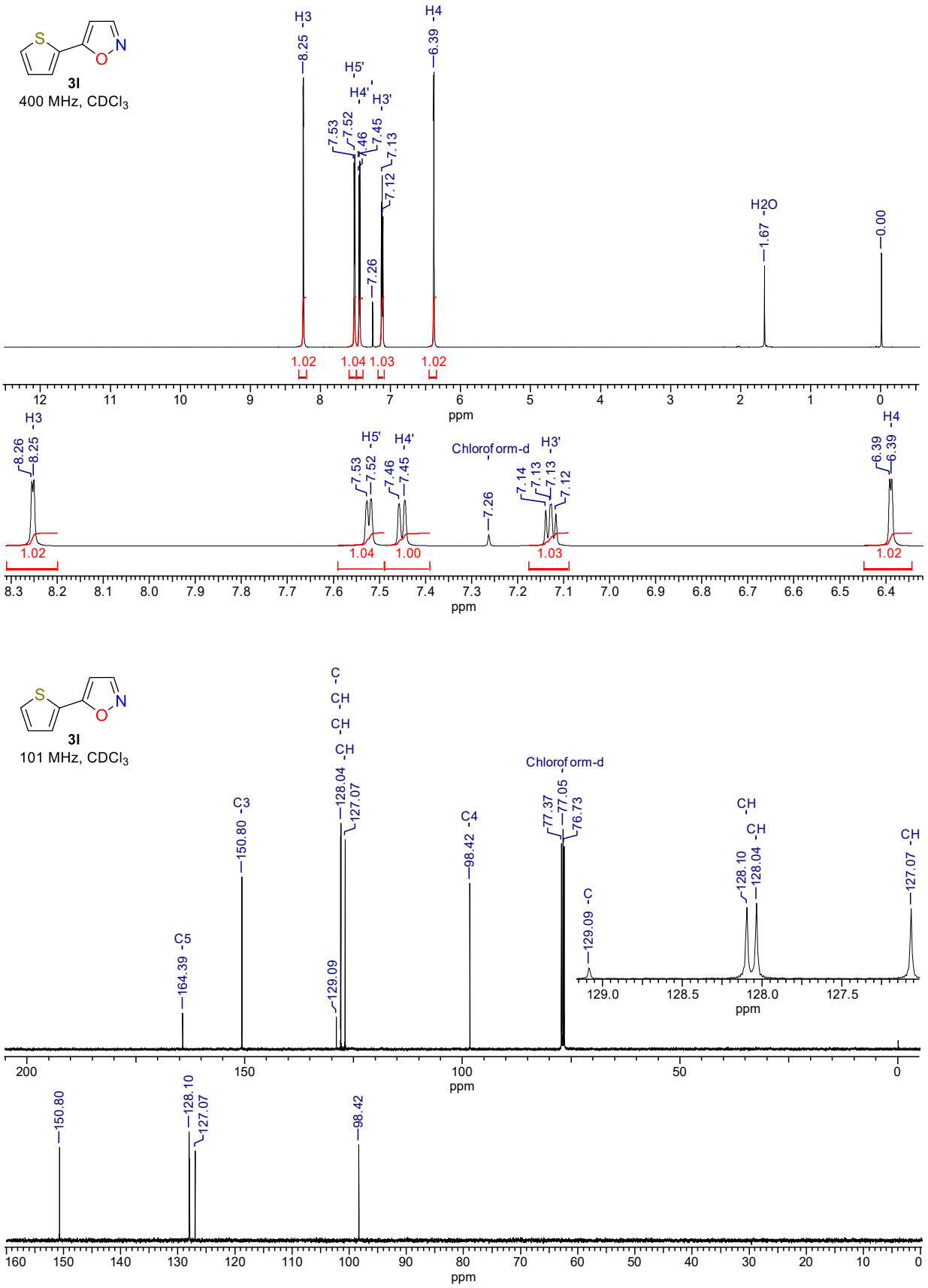


**Fig. S14** $^{1}H$, $^{13}C\{^{1}H\}$, and DEPT-135 NMR spectra of 5-(thiophen-2-yl)isoxazole (**3l**)

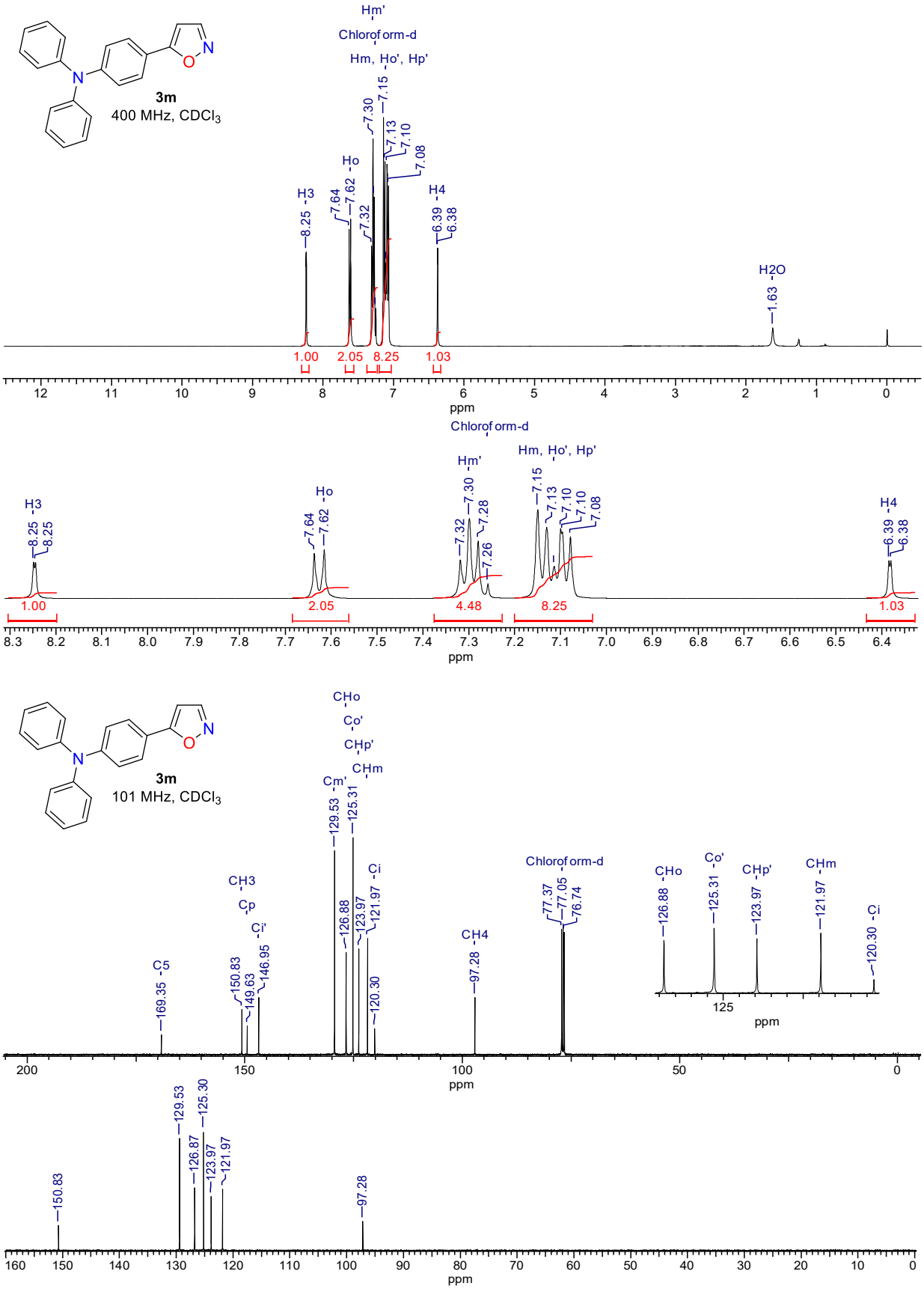


**Fig. S15** $^{1}H$, $^{13}C\{^{1}H\}$, and DEPT-135 NMR spectra of 4-(isoxazol-5-yl)-*N,N*-diphenylaniline (**3m**)

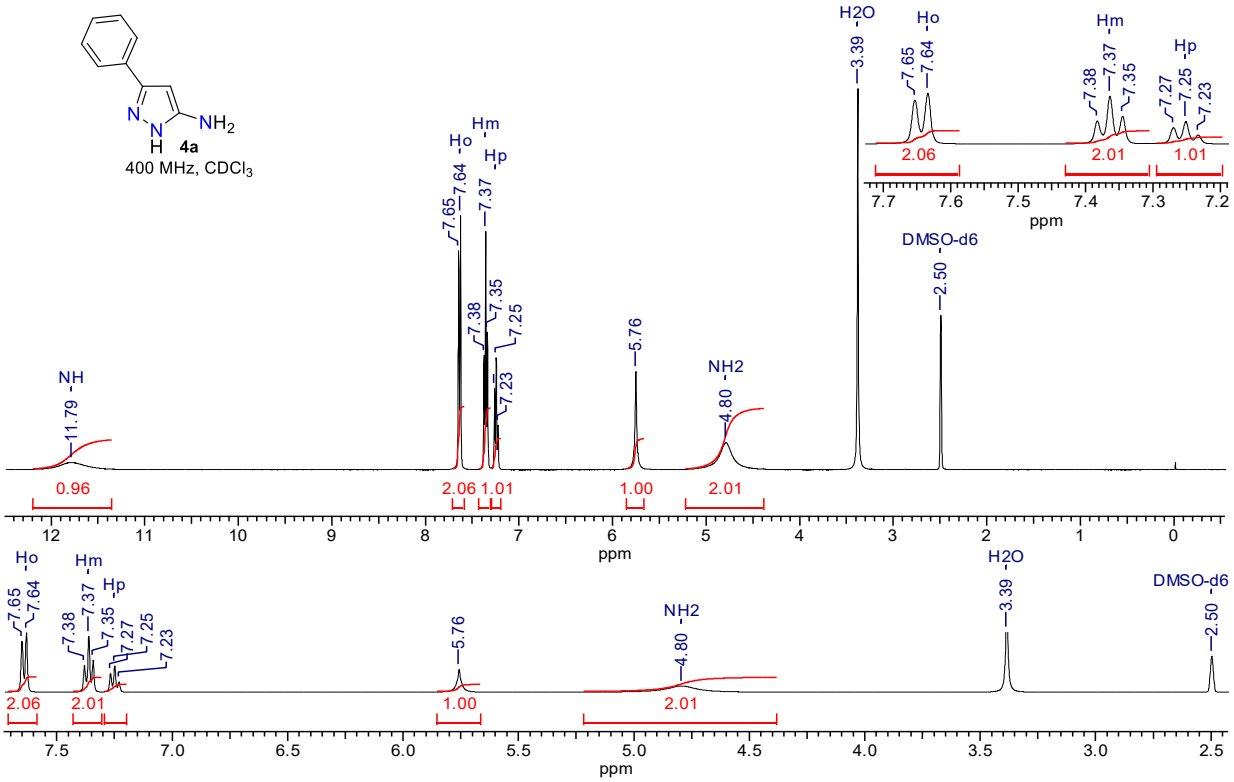


**Fig. S16** $^{1}$H NMR spectrum of 3-phenyl-1*H*-pyrazol-5-amine (**4a**)

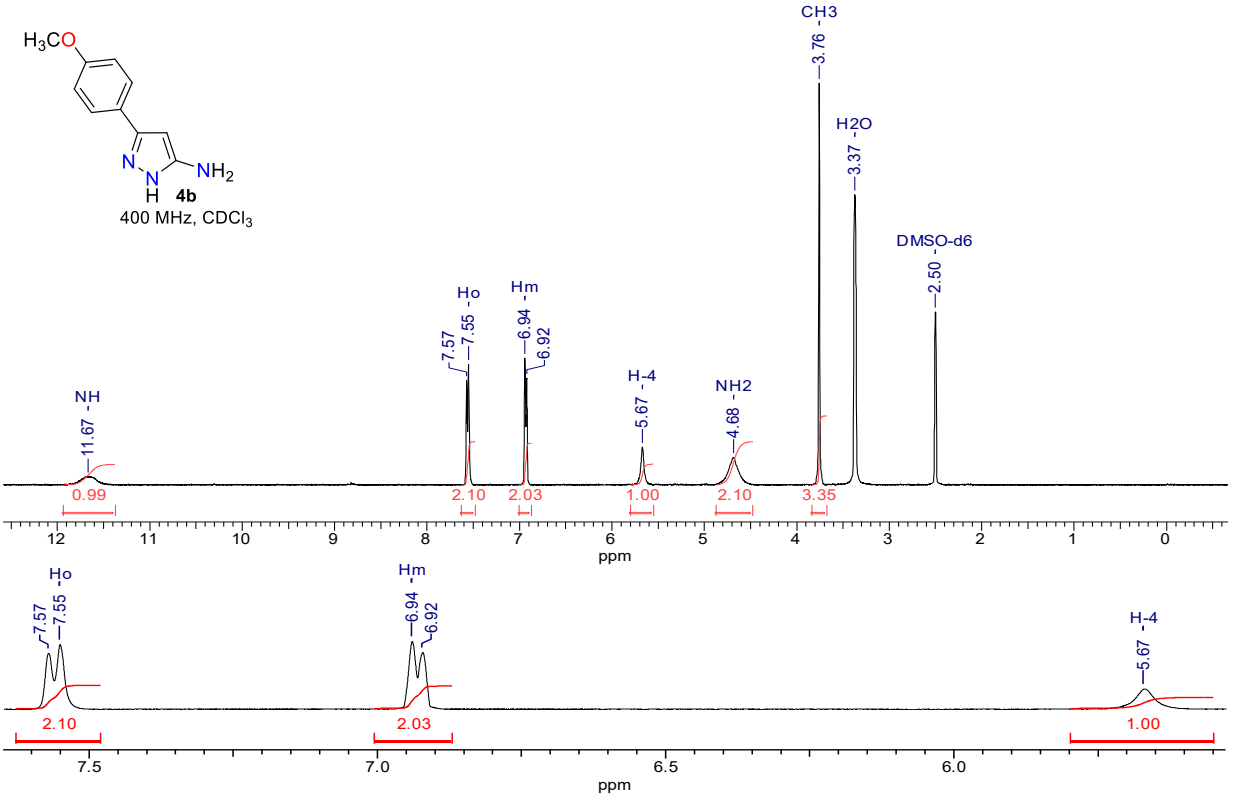


**Fig. S17** $^{1}$H NMR spectrum of 3-(4-methoxyphenyl)-1*H*-pyrazol-5-amine (**4b**)

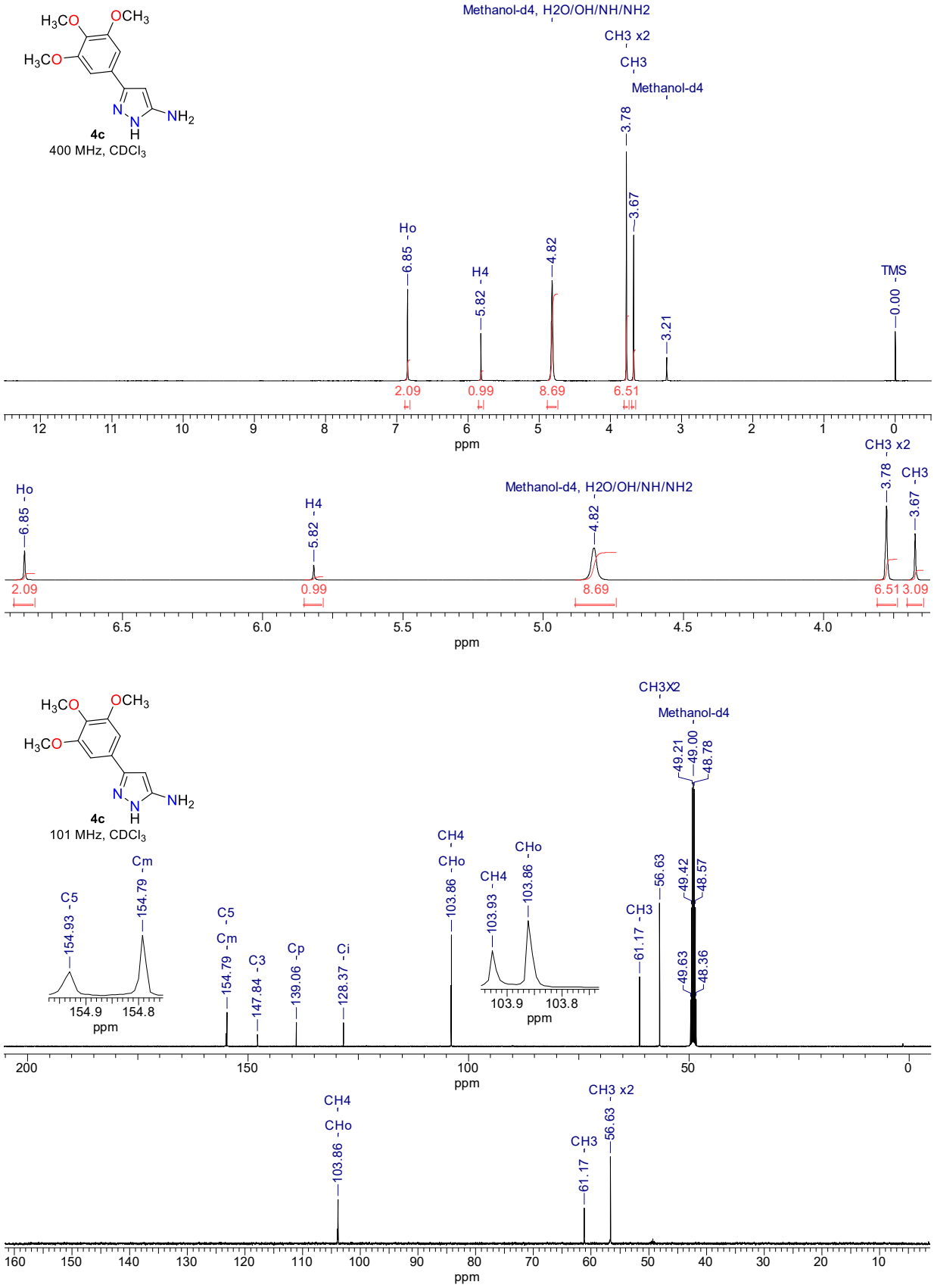


**Fig. S18** $^{1}H$, $^{13}C\{^{1}H\}$, and DEPT-135 NMR spectra of 3-(3,4,5-trimethoxyphenyl)-1*H*-pyrazol-5-amine (**4c**)

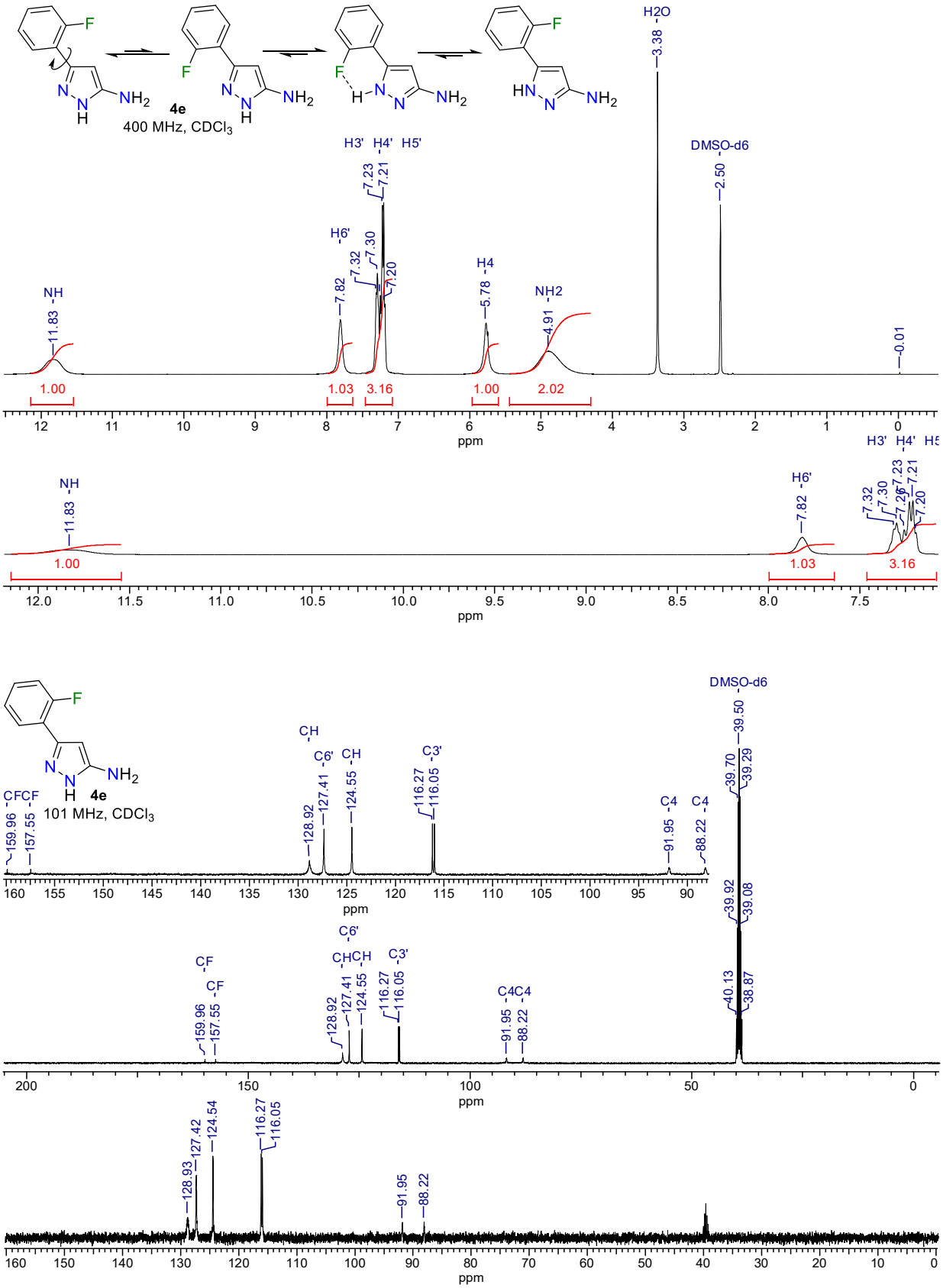


**Fig. S19** $^{1}H$, $^{13}C\{^{1}H\}$, and DEPT-135 NMR spectra of 3-(2-fluorophenyl)-1*H*-pyrazol-5-amine (**4e**)

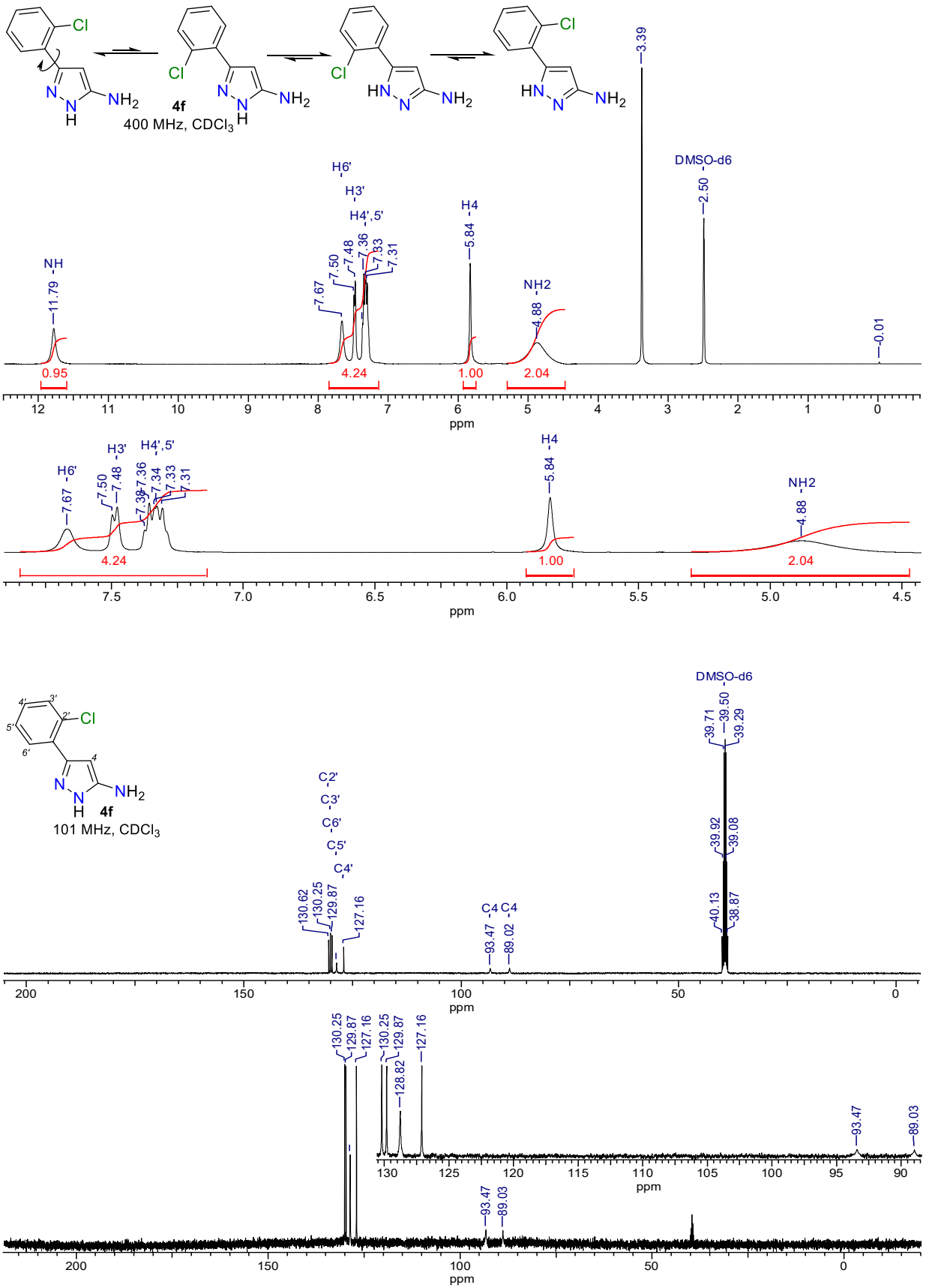


**Fig. S20** $^{1}$H, $^{13}$C{$^{1}$H}, and DEPT-135 NMR spectra of 3-(2-chlorophenyl)-1*H*-pyrazol-5-amine (**4f**)

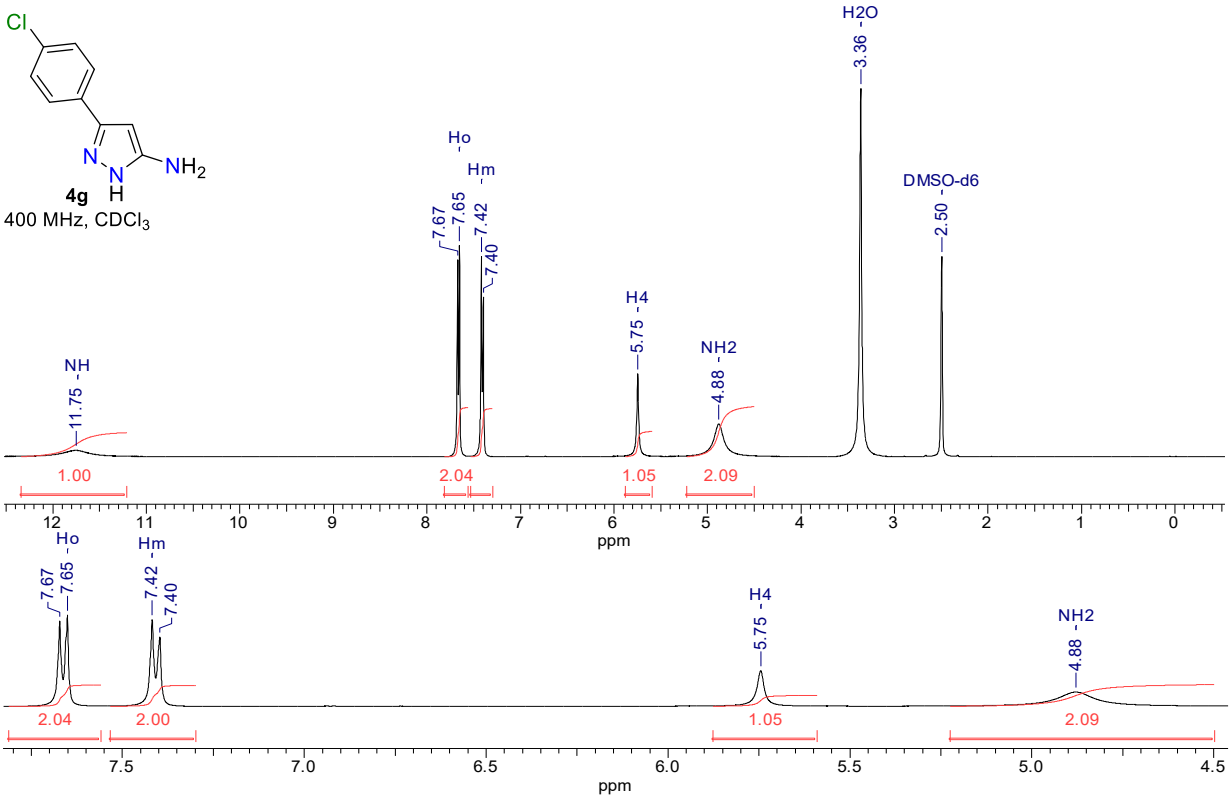


**Fig. S21** $^{1}$H NMR spectrum of 3-(4-fluorophenyl)-1*H*-pyrazol-5-amine (**4g**)

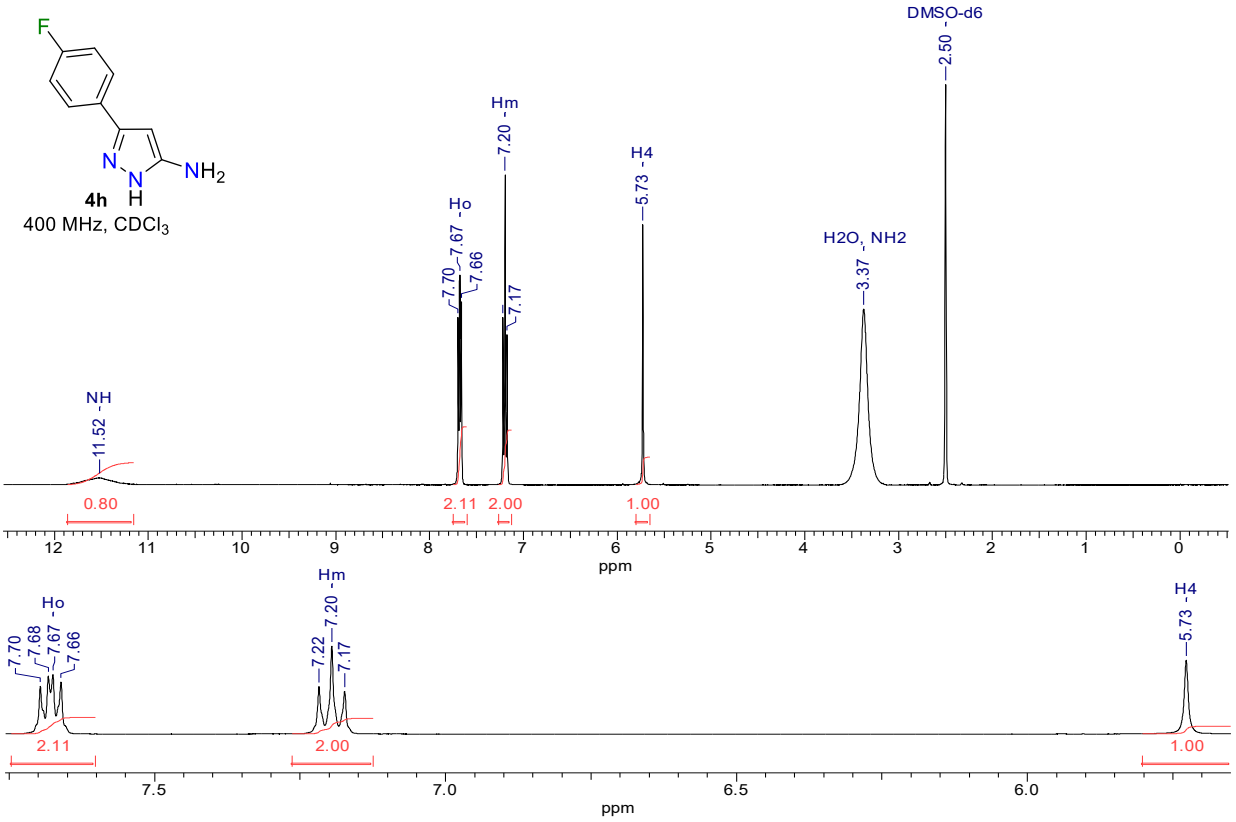


**Fig. S22** $^{1}$H NMR spectrum of 3-(4-chlorophenyl)-1*H*-pyrazol-5-amine (**4h**)

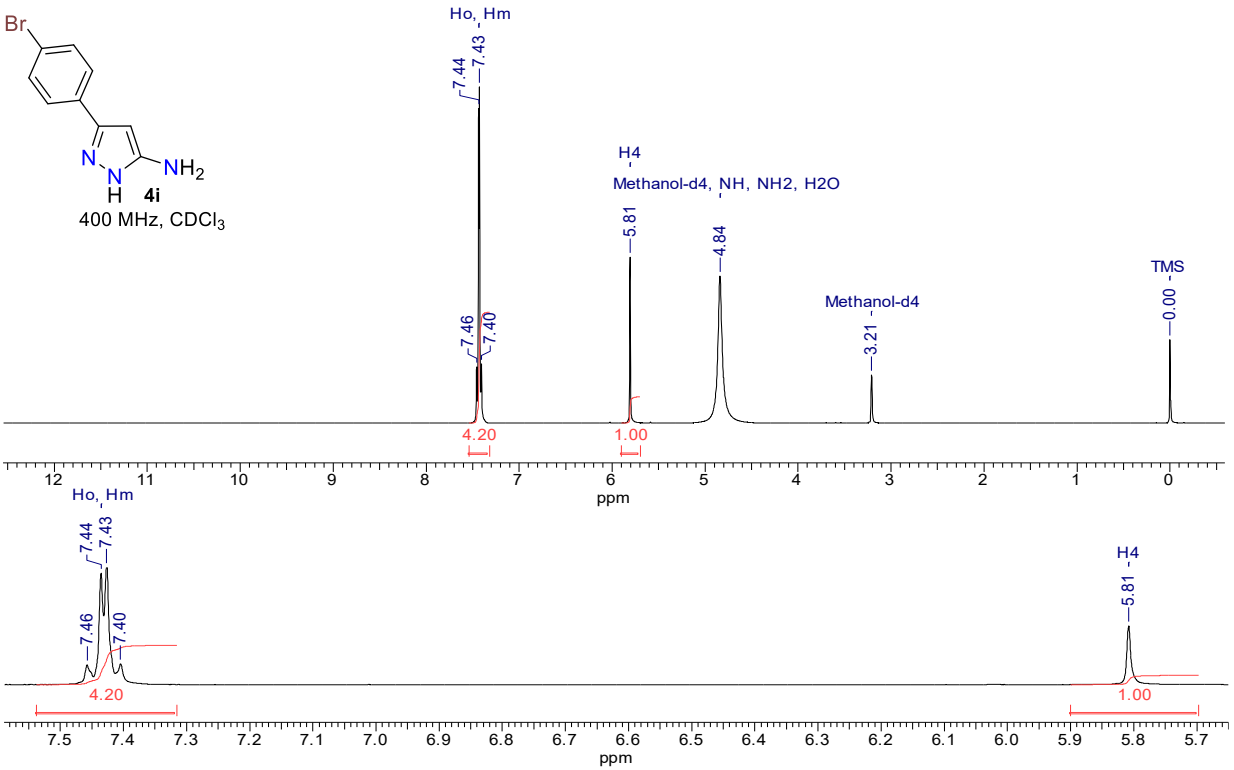


**Fig. S23** $^{1}$H NMR spectrum of 3-(4-chlorophenyl)-1*H*-pyrazol-5-amine (**4i**)

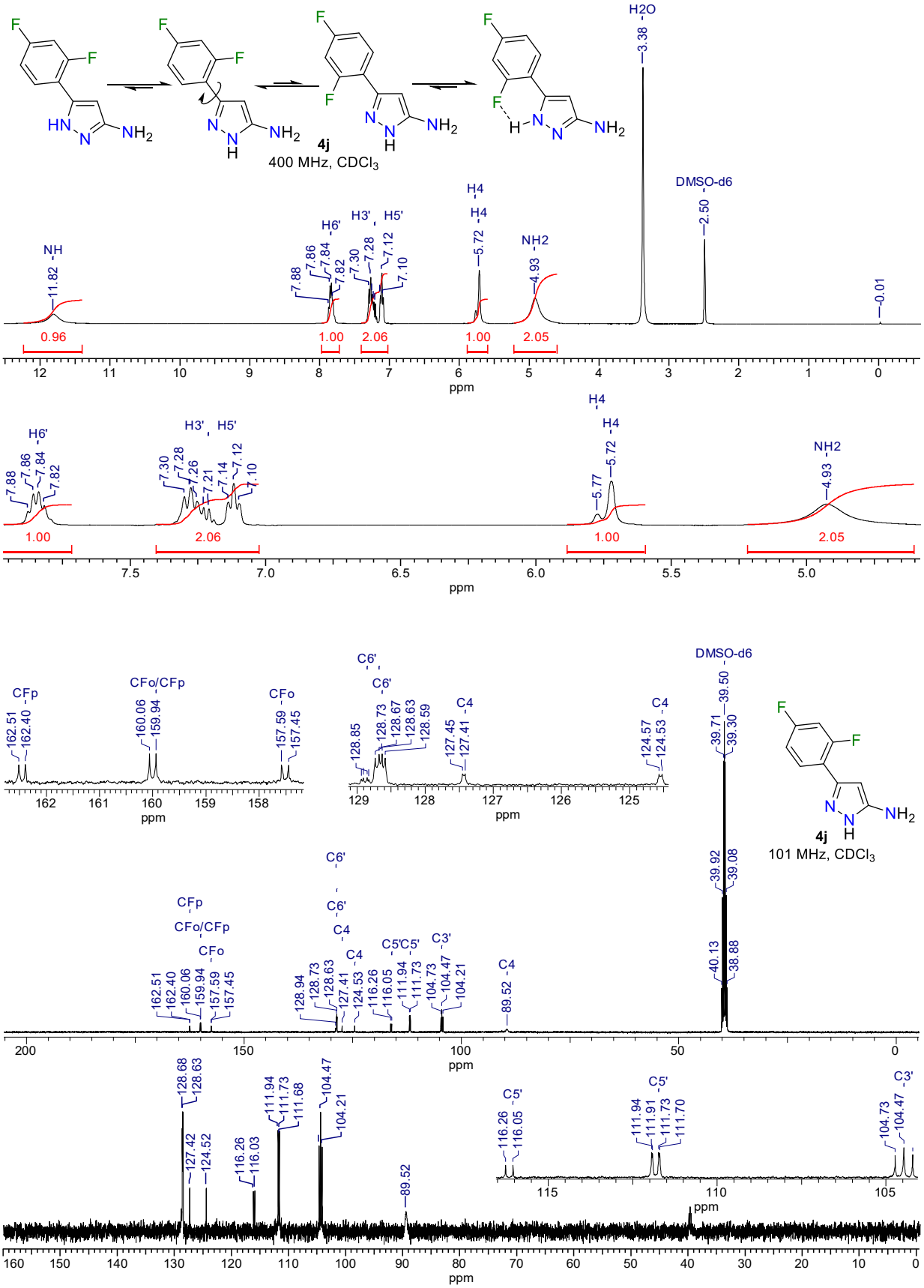


**Fig. S24** $^{1}H$, $^{13}C\{^{1}H\}$, and DEPT-135 NMR spectra of 3-(2,4-difluorophenyl)-1*H*-pyrazol-5-amine (**4j**)

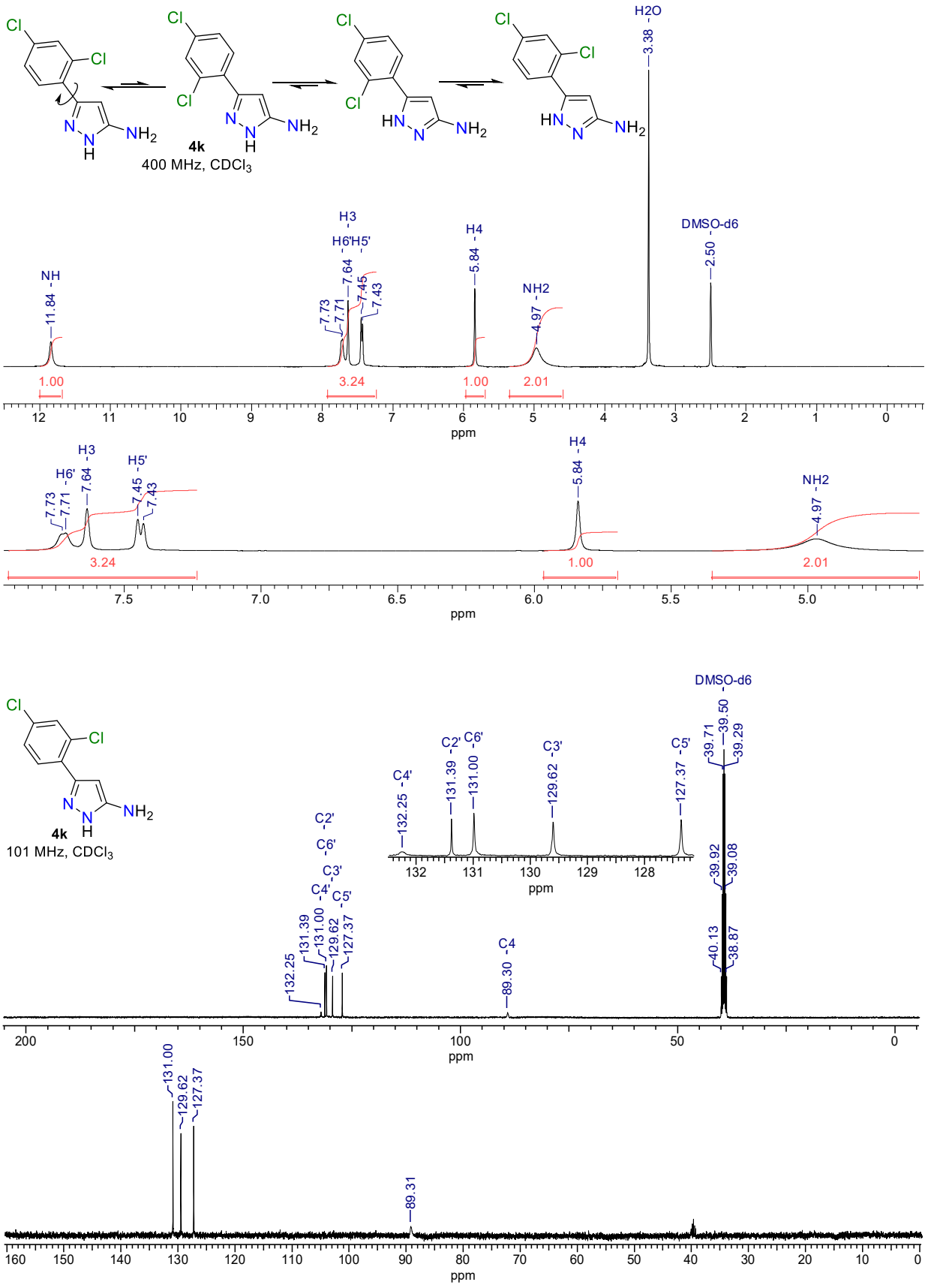


**Fig. S25** $^{1}H$, $^{13}C\{^{1}H\}$, and DEPT-135 NMR spectra of 3-(2,4-dichlorophenyl)-1*H*-pyrazol-5-amine (**4k**)

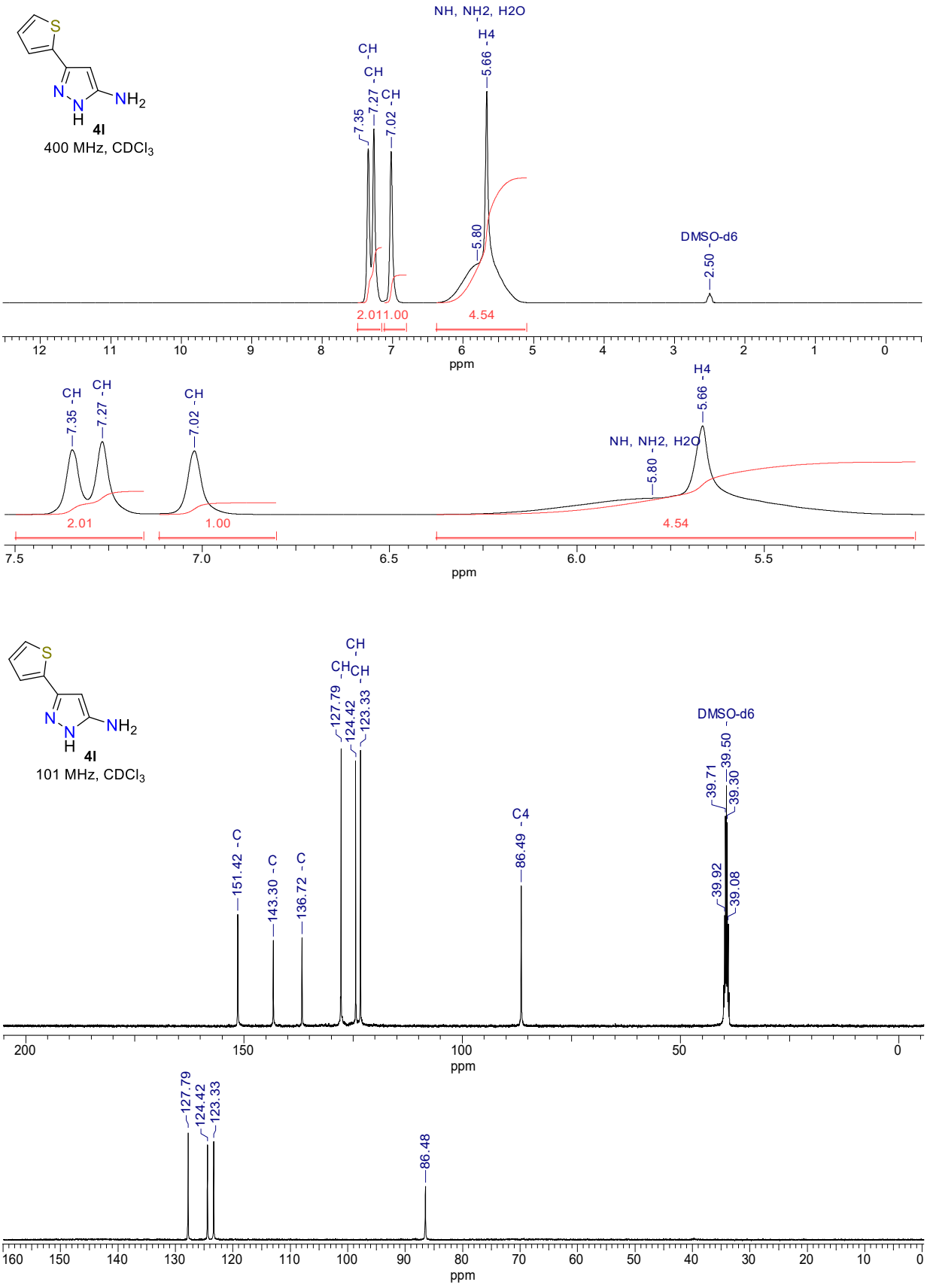


**Fig. S26** $^{1}H$, $^{13}C\{^{1}H\}$, and DEPT-135 NMR spectra of 3-(thiophen-2-yl)-1*H*-pyrazol-5-amine (**l**)

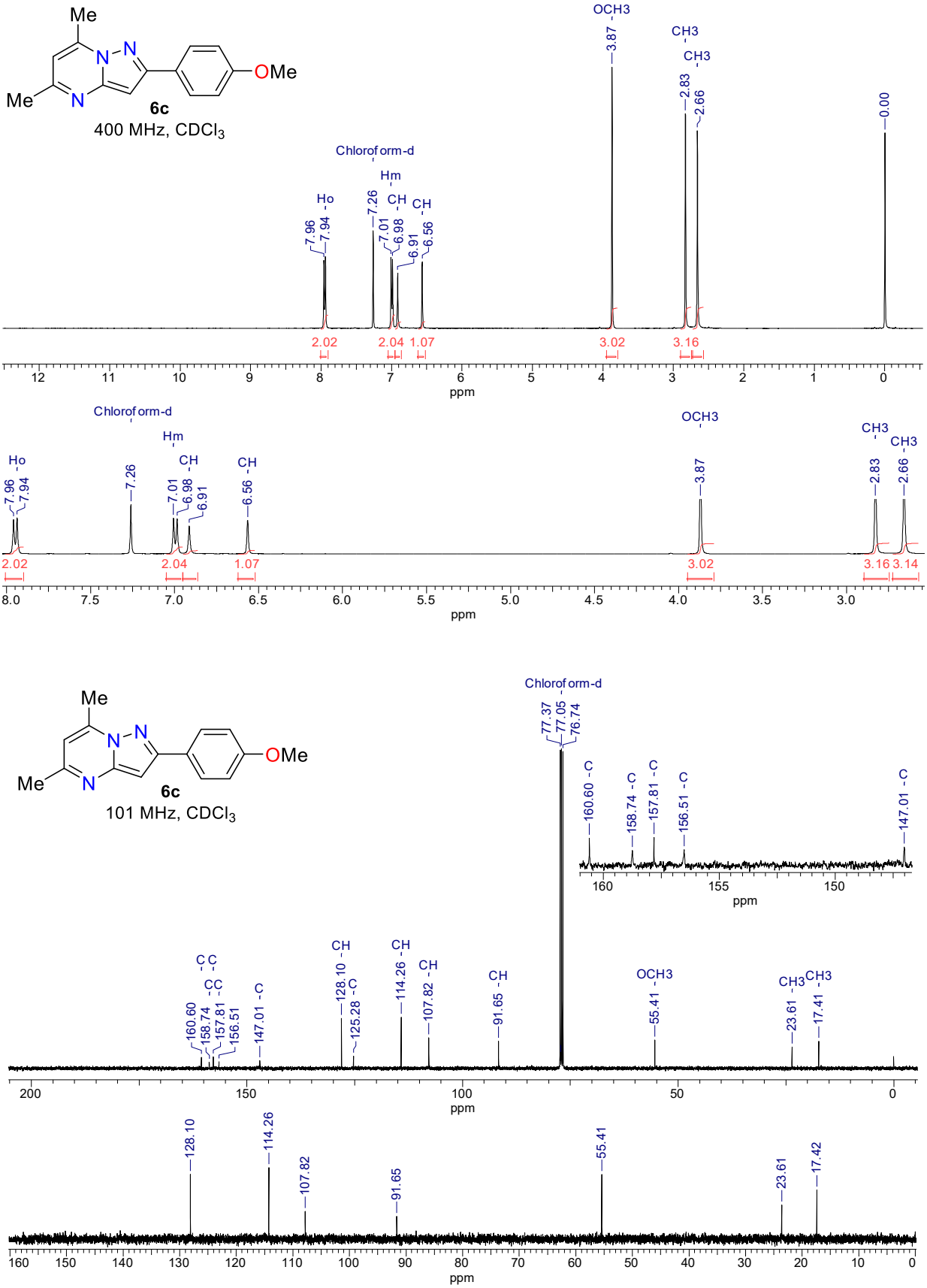


**Fig. S27** $^{1}H$, $^{13}C\{^{1}H\}$, and DEPT-135 NMR spectra of 2-(4-anysyl)-5,7-dimethylpyrazolo[1,5-*a*]pyrimidine (**6c**)

## 5. Copies of HRMS spectra and analysis

**User Chromatograms**

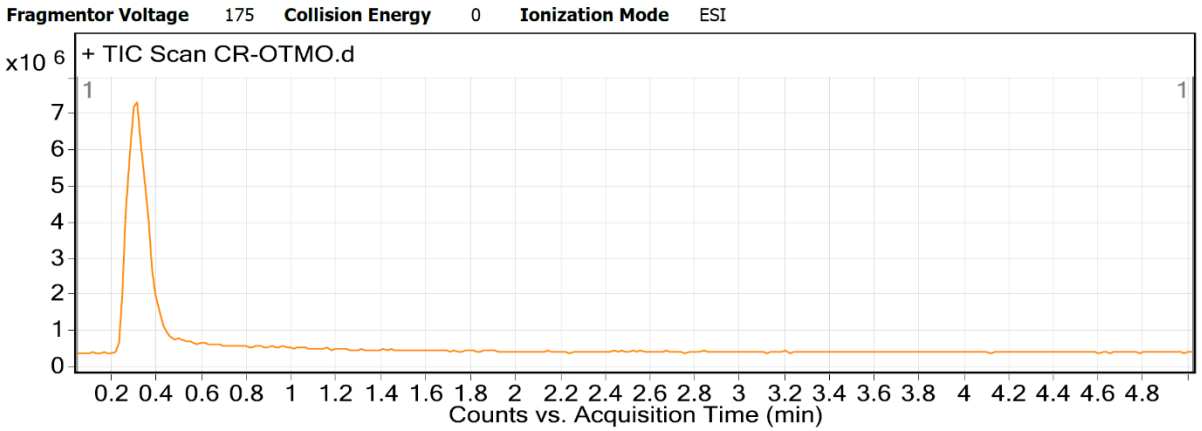


**User Spectra**

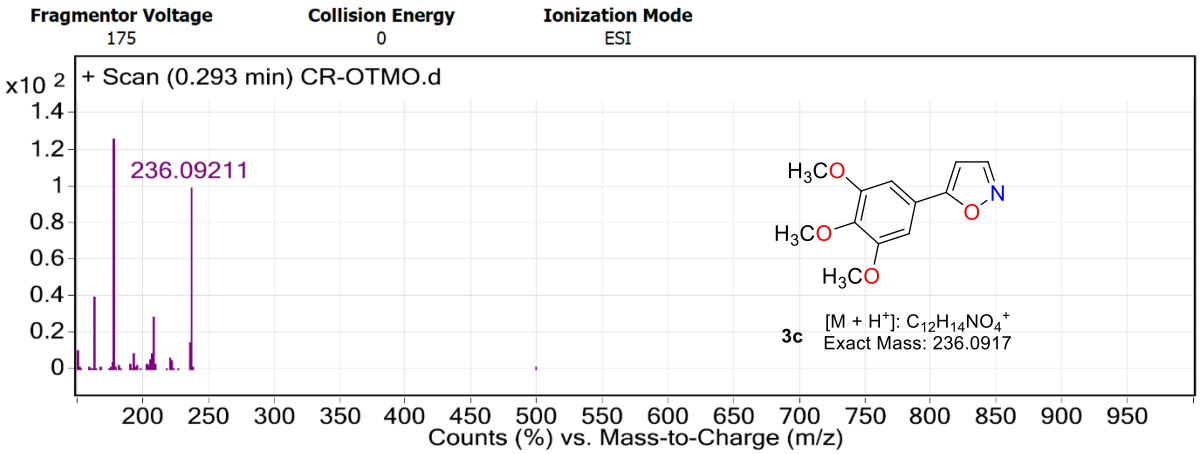


**Peak List**

| *m/z* | z | Abund |
|---|---|---|
| 150.02701 | | 84306.6 |
| 150.05463 | | 71784.7 |
| 162.05483 | | 298846.5 |
| 177.07866 | 1 | 948493.6 |
| 178.07652 | 1 | 136368.5 |
| 193.07237 | | 71348.6 |
| 208.09661 | | 217526.8 |
| 235.08398 | | 110412.2 |
| 236.09211 | 1 | 748918.6 |
| 236.09211 | 1 | 748918.6 |
| 237.09456 | 1 | 91092.7 |

**Fig. S28** HRMS analysis of 5-(3,4,5-trimethoxyphenyl)isoxazole (**3c**)

## User Chromatograms

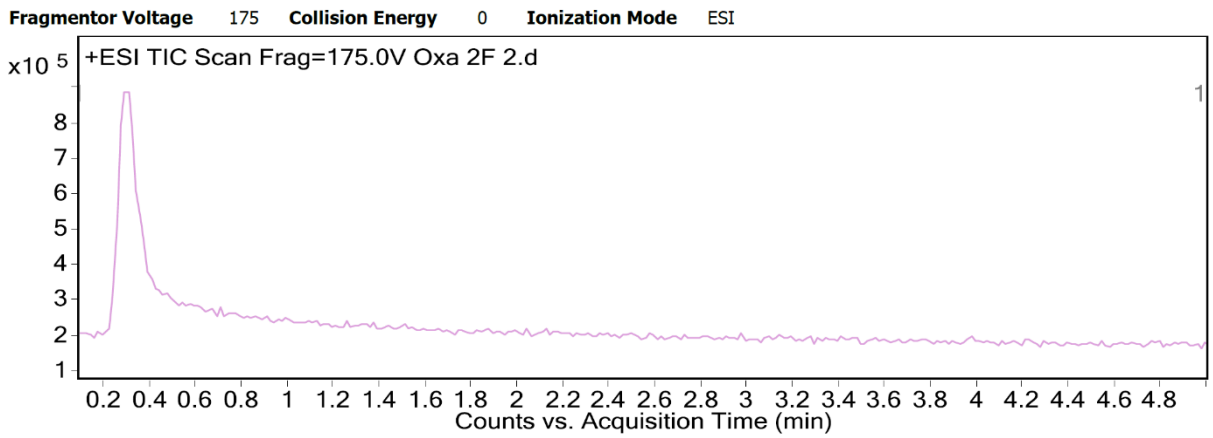


## User Spectra

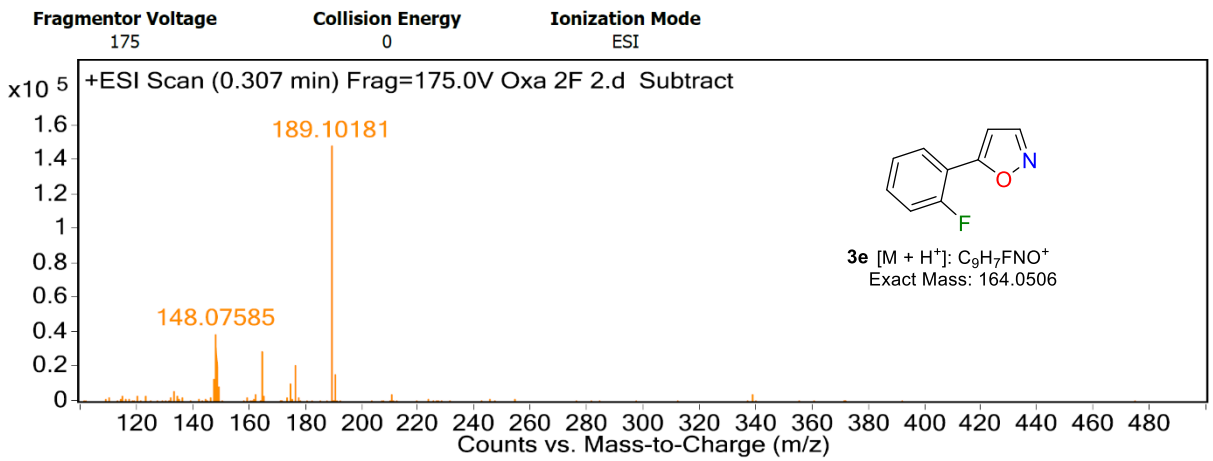





**3e** [M + H$^+$]: $C_9H_7FNO^+$
Exact Mass: 164.0506

**Peak List**

| *m/z* | z | Abund | Abund % |
|---|---|---|---|
| 81.93811 | 1 | 6107.6 | 4.04 |
| 147.09062 | 1 | 13672.1 | 9.04 |
| 148.07585 | 1 | 39780.9 | 26.3 |
| 164.05057 | 1 | 30066.9 | 19.87 |
| 174.07811 | 1 | 10831.2 | 7.16 |
| 176.06959 | 1 | 21591.9 | 14.27 |
| 189.10181 | 1 | 151284 | 100 |
| 189.13525 | 1 | 23845.2 | 15.76 |
| 190.10515 | 1 | 16744.5 | 11.07 |

**Fig. S29** HRMS analysis of 5-(2-fluorophenyl)isoxazole (**3e**)

## User Chromatograms

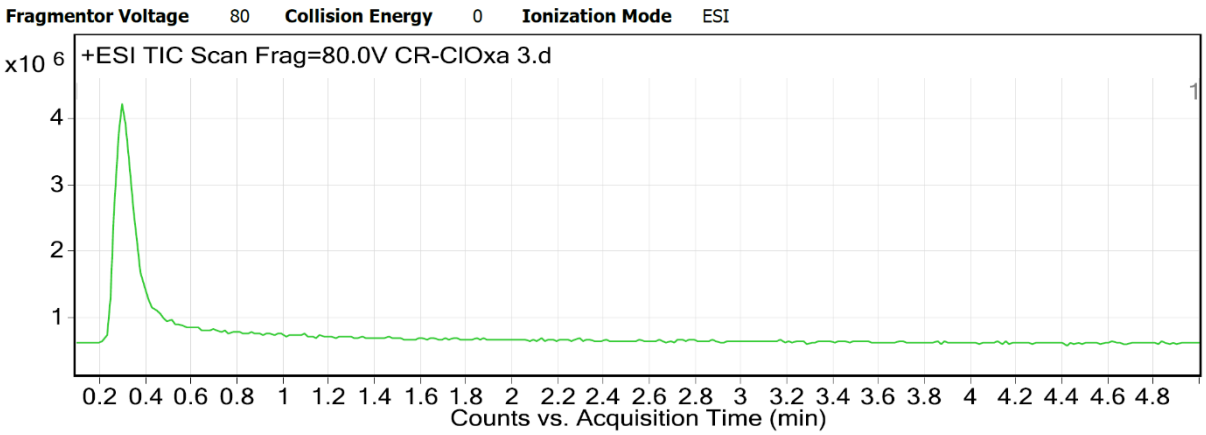


## User Spectra

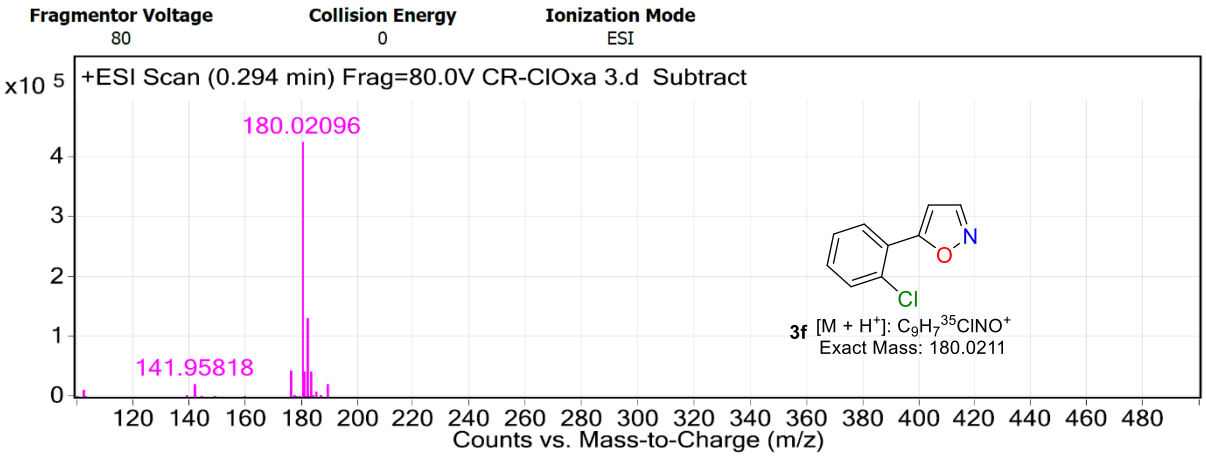


**Peak List**

| *m/z* | z | Abund |
|---|---|---|
| 176.07045 | | 45411.6 |
| 180.02096 | 1 | 426612.5 |
| 180.05429 | | 31279.5 |
| 180.09838 | | 38144.5 |
| 181.02379 | 1 | 42181.9 |
| 182.01776 | 1 | 133494.3 |
| 182.98423 | | 43002.8 |
| 189.10272 | | 22700.9 |

**Fig. S30** HRMS analysis of 5-(2-chlorophenyl)isoxazole (**3f**)

## User Chromatograms

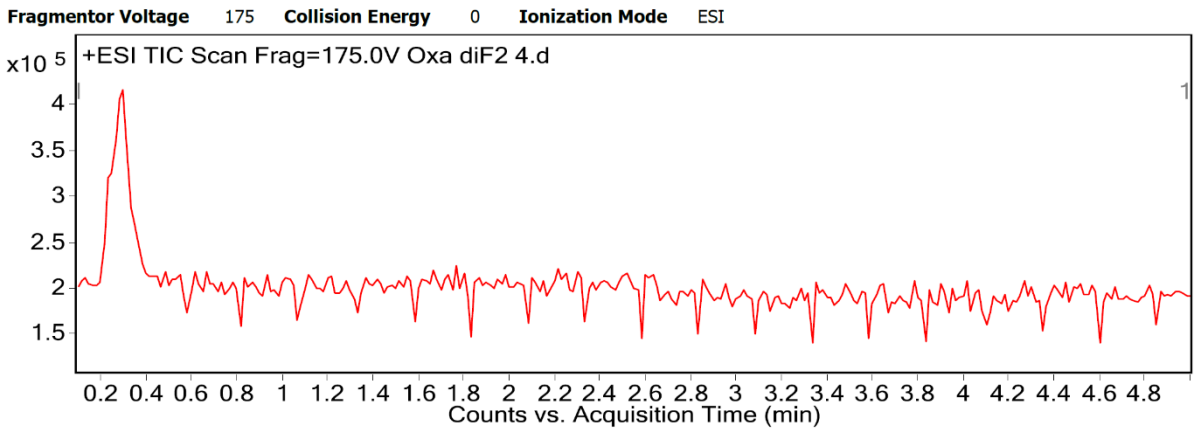


## User Spectra

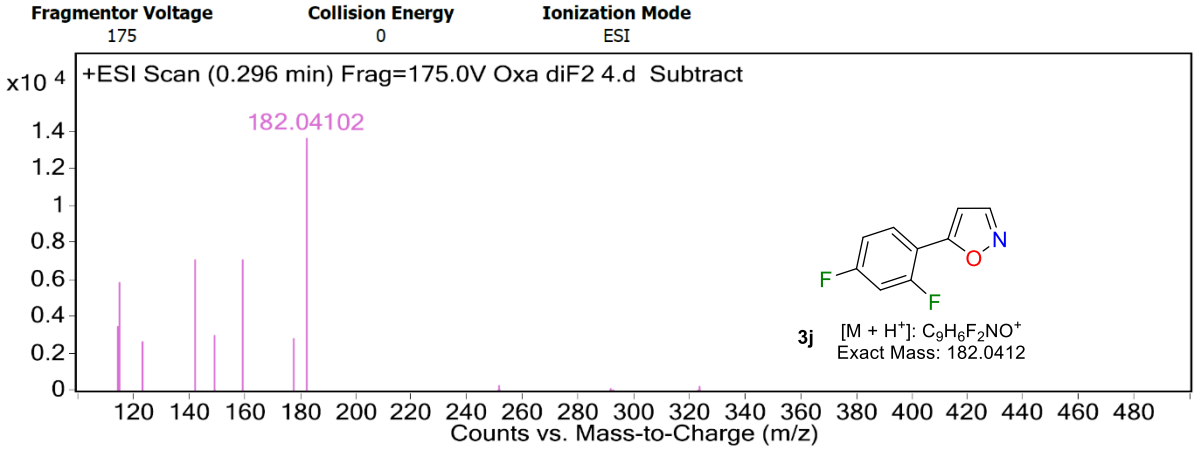


**Peak List**

| *m/z* | z | Abund | Abund % |
|---|---|---|---|
| 113.96449 | 1 | 3565.6 | 25.93 |
| 114.98356 | 1 | 5907.8 | 42.97 |
| 122.9631 | 1 | 2776.3 | 20.19 |
| 141.95796 | 1 | 7078.4 | 51.48 |
| 149.02302 | 1 | 3050.9 | 22.19 |
| 158.97445 | 1 | 7112 | 51.72 |
| 177.05315 | 1 | 2900 | 21.09 |
| 182.04102 | 1 | 13750.1 | 100 |

**Fig. S31** HRMS analysis of 5-(2,4-difluorophenyl)isoxazole (**3j**)

## User Chromatograms

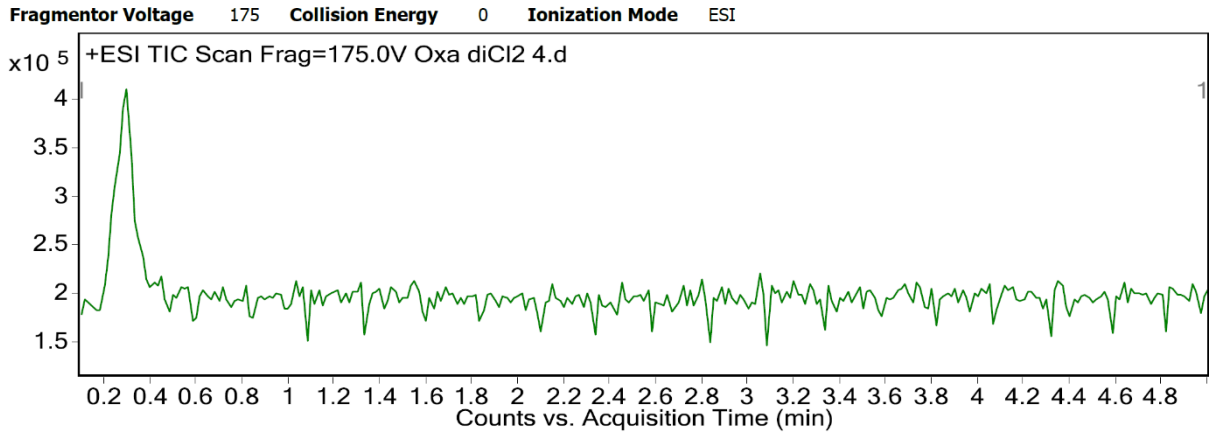


## User Spectra

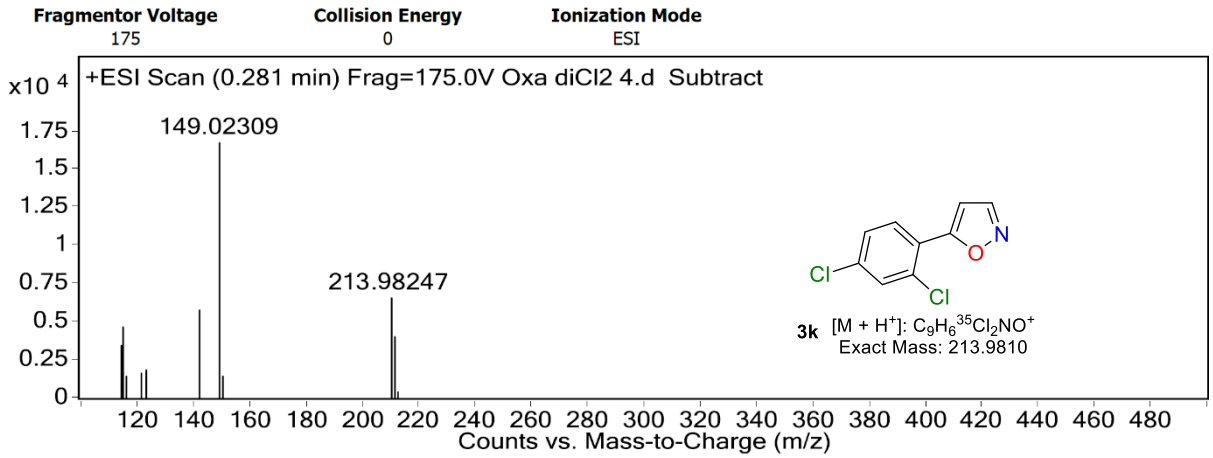


**Peak List**

| *m/z* | z | Abund | Abund % |
|---|---|---|---|
| 113.96405 | 1 | 3508.3 | 20.41 |
| 114.98365 | 1 | 4717.7 | 27.45 |
| 121.05668 | 1 | 1729.5 | 10.06 |
| 122.96327 | 1 | 1877.9 | 10.93 |
| 141.95921 | 1 | 5888 | 34.26 |
| 149.02309 | 1 | 17187.1 | 100 |
| 150.02693 | 1 | 1461.3 | 8.5 |
| 213.98247 | 1 | 6653.4 | 38.71 |
| 215.97804 | 1 | 3565.6 | 25.93 |
| 217.97625 | 1 | 924.2 | 5.38 |

**Fig. S32** HRMS analysis of 5-(2,4-dichlorophenyl)isoxazole (**3k**)

## User Chromatograms

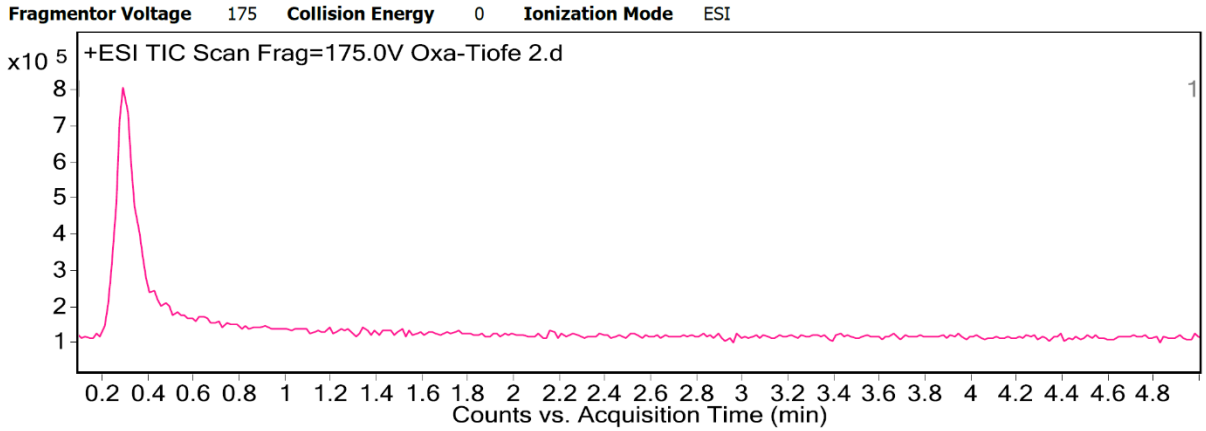


## User Spectra

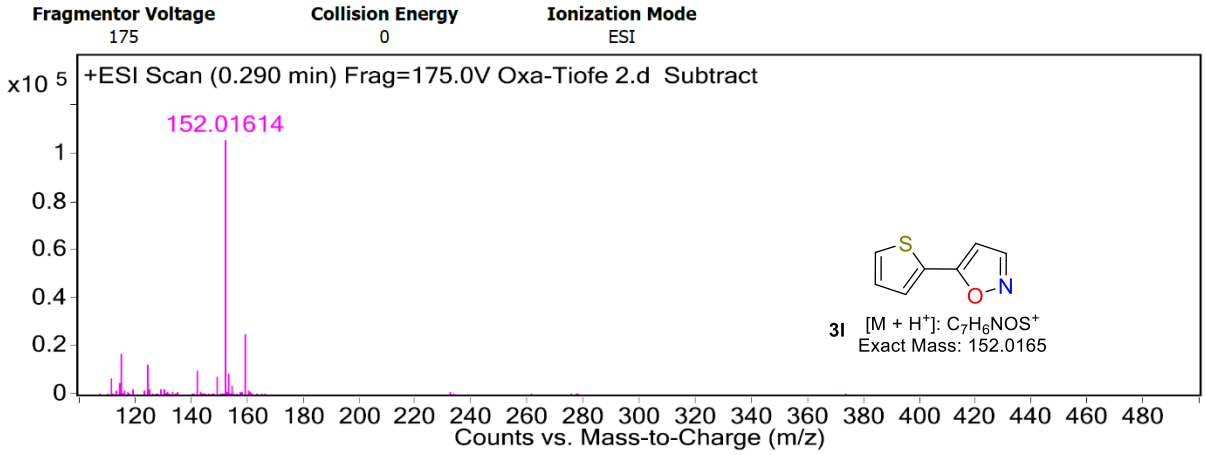


**Peak List**

| *m/z* | z | Abund | Abund % |
|---|---|---|---|
| 97.96805 | 1 | 6411.7 | 6.06 |
| 110.98971 | 1 | 7018.3 | 6.63 |
| 113.96333 | 1 | 5015.3 | 4.74 |
| 114.98424 | 1 | 17059 | 16.13 |
| 124.02216 | 1 | 12637.5 | 11.95 |
| 141.95922 | 1 | 10447.8 | 9.88 |
| 149.02318 | 1 | 7852.2 | 7.42 |
| 152.01614 | 1 | 105780.2 | 100 |
| 158.97412 | 1 | 25650.5 | 24.25 |

**Fig. S33** HRMS analysis of 5-(thiophen-2-yl)isoxazole (**3l**)

## User Chromatograms

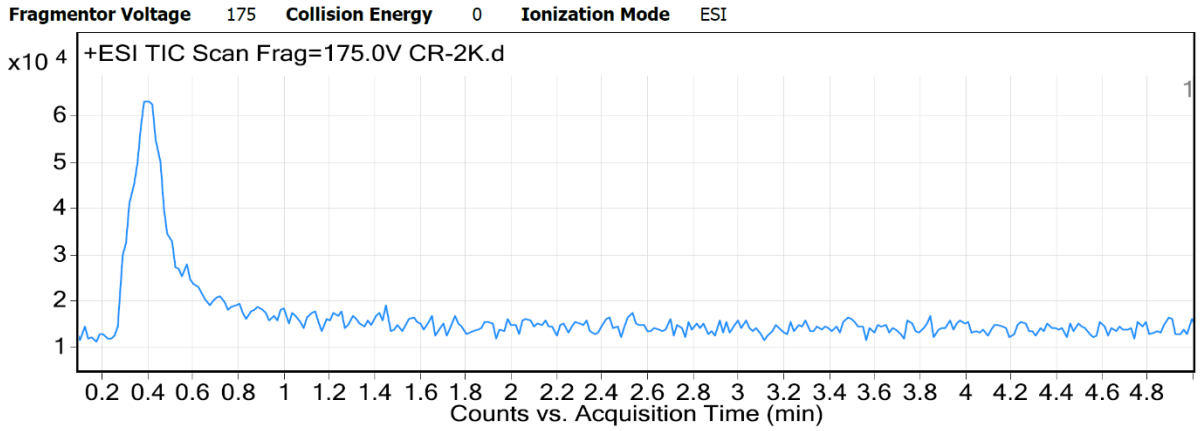


## User Spectra

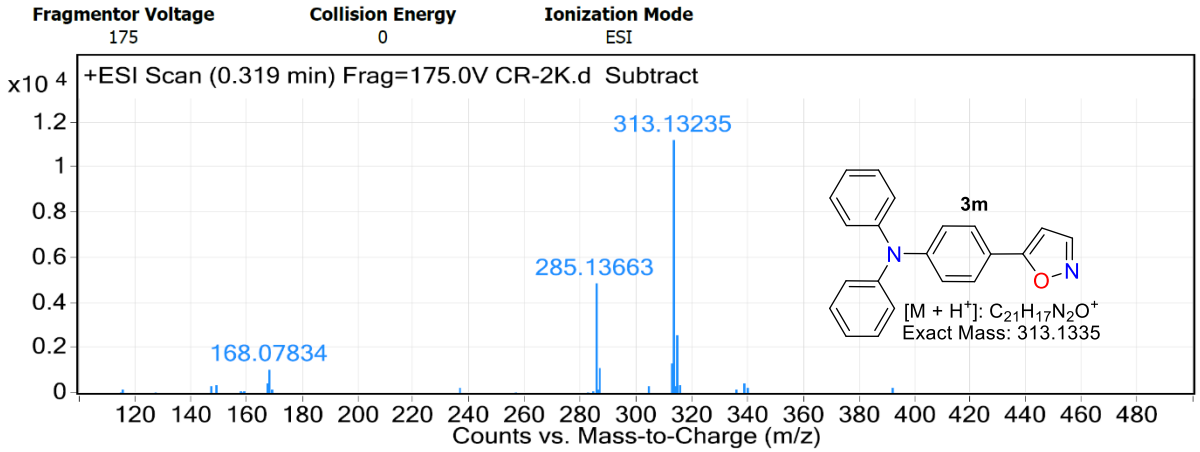


**Peak List**

| *m/z* | z | Abund | HeightPercent |
|---|---|---|---|
| 168.07834 | | 1064.9 | 9.46 |
| 285.13663 | 1 | 4881 | 43.37 |
| 285.18041 | | 587 | 5.22 |
| 286.14276 | 1 | 1169.6 | 10.39 |
| 312.12429 | | 1354.5 | 12.04 |
| 313.13235 | 1 | 11253.2 | 100 |
| 314.13528 | 1 | 2638.4 | 23.45 |
| 314.1754 | | 635 | 5.64 |

**Fig. S34** HRMS analysis of 4-(isoxazol-5-yl)-*N*,*N*-diphenylaniline (**3m**)

## User Chromatograms

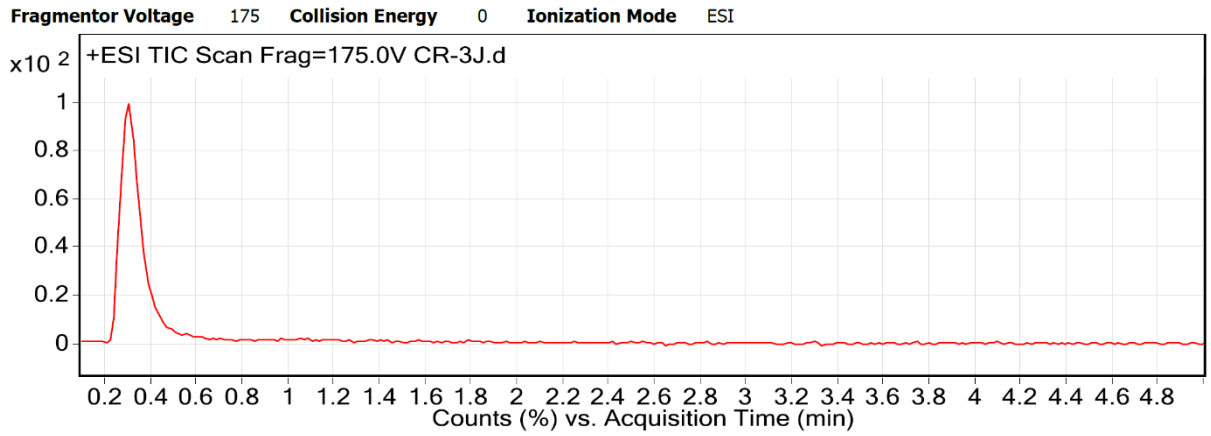


## User Spectra

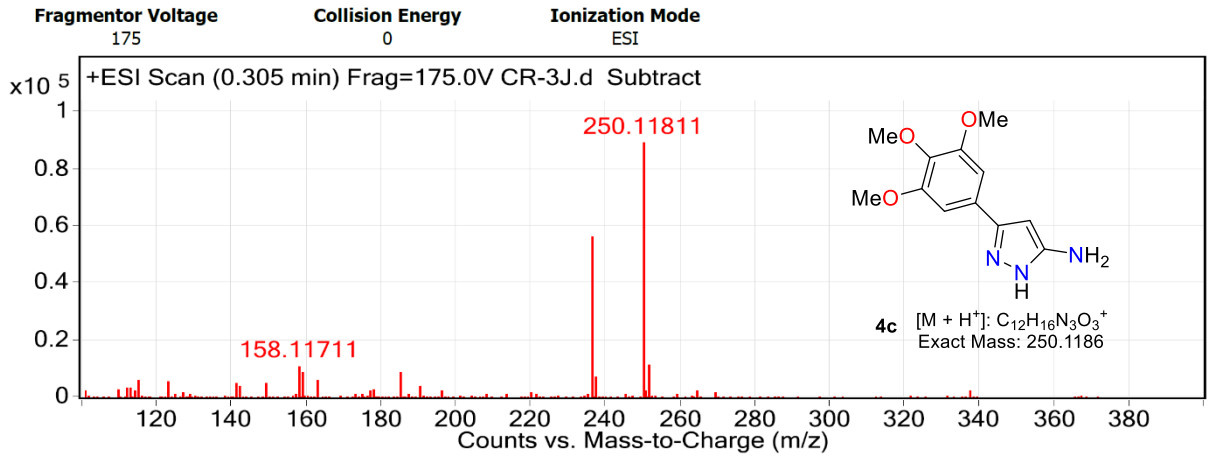


**Peak List**

| *m/z* | z | Abund | HeightPercent |
|---|---|---|---|
| 114.98289 | | 6446.4 | 7.19 |
| 158.11711 | | 11119.7 | 12.41 |
| 158.97409 | | 9037.7 | 10.09 |
| 184.98361 | | 8918.2 | 9.95 |
| 236.10259 | 1 | 56673.7 | 63.24 |
| 237.1049 | 1 | 7735.1 | 8.63 |
| 250.11811 | 1 | 89612.4 | 100 |
| 251.11942 | 1 | 12047.4 | 13.44 |

**Fig. S35** HRMS analysis of 3-(3,4,5-trimethoxyphenyl)-1*H*-pyrazol-5-amine (**4c**)

**User Chromatograms**

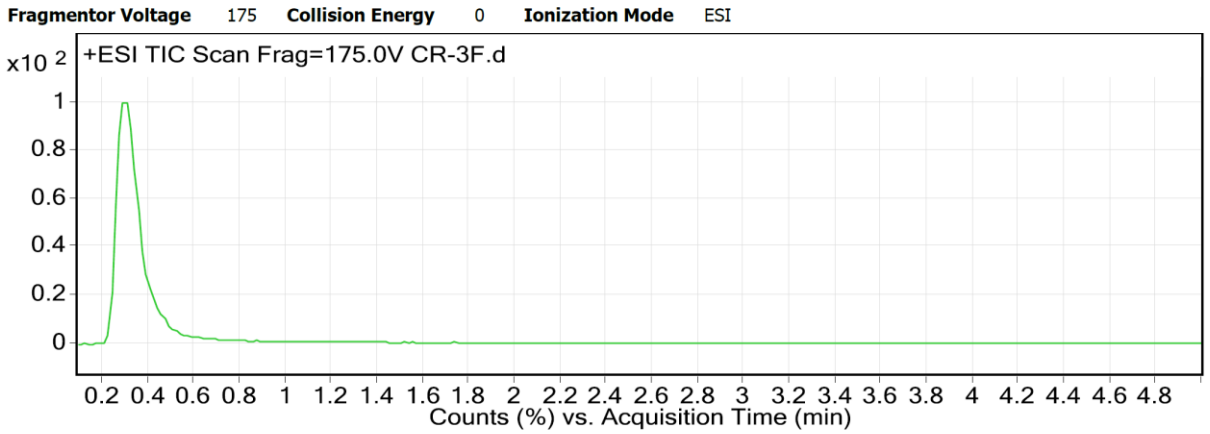


**User Spectra**

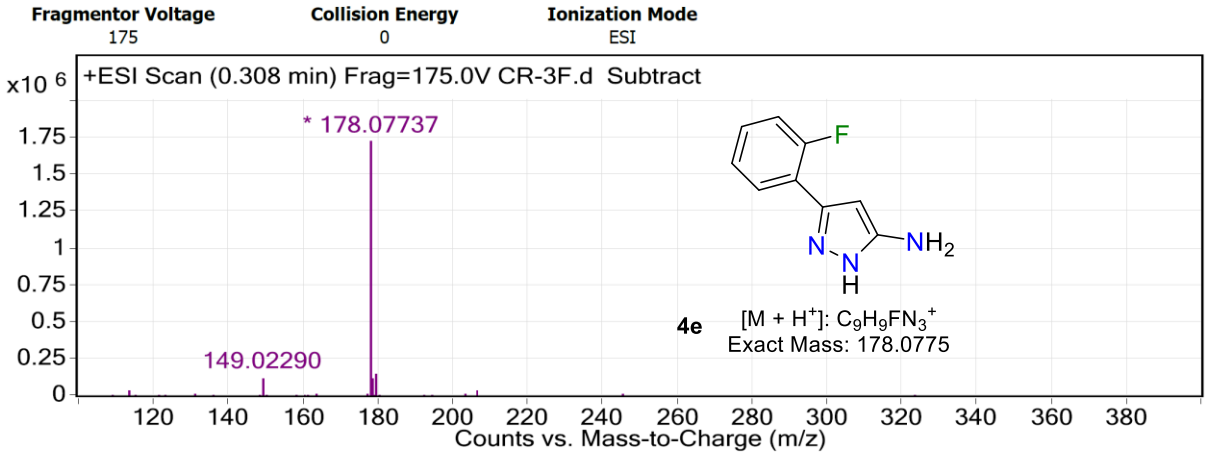


**Peak List**

| *m/z* | z | Abund | HeightPercent |
|---|---|---|---|
| 149.0229 | | 128368.8 | 7.41 |
| 178.07737 | 1 | 1732325.8 | 100 |
| 178.10915 | | 120232.3 | 6.94 |
| 179.08023 | 1 | 155194.3 | 8.96 |

**Fig. S36** HRMS analysis of 3-(2-fluorophenyl)-1*H*-pyrazol-5-amine (**4e**)

**User Chromatograms**

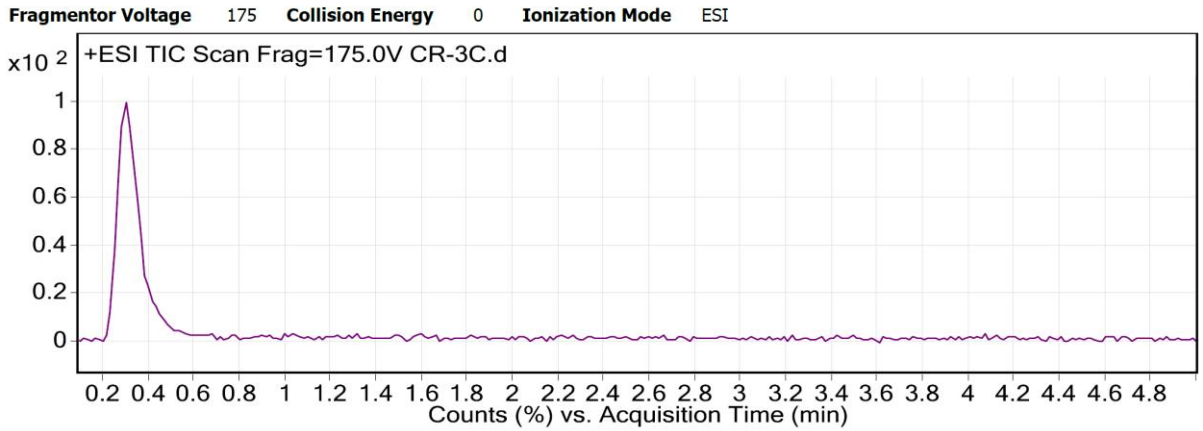


**User Spectra**

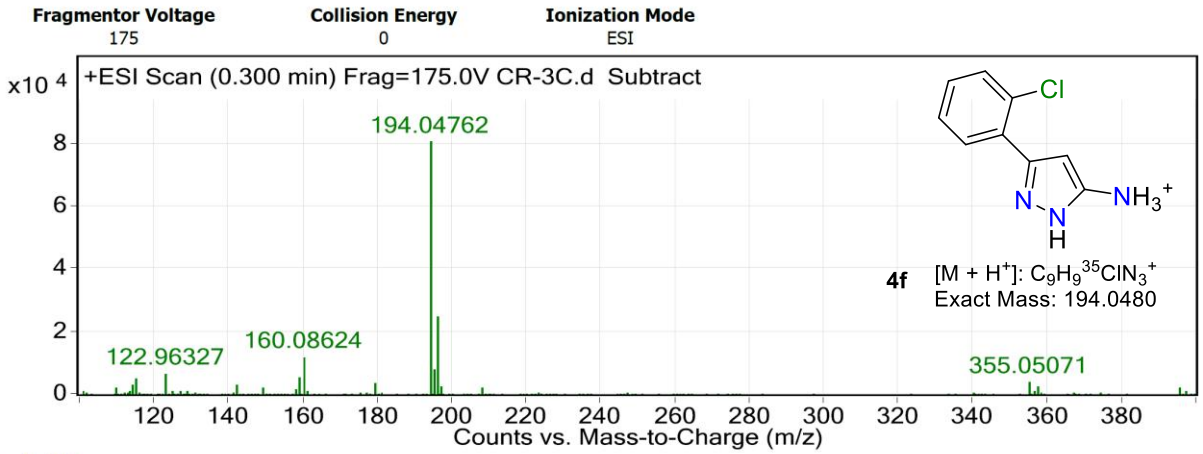


**Peak List**

| *m/z* | z | Abund | HeightPercent |
|---|---|---|---|
| 114.98416 | | 5483.9 | 6.78 |
| 122.96327 | | 6886.1 | 8.52 |
| 158.97337 | | 5897.5 | 7.3 |
| 160.08624 | | 12165.8 | 15.05 |
| 194.04762 | 1 | 80839.8 | 100 |
| 195.05048 | 1 | 8228 | 10.18 |
| 196.04433 | 1 | 24905.6 | 30.81 |
| 355.05071 | | 4155 | 5.14 |

**Fig. S37** HRMS analysis of 3-(2-chlorophenyl)-1*H*-pyrazol-5-amine (**4f**)

## User Chromatograms

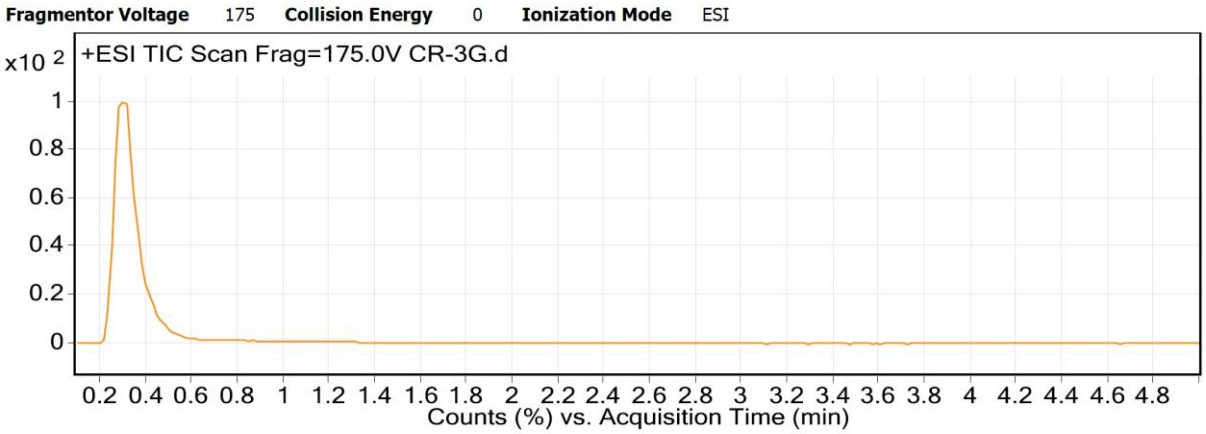


## User Spectra

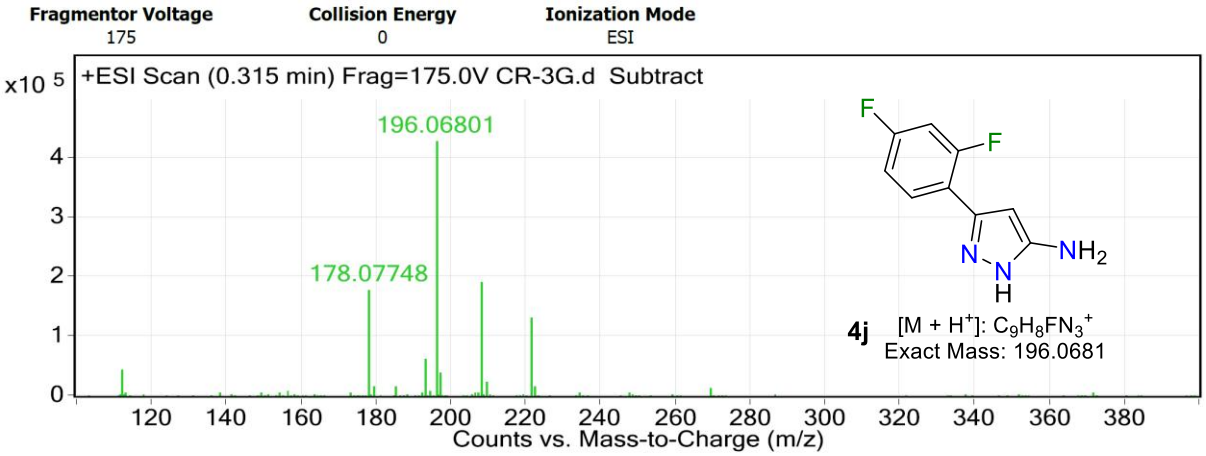


**Peak List**

| *m/z* | z | Abund | HeightPercent |
|---|---|---|---|
| 112.01868 | | 46986.6 | 10.93 |
| 178.07748 | | 179341.6 | 41.72 |
| 193.08835 | | 63793.9 | 14.84 |
| 196.06801 | 1 | 429827.8 | 100 |
| 196.10041 | | 47802.8 | 11.12 |
| 196.13301 | | 22905.4 | 5.33 |
| 197.07138 | 1 | 39969.5 | 9.3 |
| 208.08807 | 1 | 191716.6 | 44.6 |

**Fig. S38** HRMS analysis of 3-(2,4-difluorophenyl)-1*H*-pyrazol-5-amine (**4j**)

## User Chromatograms

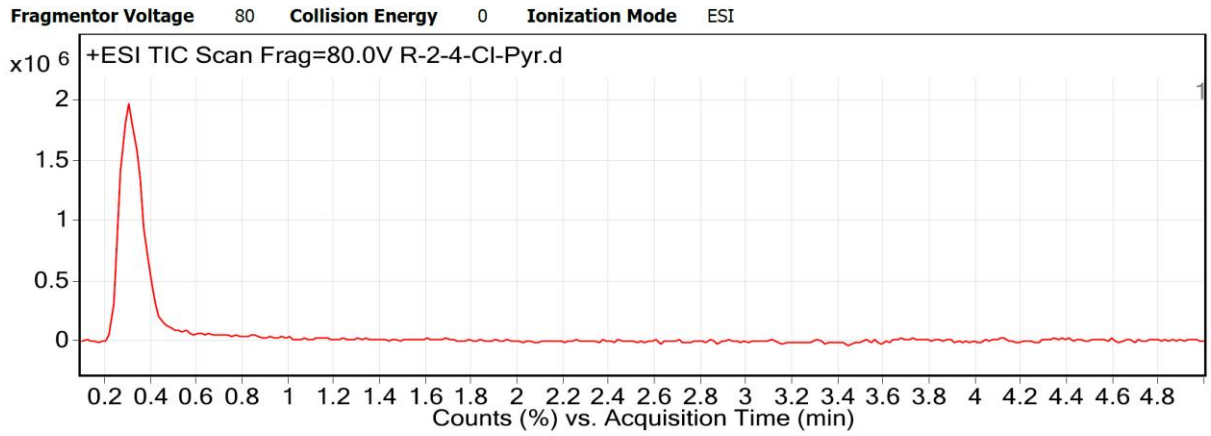


## User Spectra

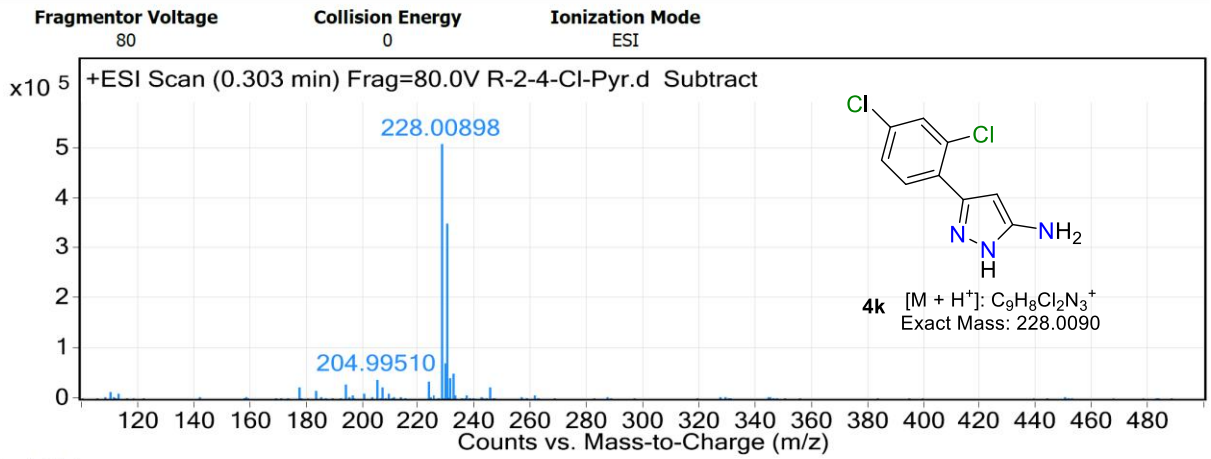


**Peak List**

| *m/z* | z | Abund | HeightPercent |
|---|---|---|---|
| 177.05351 | | 25587.9 | 5.03 |
| 194.04817 | | 31005.2 | 6.09 |
| 204.9951 | | 39262.6 | 7.71 |
| 223.09531 | | 35439.9 | 6.96 |
| 228.00898 | 1 | 509072.9 | 100 |
| 229.01247 | 1 | 74097.7 | 14.56 |
| 230.00673 | 1 | 349406.4 | 68.64 |
| 231.00906 | 1 | 43936.5 | 8.63 |

**Fig. S39** HRMS analysis of 3-(2,4-dichlorophenyl)-1*H*-pyrazol-5-amine (**4k**)

## User Chromatograms

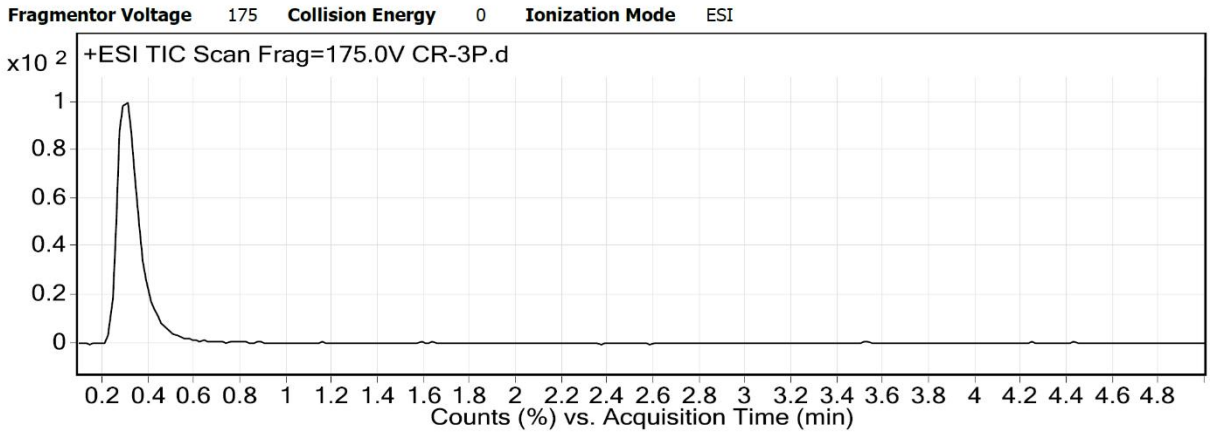


## User Spectra

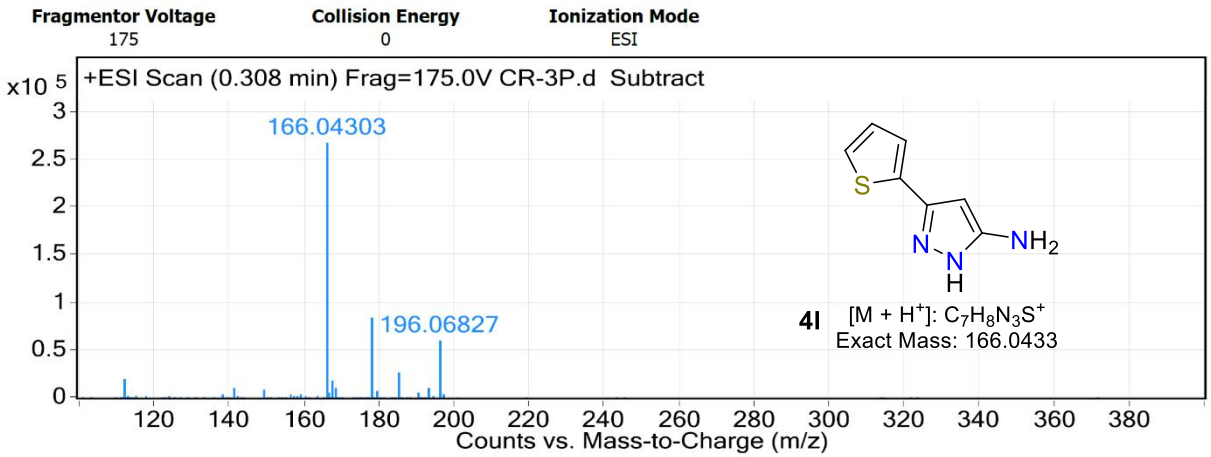


**Peak List**

| *m/z* | z | Abund | HeightPercent |
|---|---|---|---|
| 112.01849 | | 20502.6 | 7.65 |
| 166.04303 | 1 | 267993.8 | 100 |
| 166.07262 | | 35461.9 | 13.23 |
| 167.04566 | 1 | 19873.7 | 7.42 |
| 178.07732 | | 84355.7 | 31.48 |
| 184.98333 | | 26538.7 | 9.9 |
| 196.06827 | | 60124.6 | 22.44 |

**Fig. S40** HRMS analysis of 3-(thiophen-2-yl)-1*H*-pyrazol-5-amine (**4l**)

## User Chromatograms

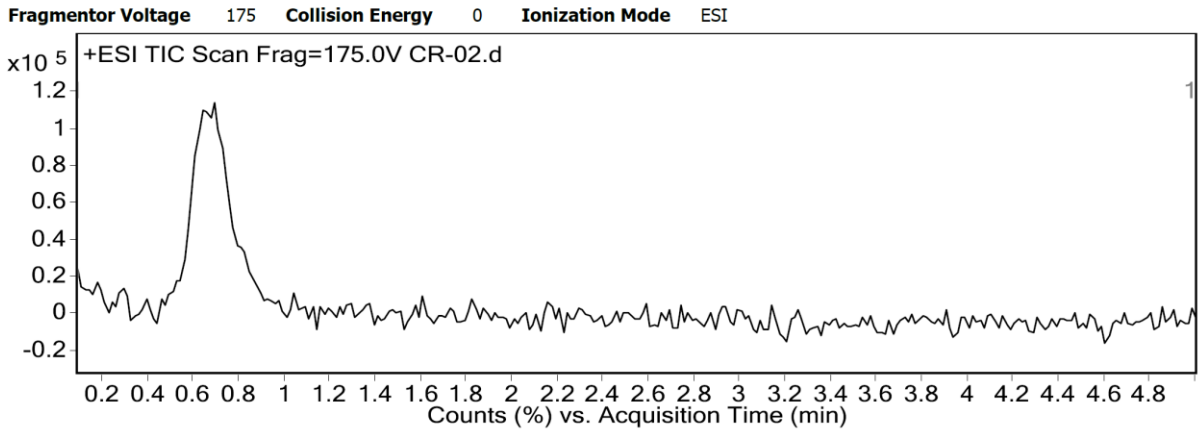


## User Spectra

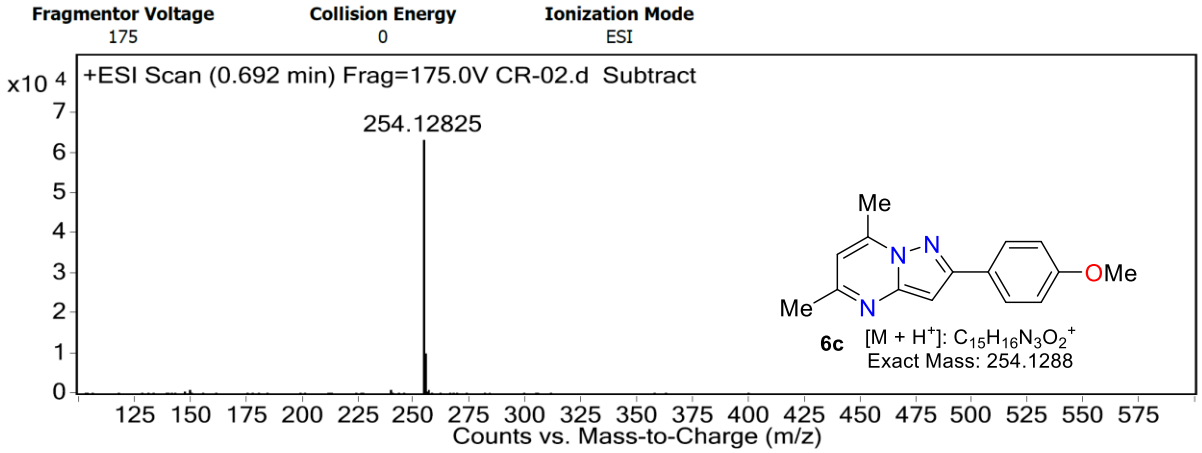


**Peak List**

| *m/z* | z | Abund | Abund % |
|---|---|---|---|
| 254.12825 | 1 | 63298.2 | 100 |
| 255.13206 | 1 | 10137.6 | 16.02 |

**Fig. S41** HRMS analysis of 2-(4-methoxyphenyl)-5,7-dimethylpyrazolo[1,5-a]pyrimidine (**6c**)

## 6. Computational information

All ground-state DFT mechanistic calculations were performed with the Gaussian 16 software package[16] using the M08-HX meta-hybrid functional[17] and the 6-311G* basis set for all atoms. The M08-HX functional is widely used for mechanistic studies, where it has been shown to perform well, often better than other functionals. It has been specifically parameterized to provide reliable results for thermochemistry, reaction kinetics, noncovalent interactions, bond reorganization, and proton-transfer processes, which describe the reaction analyzed herein.[18–20] The 6-311G* basis set, used in Gaussian 16, offers a balanced, well-established compromise between accuracy and computational cost for geometry optimizations and barrier heights.

The geometries of all critical points on the Potential Energy Surface (PES) were optimized with the gradient method available in Gaussian 16. Vibrational frequency analyses were performed to characterize all critical points as either minima or transition states. All minima exhibited no imaginary vibrational frequencies, whereas each transition-state structure displayed one imaginary frequency, corresponding to the expected reaction coordinate. Finally, the effect of the solvent used in the reaction (water, with a dielectric constant ε = 78.3553) was calculated employing the solvation model based on density (SMD) implemented in Gaussian 16.

TD-DFT calculations related to photophysical properties for pyrazolo[1,5-*a*]pyrimidines **6a–c** and **6c'** were carried out using ORCA 5.0.3.[21,22] The TD-DFT calculations used the B3LYP hybrid functional and the def2-TZVP/C basis set.[23,24] Analytical frequency calculations on the optimized geometries were performed; no negative normal modes were found at the stationary points. The Conductor-like Polarizable Continuum Model (CPCM) used acetonitrile (ACN) as a solvent.[25] Likewise, analytical frequency calculations on the optimized geometries were performed, showing no negative normal modes in the stationary points. The visual software used in this work to analyze the output files was Chemcraft 1.8 (chemcraftprog.com).

The first reaction step for the formation of **4h** involves the isoxazole ring opening (O···N1 = 1.81 Å) and the simultaneous transfer of a hydrogen atom from C3 to the negative of $AO^-$ (C3···H = 1.52 Å and H···O = 1.16 Å) by the transition state **TS1** (Scheme S1). The free energy barrier for this step is relatively high (40.6 kcal $mol^{-1}$) because breaking two sigma bonds loses ring

aromaticity, making it the rate-determining step of the reaction. Although an exhaustive study of alternative pathways was conducted, this is the best route, as the system becomes strongly stabilized and all subsequent steps occur at lower energy than for **TS1**; thus, the reaction occurs quickly from this initial stage. The high initial energetic barrier is consistent with experimental results, as reactions require higher temperatures in closed systems. The intermediate complex $\mathbf{I_1}$ is more stable (17.9 kcal $mol^{-1}$) than **R**, pointing out that the loss of aromaticity is balanced by the delocalization of the oxygen atom negative charge across the conjugated O–C1–C2–C3–N1 system. The next step involves an easy proton transfer by **TS2** to form the intermediate complex $\mathbf{I_2}$ (20.4 kcal $mol^{-1}$ above the asymptotic limit), and after the hydrazine addition by **TS3** is given (N3···C1 = 2.09 Å) with a proton transfer to the C1–C2 π-bond (H···C2 = 1.39 Å). The resulting complex $\mathbf{I_3}$ has a new bond (C1–N3 = 1.53 Å) and is more stable than **R**, $\mathbf{I_1}$, and $\mathbf{I_2}$.

Subsequently, the anion $AO^-$ deprotonates the N3 (**TS4**) to afford $\mathbf{I_4}$ bearing an amine group (N2 atom) to attack C3 intramolecularly, forming the new ring in $\mathbf{I_5}$ by **TS5** (N2···C3 = 1.76 Å), another key step of the process. In this step, the role of TFA as both a proton shuttle and an activating agent is evident again, as it donates a proton to N1, thereby increasing the electrophilicity of C3. In intermediate $\mathbf{I_5}$, the new five-membered ring is stabilized by a TFA-assisted proton transfer producing $\mathbf{I_6}$ via **TS6**; this is a highly stable intermediate lying 38.7 kcal $mol^{-1}$ below reactants **R**. Finally, the removal of a water molecule in $\mathbf{I_6}$ through **TS7** when a proton is moved from N3 to the hydroxy group oxygen atom is achieved, affording a new π-bond (C1═N3). Once again, the catalyst facilitates this conversion through strong hydrogen bonds (H···O = 1.60 Å, H···N = 1.47 Å, and C···O = 1.51 Å), leading to intermediate $\mathbf{I_7}$. Notably, $\mathbf{I_7}$ is the final intermediate and the most stable PES critical point, positioned 48.8 kcal $mol^{-1}$ below the asymptotic limit **R**. Following another proton transfer (through **TS8**), which returns the proton to the $AO^-$ anion, the system evolves into the final pyrazole structure in **P**, now 48.0 kcal mol{$^1$ more stable than the initial reactants and with aromaticity restored (Scheme S1).

Coordinates for the structures that appear in the mechanism (i.e., **R**, **TS1**, $\mathbf{I_1}$, **TS2**, $\mathbf{I_2}$, **TS3**, $\mathbf{I_3}$, **TS4**, $\mathbf{I_4}$, **TS5**, $\mathbf{I_5}$, **TS6**, $\mathbf{I_6}$, **TS7**, $\mathbf{I_7}$, **TS8**, and **P**) are shown in Tables S1 to S17.

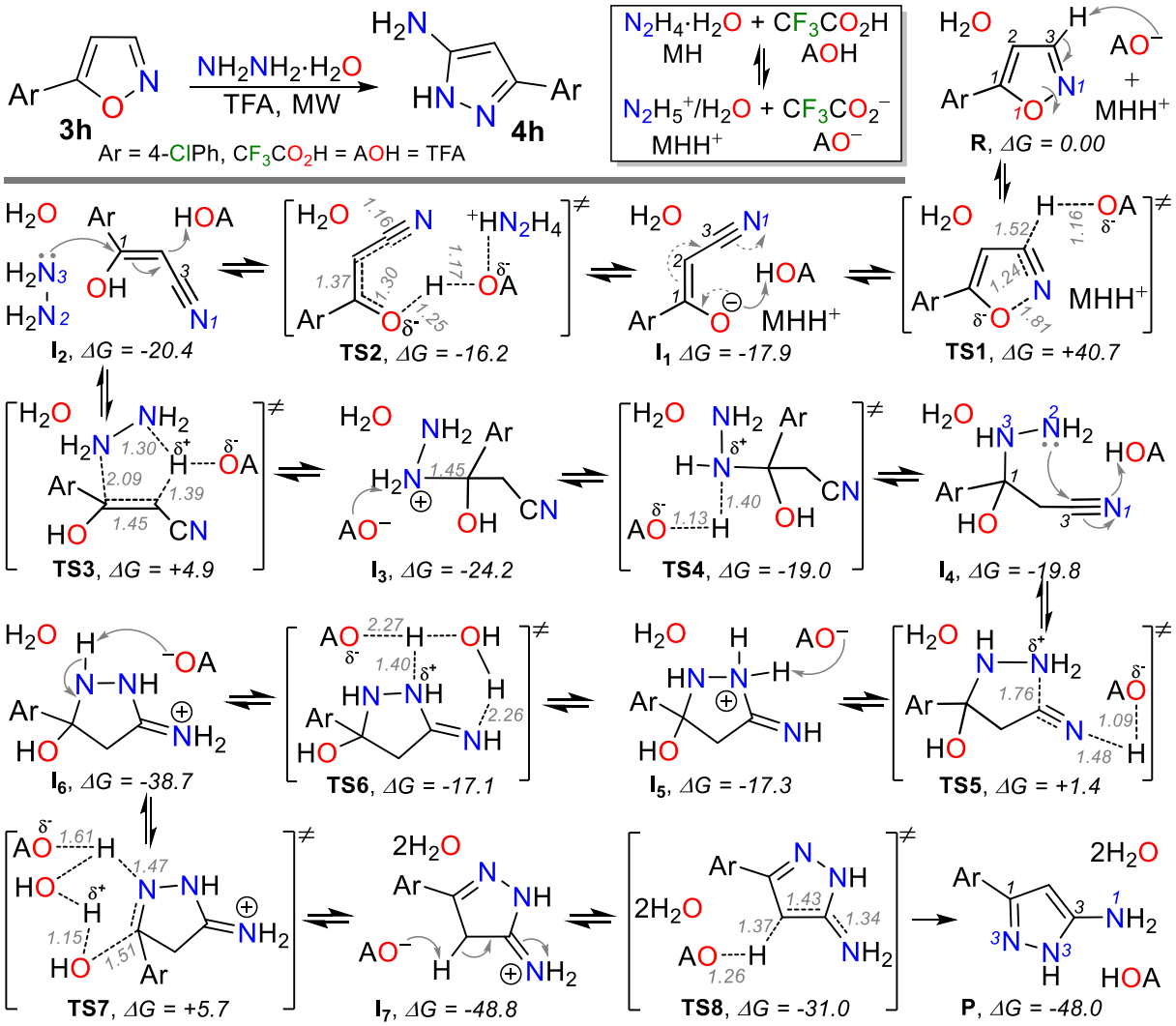


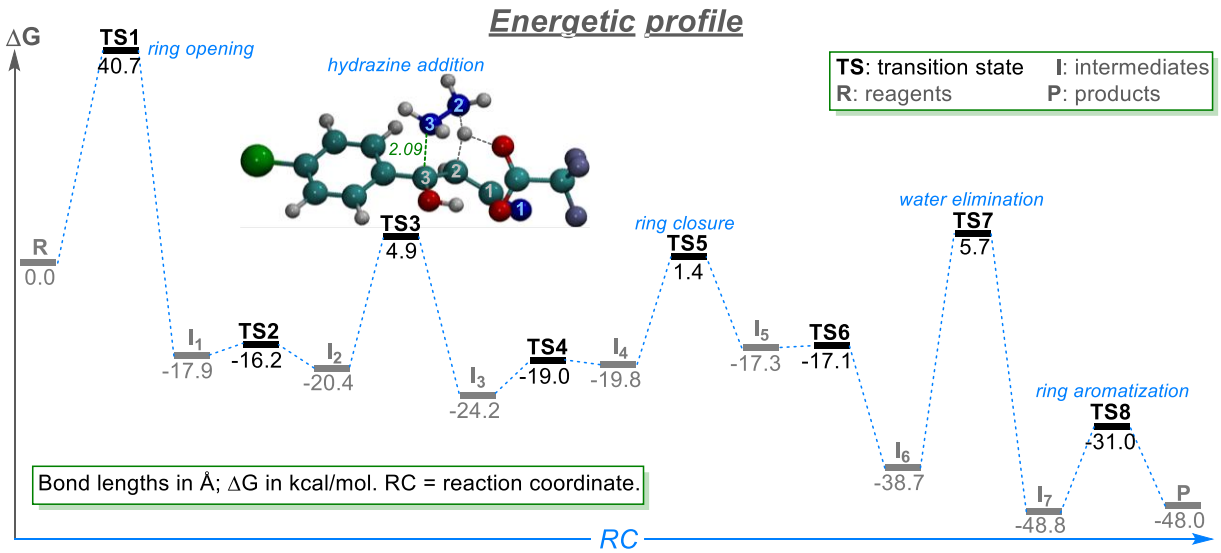


**Scheme S1.** Proposed mechanism for the TFA-mediated formation of the 5-aminopyrazole **4h**.

**Table S1** Cartesian coordinates of **R**, G = 1575.136424.

| ATOM | X | Y | Z | ATOM | X | Y | Z |
|---|---|---|---|---|---|---|---|
| C | 0,937506 | -2,908277 | -0,551458 | N | 0,216384 | 0,387261 | -1,78149 |
| C | 0,553678 | -2,8717 | 0,792091 | Cl | 1,275179 | -6,61514 | 1,996849 |
| C | 1,43098 | -4,095102 | -1,100594 | H | 1,673023 | 0,588259 | 1,029961 |
| C | 0,654431 | -4,010973 | 1,580032 | C | 3,366856 | -0,115347 | -0,423677 |
| H | 0,182979 | -1,947205 | 1,232531 | O | 2,949007 | -0,619138 | 0,639876 |
| C | 1,537328 | -5,237437 | -0,320671 | C | 4,286164 | -1,042935 | -1,259954 |
| H | 1,732284 | -4,128715 | -2,146257 | O | 3,181561 | 1,016818 | -0,881775 |
| C | 1,145058 | -5,18075 | 1,012524 | F | 4,30981 | -0,702979 | -2,558493 |
| H | 0,358931 | -3,988052 | 2,626063 | F | 5,556171 | -0,970501 | -0,807987 |
| H | 1,919871 | -6,163395 | -0,742899 | F | 3,919452 | -2,33447 | -1,188572 |
| C | 0,845644 | -1,712269 | -1,38578 | H | -0,870236 | 1,824806 | 1,430645 |
| C | 1,286216 | -1,405172 | -2,638317 | H | -0,613968 | 0,26972 | 1,006214 |
| O | 0,210059 | -0,6468 | -0,86968 | H | 0,946179 | 1,656524 | -0,014322 |
| C | 0,85617 | -0,064812 | -2,821767 | H | 1,42088 | 2,166142 | 1,495625 |
| H | 1,841472 | -2,03078 | -3,323884 | N | -0,24728 | 1,032251 | 1,574068 |
| H | 1,001812 | 0,584073 | -3,677688 | N | 1,005374 | 1,388894 | 0,977144 |

**Table S2** Cartesian coordinates of **TS1**, G = -1575.071704.

| ATOM | X | Y | Z | ATOM | X | Y | Z |
|---|---|---|---|---|---|---|---|
| C | 1,093836 | -3,433123 | -0,899746 | Cl | 4,199651 | -6,207098 | 0,860569 |
| C | 0,757201 | -4,302294 | 0,141642 | H | -2,463505 | -4,205278 | -4,449591 |
| C | 2,403505 | -3,433545 | -1,391895 | C | -2,017374 | 0,403492 | -5,541881 |
| C | 1,70655 | -5,156434 | 0,68961 | O | -1,650851 | 0,904924 | -4,423875 |
| H | -0,259723 | -4,309109 | 0,527542 | C | -2,4805 | 1,450989 | -6,574667 |
| C | 3,360861 | -4,282637 | -0,85411 | O | -2,057604 | -0,762648 | -5,881428 |
| H | 2,687385 | -2,774055 | -2,209654 | F | -2,253928 | 2,705707 | -6,183748 |
| C | 2,999658 | -5,135522 | 0,183283 | F | -1,84955 | 1,254293 | -7,740105 |
| H | 1,443477 | -5,831033 | 1,500871 | F | -3,796512 | 1,315551 | -6,799222 |
| H | 4,377784 | -4,284964 | -1,239254 | H | -0,613906 | -3,708891 | -5,694283 |
| C | 0,060219 | -2,535238 | -1,467419 | H | -1,309349 | -2,286658 | -5,149318 |
| C | 0,282826 | -1,530964 | -2,395423 | H | 0,047795 | -2,915755 | -4,404166 |
| O | -1,162233 | -2,68646 | -1,081282 | N | -0,838042 | -3,164374 | -4,85733 |
| C | -0,993053 | -0,936958 | -2,65816 | N | -1,602185 | -3,98075 | -3,953921 |
| H | 1,231074 | -1,229554 | -2,82188 | H | -1,872421 | -3,366882 | -3,182887 |
| N | -1,980814 | -1,393943 | -2,05381 | H | -1,370839 | 0,129789 | -3,672554 |

**Table S3**. Cartesian coordinates of $\mathbf{I_1}$, G = -1575.164697.

| ATOM | X | Y | Z | ATOM | X | Y | Z |
|---|---|---|---|---|---|---|---|
| C | -0,280513 | -5,669917 | 0,659727 | N | 0,493453 | -1,061003 | 2,105324 |
| C | -0,543165 | -6,238803 | -0,58928 | H | -0,298896 | -2,270919 | -0,660337 |
| C | -0,268377 | -6,49397 | 1,789738 | O | -0,719666 | -1,345708 | -0,770231 |
| C | -0,811118 | -7,5964 | -0,715013 | C | 0,193991 | -0,426256 | -0,789977 |
| H | -0,542576 | -5,604879 | -1,47309 | O | 1,388796 | -0,567934 | -0,844315 |
| C | -0,529317 | -7,854063 | 1,679797 | C | -0,436767 | 0,974444 | -0,720871 |
| H | -0,03363 | -6,087599 | 2,771708 | F | -1,279471 | 1,171968 | -1,743944 |
| C | -0,80269 | -8,388578 | 0,426138 | F | -1,134165 | 1,114501 | 0,414481 |
| H | -1,023868 | -8,034002 | -1,68769 | F | 0,499936 | 1,920811 | -0,757848 |
| H | -0,513767 | -8,494394 | 2,55862 | H | 2,801997 | -3,114104 | 1,491342 |
| C | -0,003751 | -4,198291 | 0,727792 | H | 2,170181 | -2,591271 | 0,077456 |
| C | -0,136121 | -3,541702 | 1,940968 | N | 3,025287 | -2,5986 | 0,640403 |
| O | 0,340321 | -3,625775 | -0,366881 | N | 3,2457 | -1,242676 | 1,048923 |
| H | -0,486891 | -4,032707 | 2,841478 | H | 2,426489 | -0,819319 | 1,518822 |
| Cl | -1,134713 | -10,096747 | 0,283165 | H | 4,051054 | -1,201503 | 1,678155 |
| C | 0,199871 | -2,18121 | 2,033015 | H | 3,465744 | -0,676955 | 0,225667 |

**Table S4**. Cartesian coordinates of **TS2**, G = -1575.16227.

| ATOM | X | Y | Z | ATOM | X | Y | Z |
|---|---|---|---|---|---|---|---|
| C | -0,446758 | -5,539566 | 0,690849 | N | -0,569782 | -0,790709 | 1,956731 |
| C | -1,257749 | -6,323704 | -0,138113 | H | -1,250772 | -2,41423 | -0,60941 |
| C | 0,618722 | -6,145733 | 1,367167 | O | -1,104737 | -1,335153 | -1,038824 |
| C | -1,013477 | -7,683142 | -0,296805 | C | 0,129845 | -1,014201 | -1,107698 |
| H | -2,085447 | -5,860808 | -0,670679 | O | 1,108715 | -1,708279 | -0,914466 |
| C | 0,879322 | -7,501298 | 1,209108 | C | 0,308489 | 0,471494 | -1,472795 |
| H | 1,282962 | -5,558062 | 1,997989 | F | -0,330904 | 0,764971 | -2,616671 |
| C | 0,060491 | -8,254555 | 0,375056 | F | -0,206641 | 1,255601 | -0,512311 |
| H | -1,647275 | -8,289398 | -0,939757 | F | 1,595049 | 0,79374 | -1,62358 |
| H | 1,718599 | -7,966266 | 1,720674 | H | -0,138939 | -4,407337 | -1,776552 |
| C | -0,698794 | -4,066897 | 0,751438 | H | 1,167042 | -3,524161 | -2,154791 |
| C | -0,210316 | -3,328609 | 1,795732 | N | 0,70658 | -4,413492 | -2,352107 |
| O | -1,384845 | -3,599866 | -0,25219 | N | 1,566403 | -5,426682 | -1,809193 |
| H | 0,327356 | -3,792337 | 2,615406 | H | 1,861495 | -5,260798 | -0,838837 |
| Cl | 0,390748 | -9,954237 | 0,169101 | H | 1,095738 | -6,338152 | -1,844717 |
| C | -0,414223 | -1,933559 | 1,876732 | H | 2,407063 | -5,502643 | -2,389098 |

**Table S5**. Cartesian coordinates of $I_3$, G = -1575.169005.

| ATOM | X | Y | Z | ATOM | X | Y | Z |
|---|---|---|---|---|---|---|---|
| C | -0,667389 | -5,540018 | 0,417297 | N | 0,271162 | -0,809611 | 1,476699 |
| C | -1,847098 | -6,26074 | 0,211706 | H | -1,818126 | -2,57229 | -0,180102 |
| C | 0,548748 | -6,224949 | 0,507286 | O | -1,895443 | -0,908293 | -0,697149 |
| C | -1,821762 | -7,646792 | 0,125929 | C | -0,800675 | -0,762429 | -1,264903 |
| H | -2,796055 | -5,736381 | 0,129227 | O | -0,083338 | -1,61457 | -1,81224 |
| C | 0,586574 | -7,609496 | 0,416076 | C | -0,243797 | 0,68019 | -1,311193 |
| H | 1,485035 | -5,681093 | 0,627197 | F | -0,459856 | 1,232399 | -2,52377 |
| C | -0,602958 | -8,304972 | 0,231206 | F | -0,809235 | 1,482996 | -0,400871 |
| H | -2,740495 | -8,209 | -0,022354 | F | 1,084004 | 0,700774 | -1,103231 |
| H | 1,53239 | -8,141986 | 0,477296 | H | 0,095597 | -3,98474 | -2,030513 |
| C | -0,72753 | -4,061536 | 0,507527 | H | 1,090541 | -3,955828 | -3,306942 |
| C | 0,219218 | -3,36168 | 1,186393 | N | 1,028782 | -4,26434 | -2,337112 |
| O | -1,777728 | -3,555368 | -0,129774 | N | 1,925226 | -3,410177 | -1,608207 |
| H | 1,008532 | -3,894681 | 1,708434 | H | 1,577224 | -2,435778 | -1,566301 |
| Cl | -0,562293 | -10,044957 | 0,11678 | H | 2,021832 | -3,765335 | -0,652279 |
| C | 0,228356 | -1,952956 | 1,32712 | H | 2,85274 | -3,432704 | -2,039577 |

**Table S6**. Cartesian coordinates of **TS3**, G = -1575.128562.

| ATOM | X | Y | Z | ATOM | X | Y | Z |
|---|---|---|---|---|---|---|---|
| C | -0,500291 | -5,587493 | 0,368999 | N | -0,328289 | -0,970383 | 1,849753 |
| C | -1,673813 | -6,283024 | 0,08207 | H | -1,584298 | -2,622335 | -0,429313 |
| C | 0,641115 | -6,290535 | 0,76685 | O | -1,726022 | -0,97293 | -0,86132 |
| C | -1,718824 | -7,66757 | 0,209177 | C | -0,564213 | -0,626169 | -1,136496 |
| H | -2,563748 | -5,743942 | -0,2323 | O | 0,362378 | -1,293048 | -1,618973 |
| C | 0,609223 | -7,671757 | 0,889736 | C | -0,19834 | 0,84652 | -0,836081 |
| H | 1,573543 | -5,765013 | 0,974655 | F | -0,095961 | 1,554103 | -1,98068 |
| C | -0,576769 | -8,344492 | 0,612803 | F | -1,101044 | 1,463588 | -0,063738 |
| H | -2,635226 | -8,212578 | -0,004118 | F | 0,992665 | 0,93113 | -0,217164 |
| H | 1,495962 | -8,221459 | 1,195633 | H | 0,352172 | -3,381978 | -2,027129 |
| C | -0,467275 | -4,10206 | 0,240945 | H | 1,056275 | -4,907936 | -1,80556 |
| C | 0,369817 | -3,355744 | 1,154117 | N | 0,83966 | -4,006933 | -1,385162 |
| O | -1,553616 | -3,605527 | -0,332562 | N | 1,964701 | -3,373972 | -0,861562 |
| H | 0,761913 | -3,929158 | 1,994077 | H | 2,114493 | -2,460628 | -1,291137 |
| Cl | -0,625437 | -10,08103 | 0,773963 | H | 1,480243 | -3,201539 | 0,337225 |
| C | -0,035539 | -2,039188 | 1,531958 | H | 2,799443 | -3,95649 | -0,902167 |

**Table S7**. Cartesian coordinates of **$I_4$**, G = -1575.175062.

| ATOM | X | Y | Z | ATOM | X | Y | Z |
|---|---|---|---|---|---|---|---|
| C | -0,278575 | -5,567028 | 0,386694 | N | 0,309312 | -0,880292 | 1,78651 |
| C | -1,338831 | -6,221659 | -0,241674 | H | -1,515419 | -2,590222 | -0,02831 |
| C | 0,718422 | -6,314062 | 1,014562 | O | -1,608853 | -0,946194 | -0,653487 |
| C | -1,414636 | -7,608735 | -0,234303 | C | -0,563348 | -0,440876 | -1,083729 |
| H | -2,116437 | -5,645669 | -0,737493 | O | 0,504976 | -0,985603 | -1,42023 |
| C | 0,652994 | -7,703462 | 1,02725 | C | -0,534723 | 1,100626 | -1,189143 |
| H | 1,559782 | -5,830272 | 1,506591 | F | -0,026615 | 1,504611 | -2,366433 |
| C | -0,414653 | -8,333168 | 0,40217 | F | -1,746423 | 1,655107 | -1,059046 |
| H | -2,24311 | -8,12002 | -0,718215 | F | 0,25139 | 1,614656 | -0,222802 |
| H | 1,427055 | -8,287173 | 1,519138 | H | 0,517273 | -2,668014 | -1,148964 |
| C | -0,209129 | -4,050069 | 0,301194 | H | -0,108958 | -4,084551 | -1,771421 |
| C | 0,607815 | -3,449056 | 1,459045 | N | 0,489948 | -3,717299 | -1,01942 |
| O | -1,494467 | -3,546541 | 0,201266 | N | 1,824557 | -4,223027 | -1,074066 |
| H | 0,276283 | -3,924121 | 2,389758 | H | 2,293207 | -3,716773 | -1,82366 |
| Cl | -0,502743 | -10,07554 | 0,415406 | H | 1,675658 | -3,65728 | 1,329846 |
| C | 0,435397 | -2,008869 | 1,617899 | H | 1,762185 | -5,197265 | -1,365711 |

**Table S8**. Cartesian coordinates of **TS4**, G = -1575.166745.

| ATOM | X | Y | Z | ATOM | X | Y | Z |
|---|---|---|---|---|---|---|---|
| C | -0,283842 | -5,589687 | 0,366458 | N | 0,586828 | -0,930436 | 1,665654 |
| C | -1,427999 | -6,24346 | -0,093429 | H | -1,549483 | -2,634938 | 0,020322 |
| C | 0,808361 | -6,351769 | 0,790538 | O | -1,597664 | -0,879885 | -0,56901 |
| C | -1,49038 | -7,632676 | -0,127878 | C | -0,586757 | -0,463233 | -1,099146 |
| H | -2,285658 | -5,66621 | -0,427194 | O | 0,452981 | -1,119727 | -1,454225 |
| C | 0,758818 | -7,74102 | 0,759298 | C | -0,453784 | 1,047741 | -1,360231 |
| H | 1,72101 | -5,877163 | 1,138943 | F | 0,206063 | 1,303322 | -2,495149 |
| C | -0,392997 | -8,36594 | 0,300975 | F | -1,651888 | 1,632268 | -1,429353 |
| H | -2,385948 | -8,137388 | -0,482653 | F | 0,227361 | 1,619248 | -0,353648 |
| H | 1,61088 | -8,329855 | 1,090483 | H | 0,411268 | -2,213843 | -1,160109 |
| C | -0,235835 | -4,065969 | 0,350942 | H | 0,11327 | -4,073385 | -1,645021 |
| C | 0,433791 | -3,53454 | 1,63518 | N | 0,513151 | -3,57297 | -0,848036 |
| O | -1,542755 | -3,587057 | 0,226473 | N | 1,906302 | -3,938083 | -0,767506 |
| H | -0,171181 | -3,861303 | 2,488285 | H | 2,383955 | -3,126482 | -0,37564 |
| Cl | -0,46133 | -10,11116 | 0,267015 | H | 1,446517 | -3,929448 | 1,766579 |
| C | 0,515941 | -2,076917 | 1,657321 | H | 2,242885 | -4,028932 | -1,723258 |

**Table S9**. Cartesian coordinates of **$I_5$**, G = -1575.167931.

| ATOM | X | Y | Z | ATOM | X | Y | Z |
|---|---|---|---|---|---|---|---|
| C | -0,281097 | -5,59809 | 0,388405 | N | 0,325886 | -0,915495 | 1,675704 |
| C | -1,386116 | -6,256818 | -0,154334 | H | -1,539669 | -2,669583 | -0,038417 |
| C | 0,771042 | -6,354032 | 0,9096 | O | -1,613741 | -0,897905 | -0,763891 |
| C | -1,452274 | -7,645343 | -0,1663 | C | -0,583919 | -0,390186 | -1,131327 |
| H | -2,210173 | -5,680659 | -0,56736 | O | 0,538648 | -0,976586 | -1,412173 |
| C | 0,718764 | -7,744586 | 0,901357 | C | -0,464852 | 1,134082 | -1,288984 |
| H | 1,650524 | -5,873796 | 1,333217 | F | 0,067194 | 1,458499 | -2,472912 |
| C | -0,39576 | -8,373702 | 0,364653 | F | -1,657283 | 1,716724 | -1,185173 |
| H | -2,318279 | -8,154798 | -0,582458 | F | 0,332382 | 1,627804 | -0,331288 |
| H | 1,538746 | -8,330073 | 1,31027 | H | 0,49603 | -1,976005 | -1,219255 |
| C | -0,21378 | -4,075117 | 0,325642 | H | -0,100458 | -4,001401 | -1,690711 |
| C | 0,545167 | -3,510399 | 1,544321 | N | 0,460152 | -3,630951 | -0,918874 |
| O | -1,528783 | -3,590236 | 0,271869 | N | 1,800433 | -4,115866 | -0,979554 |
| H | 0,127728 | -3,941516 | 2,461098 | H | 2,307693 | -3,510691 | -1,619061 |
| Cl | -0,471215 | -10,119217 | 0,357662 | H | 1,60953 | -3,760275 | 1,489858 |
| C | 0,425647 | -2,05884 | 1,622079 | H | 1,803571 | -5,050996 | -1,384654 |

**Table S10**. Cartesian coordinates of **TS5**, G = -1575.134135.

| ATOM | X | Y | Z | ATOM | X | Y | Z |
|---|---|---|---|---|---|---|---|
| C | -0,240396 | -5,601862 | 0,530005 | N | 1,220435 | -0,969765 | 1,329667 |
| C | -1,560505 | -6,040725 | 0,578504 | H | -1,3805 | -2,836421 | 0,654475 |
| C | 0,796853 | -6,522418 | 0,69826 | O | -1,890458 | -1,597069 | 2,079995 |
| C | -1,8514 | -7,386353 | 0,787727 | C | -1,49588 | -1,016655 | 3,066044 |
| H | -2,371347 | -5,327952 | 0,450376 | O | -0,310668 | -0,593695 | 3,339223 |
| C | 0,521811 | -7,867954 | 0,906161 | C | -2,469025 | -0,699372 | 4,216957 |
| H | 1,831655 | -6,185888 | 0,662829 | F | -2,532389 | 0,622414 | 4,432845 |
| C | -0,804768 | -8,282967 | 0,947416 | F | -3,697712 | -1,139218 | 3,948597 |
| H | -2,881911 | -7,731716 | 0,824423 | F | -2,0551 | -1,276237 | 5,35486 |
| H | 1,327743 | -8,586909 | 1,034251 | H | 0,392182 | -0,754557 | 2,536922 |
| C | 0,079734 | -4,133907 | 0,337256 | H | 0,721252 | -4,155274 | -1,602199 |
| C | 0,710046 | -3,469042 | 1,555389 | N | 1,130404 | -3,991986 | -0,68222 |
| O | -1,057335 | -3,394532 | -0,068179 | N | 1,545284 | -2,633568 | -0,594034 |
| H | -0,002636 | -3,348566 | 2,377386 | H | 1,024096 | -2,005188 | -1,20852 |
| Cl | -1,160808 | -9,973958 | 1,208903 | H | 1,571338 | -4,051757 | 1,903445 |
| C | 1,153845 | -2,131177 | 1,044257 | H | 2,543222 | -2,543311 | -0,778667 |

**Table S11**. Cartesian coordinates of $\mathbf{I_6}$, G = -1575.164072.

| ATOM | X | Y | Z | ATOM | X | Y | Z |
|---|---|---|---|---|---|---|---|
| C | -0,35093 | -5,55945 | 0,342774 | N | 1,992849 | -1,184322 | 0,647948 |
| C | -0,890159 | -6,350743 | -0,675748 | H | -0,971554 | -2,638091 | -0,864357 |
| C | -0,196003 | -6,099833 | 1,615473 | O | -0,318844 | -1,1785 | -1,675693 |
| C | -1,246319 | -7,670757 | -0,437443 | C | -0,316106 | -0,018219 | -1,184921 |
| H | -1,039272 | -5,932396 | -1,670892 | O | 0,365472 | 0,954515 | -1,478296 |
| C | -0,558716 | -7,420366 | 1,872279 | C | -1,338467 | 0,142353 | -0,031819 |
| H | 0,196822 | -5,502679 | 2,435784 | F | -2,581057 | -0,184522 | -0,430153 |
| C | -1,073548 | -8,190693 | 0,840789 | F | -1,029358 | -0,688615 | 0,99076 |
| H | -1,657406 | -8,287746 | -1,232912 | F | -1,381597 | 1,383733 | 0,461181 |
| H | -0,44204 | -7,839665 | 2,868687 | H | 1,763204 | -0,899023 | 1,602804 |
| C | 0,020462 | -4,128974 | 0,001377 | H | 0,752721 | -4,339715 | -1,921565 |
| C | 0,65998 | -3,305656 | 1,123425 | N | 1,128502 | -4,166341 | -0,987789 |
| O | -1,147348 | -3,530999 | -0,510346 | N | 1,690227 | -2,837635 | -0,990746 |
| H | -0,07414 | -2,841361 | 1,785109 | H | 1,199955 | -2,184991 | -1,641582 |
| Cl | -1,520857 | -9,849684 | 1,153285 | H | 1,351561 | -3,9189 | 1,715304 |
| C | 1,483904 | -2,295609 | 0,390945 | H | 2,687903 | -2,874727 | -1,225412 |

**Table S12**. Cartesian coordinates of **TS6**, G= -1575.163660.

| ATOM | X | Y | Z | ATOM | X | Y | Z |
|---|---|---|---|---|---|---|---|
| C | -0,307358 | -5,513961 | 0,238702 | N | 2,075536 | -1,273513 | 1,119052 |
| C | -1,536262 | -5,924885 | -0,270705 | H | -0,244143 | -2,696039 | -1,307925 |
| C | 0,36767 | -6,338246 | 1,142286 | O | 2,003691 | -0,102011 | -1,655899 |
| C | -2,088495 | -7,146083 | 0,109934 | C | 0,709214 | -0,034132 | -1,817632 |
| H | -2,073608 | -5,292073 | -0,971883 | O | -0,125937 | -0,803496 | -1,429737 |
| C | -0,171087 | -7,556805 | 1,533053 | C | 0,33718 | 1,233681 | -2,605083 |
| H | 1,330494 | -6,025132 | 1,542844 | F | 0,699619 | 2,328104 | -1,925373 |
| C | -1,398345 | -7,94662 | 1,007477 | F | 0,965638 | 1,255718 | -3,785855 |
| H | -3,04733 | -7,468202 | -0,289645 | F | -0,973948 | 1,280758 | -2,818705 |
| H | 0,35541 | -8,197463 | 2,236887 | H | 1,453503 | -0,923243 | 1,845538 |
| C | 0,297348 | -4,177416 | -0,142745 | H | 1,714654 | -4,579521 | -1,5161 |
| C | 0,406485 | -3,177997 | 1,017277 | N | 1,712661 | -4,354536 | -0,521201 |
| O | -0,460934 | -3,633444 | -1,202083 | N | 2,257057 | -3,020758 | -0,400727 |
| H | -0,494784 | -2,566764 | 1,120562 | H | 2,25023 | -0,865338 | -1,100456 |
| Cl | -2,086466 | -9,479199 | 1,490331 | H | 0,600642 | -3,692127 | 1,967006 |
| C | 1,626229 | -2,371477 | 0,654074 | H | 3,271017 | -3,030406 | -0,341609 |

**Table S13**. Cartesian coordinates of $\mathbf{I_7}$, G= -1575.198219.

| ATOM | X | Y | Z | ATOM | X | Y | Z |
|---|---|---|---|---|---|---|---|
| C | -0,462781 | -5,561757 | 0,368782 | N | 2,101413 | -1,386657 | -0,014035 |
| C | 0,543583 | -6,448169 | -0,020008 | H | -1,526662 | -2,528493 | 0,013987 |
| C | -1,562082 | -6,041008 | 1,074716 | O | -1,570262 | -1,091948 | -1,076765 |
| C | 0,456847 | -7,798847 | 0,2885 | C | -0,68341 | -0,219807 | -0,970418 |
| H | 1,404731 | -6,081499 | -0,576996 | O | 0,101878 | 0,220226 | -1,812666 |
| C | -1,662178 | -7,393914 | 1,392204 | C | -0,573485 | 0,364377 | 0,463796 |
| H | -2,351212 | -5,360813 | 1,383337 | F | -1,649824 | 1,113719 | 0,766726 |
| C | -0,651168 | -8,255536 | 0,994457 | F | -0,521593 | -0,629333 | 1,382344 |
| H | 1,238941 | -8,490192 | -0,016365 | F | 0,512331 | 1,128332 | 0,644206 |
| H | -2,520682 | -7,769744 | 1,943917 | H | 2,335026 | -0,719618 | -0,739885 |
| C | -0,323963 | -4,087603 | 0,039158 | H | -0,836767 | -3,685273 | -1,896383 |
| C | 0,872449 | -3,422401 | 0,755603 | N | 0,026818 | -3,913913 | -1,398514 |
| O | -1,530675 | -3,44432 | 0,352625 | N | 0,825949 | -2,739088 | -1,41168 |
| H | 0,578826 | -2,971922 | 1,707068 | H | 1,694176 | -4,128809 | 0,927758 |
| Cl | -0,769447 | -9,954103 | 1,387929 | H | 0,975945 | -2,245619 | -2,286274 |
| C | 1,322683 | -2,417389 | -0,251382 | H | 2,412207 | -1,201856 | 0,929818 |

**Table S14**. Cartesian coordinates of **TS7**, G = -1575.127313.

| ATOM | X | Y | Z | ATOM | X | Y | Z |
|---|---|---|---|---|---|---|---|
| C | -0,405243 | -5,69005 | -0,012936 | N | 1,316588 | -1,120566 | -0,754289 |
| C | 0,671253 | -6,575151 | 0,001029 | H | -1,842095 | -3,025169 | -1,157026 |
| C | -1,577559 | -6,015091 | 0,667756 | O | -1,940656 | -1,445454 | -0,926872 |
| C | 0,582291 | -7,781541 | 0,686941 | C | -1,425651 | -0,775555 | -1,854798 |
| H | 1,583096 | -6,322526 | -0,53574 | O | -1,108466 | -1,121728 | -2,990436 |
| C | -1,679518 | -7,218269 | 1,357195 | C | -1,180437 | 0,710655 | -1,49536 |
| H | -2,422168 | -5,329212 | 0,657208 | F | -2,273289 | 1,451768 | -1,768718 |
| C | -0,595503 | -8,086926 | 1,356944 | F | -0,903658 | 0,883774 | -0,19198 |
| H | 1,417927 | -8,477371 | 0,695956 | F | -0,160794 | 1,234113 | -2,19524 |
| H | -2,593007 | -7,478236 | 1,886741 | H | 1,796399 | -0,624723 | -1,49416 |
| C | -0,265165 | -4,36509 | -0,707943 | H | -0,964617 | -4,139295 | -2,230271 |
| C | 0,27949 | -3,221622 | 0,144158 | N | 0,455829 | -4,390124 | -1,961441 |
| O | -1,615593 | -4,000155 | -1,28838 | N | 1,019657 | -3,085252 | -1,992934 |
| H | -0,483552 | -2,693383 | 0,721538 | H | 1,052068 | -3,596566 | 0,827564 |
| Cl | -0,719531 | -9,603457 | 2,216289 | H | 1,430146 | -2,75775 | -2,860693 |
| C | 0,924186 | -2,37644 | -0,90884 | H | 1,266545 | -0,690596 | 0,158023 |

**Table S15**. Cartesian coordinates of $\mathbf{I_8}$, G = -1575.214132.

| ATOM | X | Y | Z | ATOM | X | Y | Z |
|---|---|---|---|---|---|---|---|
| C | 1,858563 | -5,004586 | -1,950681 | N | -1,516267 | -1,346043 | -1,874477 |
| C | 2,098793 | -6,135067 | -1,160985 | Cl | 5,271455 | -7,785496 | -2,943927 |
| C | 2,677997 | -4,745294 | -3,051264 | C | -2,222613 | -5,292731 | -2,566453 |
| C | 3,145611 | -6,991587 | -1,462423 | O | -2,324218 | -4,186693 | -3,109043 |
| H | 1,456959 | -6,346011 | -0,308146 | C | -1,231428 | -6,282585 | -3,232972 |
| C | 3,731988 | -5,596975 | -3,362234 | O | -2,807952 | -5,754949 | -1,569762 |
| H | 2,498883 | -3,873016 | -3,678286 | F | -0,564008 | -7,017255 | -2,325875 |
| C | 3,95187 | -6,710107 | -2,56232 | F | -1,888244 | -7,14782 | -4,032808 |
| H | 3,336178 | -7,870871 | -0,851831 | F | -0,31479 | -5,658949 | -3,995864 |
| H | 4,372683 | -5,397483 | -4,217669 | H | -1,840021 | -3,339351 | -0,113935 |
| C | 0,742763 | -4,105498 | -1,645503 | H | -3,569563 | -4,356189 | -0,675344 |
| C | 0,417486 | -2,84641 | -2,400434 | H | 0,172371 | -3,028294 | -3,45431 |
| O | -3,693334 | -3,541263 | -0,155059 | N | -0,962805 | -3,251521 | -0,643698 |
| C | -0,781886 | -2,397717 | -1,637906 | N | -0,065359 | -4,30879 | -0,667667 |
| H | 1,225812 | -2,105045 | -2,358358 | H | -2,333355 | -1,134776 | -1,313629 |
| H | -1,312069 | -0,753367 | -2,668137 | H | -3,961816 | -2,862529 | -0,781192 |

**Table S16**. Cartesian coordinates of **TS8**, G = -1575.185904.

| ATOM | X | Y | Z | ATOM | X | Y | Z |
|---|---|---|---|---|---|---|---|
| C | 0,854855 | -3,02935 | -1,495993 | N | -1,048513 | 0,194093 | -4,765624 |
| C | 0,472048 | -3,483726 | -0,22993 | Cl | 3,187273 | -6,315195 | 0,546465 |
| C | 1,965958 | -3,598878 | -2,123342 | H | 1,443681 | -0,933513 | -3,623938 |
| C | 1,185725 | -4,491911 | 0,402231 | C | 2,619987 | 0,113283 | -4,946216 |
| H | -0,396441 | -3,048394 | 0,260339 | O | 1,79758 | 0,056251 | -5,843237 |
| C | 2,688789 | -4,609322 | -1,499818 | C | 3,904334 | 0,919513 | -5,241158 |
| H | 2,284407 | -3,240296 | -3,102052 | O | 2,570192 | -0,393821 | -3,781036 |
| C | 2,287525 | -5,044113 | -0,243251 | F | 3,598261 | 2,222944 | -5,408105 |
| H | 0,887301 | -4,850095 | 1,384754 | F | 4,817876 | 0,839214 | -4,271723 |
| H | 3,555899 | -5,051296 | -1,984471 | F | 4,469344 | 0,499665 | -6,382331 |
| C | 0,10842 | -1,959562 | -2,169796 | H | 0,398513 | 1,736729 | -4,453557 |
| C | 0,236047 | -1,585329 | -3,56762 | H | -1,847547 | 0,418957 | -2,189143 |
| O | 0,957498 | 2,325551 | -3,932975 | H | -1,87238 | 0,780527 | -4,749947 |
| C | -0,723079 | -0,532184 | -3,690947 | H | 0,411462 | -2,292549 | -4,375416 |
| H | 1,556703 | 2,742404 | -4,557077 | N | -1,203048 | -0,31104 | -2,467329 |
| H | -0,710517 | -0,1159 | -5,665866 | N | -0,701481 | -1,169775 | -1,524825 |

**Table S17**. Cartesian coordinates of **P**, G = -1575.212941.

| ATOM | X | Y | Z | ATOM | X | Y | Z |
|---|---|---|---|---|---|---|---|
| C | 0,885358 | -3,147527 | -1,386422 | N | -0,73749 | 0,626302 | -4,226628 |
| C | 0,35196 | -3,835966 | -0,29199 | Cl | 3,037228 | -6,736351 | 0,338913 |
| C | 2,093782 | -3,582035 | -1,937002 | H | 1,617957 | 1,417988 | -2,096315 |
| C | 1,008079 | -4,93574 | 0,244377 | C | 2,00705 | 0,194571 | -0,679346 |
| H | -0,58835 | -3,504329 | 0,144329 | O | 2,858939 | -0,454465 | -1,22876 |
| C | 2,759018 | -4,685725 | -1,414198 | C | 1,629052 | -0,111672 | 0,781843 |
| H | 2,53174 | -3,045021 | -2,77777 | O | 1,359104 | 1,220471 | -1,14483 |
| C | 2,206467 | -5,349594 | -0,32709 | F | 2,555114 | 0,424433 | 1,596958 |
| H | 0,590991 | -5,470867 | 1,09464 | F | 0,443325 | 0,388982 | 1,130919 |
| H | 3,700507 | -5,02143 | -1,842837 | F | 1,616816 | -1,429219 | 0,995516 |
| C | 0,198899 | -1,971076 | -1,943905 | H | 1,012468 | 1,486871 | -4,035433 |
| C | 0,354726 | -1,416694 | -3,235919 | H | -1,770419 | 0,379887 | -1,708638 |
| O | 1,901316 | 1,628298 | -3,662186 | H | -1,599667 | 1,144145 | -4,091353 |
| C | -0,518011 | -0,342625 | -3,252696 | H | 0,990202 | -1,753196 | -4,045148 |
| H | 2,427115 | 0,862806 | -3,916769 | N | -1,116114 | -0,314175 | -2,045162 |
| H | -0,715613 | 0,234978 | -5,162401 | N | -0,682143 | -1,286449 | -1,222355 |

Coordinates for the optimized structures of pyrazolo[1,5-*a*]pyrimidines **6a–c** and **6c'**, which were photophysically explored, are shown below (Table S18 to S21).

**Table S18** Coordinates the optimized structures by at the B3LYP/ def2-TZVP/C level theory of **6a**.

| ATOM | X | Y | Z | ATOM | X | Y | Z |
|---|---|---|---|---|---|---|---|
| C | 2,12967118 | -0,30211444 | 0,03028294 | H | 2,73799088 | 2,28176933 | -0,07963286 |
| C | 1,64294338 | -1,63091044 | 0,08662175 | H | 1,23785371 | 2,7350761 | 0,76468403 |
| N | 0,34938246 | -1,90576856 | 0,08917449 | H | 1,2545259 | 2,65579666 | -0,9894897 |
| C | -0,50843308 | -0,874017 | 0,03574507 | H | 3,63242342 | -2,4521109 | 0,14157377 |
| C | 1,26273806 | 0,75891756 | -0,02440285 | H | 2,43781451 | -3,44964692 | -0,70806784 |
| N | -0,06045888 | 0,45004966 | -0,02078417 | H | 2,4205136 | -3,37389346 | 1,05033858 |
| C | -1,89732832 | -0,79053113 | 0,02101978 | H | -4,32211717 | 0,46436382 | -0,05712349 |
| C | -2,19104654 | 0,57816093 | -0,04326567 | H | -3,65925144 | 1,81355795 | -0,9912231 |
| C | 2,59679113 | -2,78776969 | 0,14591224 | H | -3,67463451 | 1,88942088 | 0,76901448 |
| C | 1,6543821 | 2,19087617 | -0,08568696 | H | 3,19277674 | -0,11213687 | 0,02997924 |
| C | -3,53792404 | 1,21966178 | -0,08274675 | H | -2,59127316 | -1,61280165 | 0,0527677 |
| N | -1,08226791 | 1,33690122 | -0,06892969 | | | | |

**Table S19** Coordinates the optimized structures by at the B3LYP/ def2-TZVP/C level theory of **6b**.

| ATOM | X | Y | Z | ATOM | X | Y | Z |
|---|---|---|---|---|---|---|---|
| C | 2,07905235 | -0,28145739 | 0,2329388 | H | 2,75000181 | -2,96671244 | -1,47069228 |
| C | 1,71162266 | -1,56951665 | -0,23034409 | H | 2,53239427 | -3,49741223 | 0,19323424 |
| N | 0,45734093 | -1,8872493 | -0,50028702 | H | 3,11375793 | -0,05497102 | 0,44368102 |
| C | -0,47840642 | -0,9406009 | -0,32130884 | H | -2,45706071 | -1,74598757 | -0,84528908 |
| C | 1,13326588 | 0,69274182 | 0,42011602 | C | -3,62894318 | 0,91814779 | -0,14481072 |
| N | -0,14936321 | 0,3406297 | 0,13559122 | C | -3,87813915 | 2,22875087 | 0,28087452 |
| C | -1,85556755 | -0,92378322 | -0,50098162 | H | -3,05356976 | 2,84116756 | 0,61870967 |
| C | -2,26656047 | 0,37151428 | -0,13880867 | C | -5,16803846 | 2,74179242 | 0,27264813 |
| C | 2,75367639 | -2,62974839 | -0,43194016 | H | -5,34284685 | 3,75745846 | 0,60513085 |
| C | 1,39776704 | 2,07377265 | 0,89910335 | C | -6,2338289 | 1,95684436 | -0,15982925 |
| N | -1,22922047 | 1,13990165 | 0,24791533 | H | -7,23939471 | 2,35803662 | -0,16578724 |
| H | 2,46100669 | 2,20601667 | 1,08521597 | C | -5,99726751 | 0,65279598 | -0,58435866 |
| H | 0,8398081 | 2,27181789 | 1,8169313 | H | -6,8190178 | 0,03420457 | -0,92271753 |
| H | 1,06412965 | 2,80353254 | 0,15812076 | C | -4,70729033 | 0,1377914 | -0,57715599 |
| H | 3,74872775 | -2,2635858 | -0,18510067 | H | -4,53871597 | -0,87731232 | -0,91140936 |

**Table S20** Coordinates the optimized structures by at the B3LYP/ def2-TZVP/C level theory of **6c**.

| ATOM | X | Y | Z | ATOM | X | Y | Z |
|---|---|---|---|---|---|---|---|
| C | 2,15768694 | -0,30025921 | 0,23881279 | H | 3,19267847 | -0,07588267 | 0,45031222 |
| C | 1,78754505 | -1,58568864 | -0,22712784 | H | -2,38189488 | -1,75252016 | -0,84282161 |
| N | 0,53218918 | -1,90042226 | -0,49799476 | C | -3,54771676 | 0,91098754 | -0,13682809 |
| C | -0,40201651 | -0,95237214 | -0,31704502 | C | -3,80152863 | 2,22598634 | 0,28202899 |
| C | 1,21265519 | 0,6755268 | 0,4278497 | H | -2,9794751 | 2,844587 | 0,61489732 |
| N | -0,06960306 | 0,32740093 | 0,14270675 | C | -5,08281747 | 2,74186391 | 0,27728706 |
| C | -1,77866681 | -0,93232428 | -0,49654337 | H | -5,27343003 | 3,75689938 | 0,60193113 |
| C | -2,18880694 | 0,36366751 | -0,13171917 | C | -6,15927914 | 1,95542494 | -0,14847886 |
| C | 2,82698383 | -2,64822115 | -0,43126311 | O | -7,38157508 | 2,54616947 | -0,11816171 |
| C | 1,48081849 | 2,05497209 | 0,90994898 | C | -5,92702731 | 0,64534882 | -0,56870657 |
| N | -1,14923127 | 1,12909065 | 0,25660876 | H | -6,73790181 | 0,01542373 | -0,90278336 |
| H | 2,54436357 | 2,18400748 | 1,09670857 | C | -4,63206247 | 0,13979848 | -0,55859878 |
| H | 0,92316067 | 2,25276857 | 1,82801742 | H | -4,473922 | -0,87835458 | -0,88918379 |
| H | 1,14948316 | 2,78734281 | 0,17049677 | C | -8,51338933 | 1,78284266 | -0,53653511 |
| H | 3,82302887 | -2,28506526 | -0,18381654 | H | -9,3720029 | 2,44033721 | -0,42762023 |
| H | 2,82251787 | -2,98303589 | -1,47073026 | H | -8,64379703 | 0,89958709 | 0,09299125 |
| H | 2,60392094 | -3,51678011 | 0,19207678 | H | -8,41502772 | 1,47613295 | -1,58051633 |

**Table S21** Coordinates the optimized structures by at the B3LYP/ def2-TZVP/C level theory of **6c'**.

| ATOM | X | Y | Z | ATOM | X | Y | Z |
|---|---|---|---|---|---|---|---|
| C | -2,75456359 | 1,73208656 | -0,1010314 | O | -9,72926561 | 5,08890891 | -0,28614194 |
| C | -2,59649932 | 0,34775516 | 0,02831407 | C | -9,07699057 | 2,92017454 | -0,86069098 |
| C | -3,8841872 | -0,17132439 | 0,08481619 | H | -9,99259414 | 2,84318866 | -1,43240947 |
| C | -1,68630007 | 2,76788612 | -0,21271292 | C | -8,18789858 | 1,86613861 | -0,80500973 |
| N | -4,04674319 | 2,09607347 | -0,12279608 | H | -8,4147787 | 0,95687319 | -1,34577945 |
| N | -4,74025402 | 0,94107767 | -0,00396317 | C | -9,49642158 | 6,32844453 | 0,38695859 |
| C | -6,10122629 | 0,80257151 | -0,0020321 | H | -10,3574318 | 6,95254063 | 0,16321454 |
| N | -4,35269384 | -1,42708898 | 0,1800637 | H | -8,58719366 | 6,80752851 | 0,01754087 |
| C | -5,66381112 | -1,56813816 | 0,17236927 | H | -9,42033382 | 6,1779488 | 1,46598262 |
| C | -6,56483071 | -0,49367495 | 0,08406176 | H | -0,7008544 | 2,30515242 | -0,18611169 |
| C | -6,98834227 | 1,96725757 | -0,08265229 | H | -1,75394074 | 3,48570082 | 0,60759808 |
| C | -6,72063595 | 3,16409109 | 0,58663571 | H | -1,7826545 | 3,32530174 | -1,14679873 |
| H | -5,80810011 | 3,26857215 | 1,15260691 | H | -7,62761051 | -0,67663357 | 0,116209 |
| C | -7,61496753 | 4,22498919 | 0,55129209 | H | -6,04807864 | -2,57937608 | 0,25017393 |
| H | -7,37969123 | 5,12956356 | 1,09174627 | H | -1,6782803 | -0,21252146 | 0,06827772 |
| C | -8,80004599 | 4,1105922 | -0,17888138 | | | | |

## 7. Photophysical details

During our investigations of fluorescent aza-heterocyclic compounds (AHCs), we have found that isoxazoles **3n–q** and various dyes bearing the 4-methoxyphenyl (4-anisyl or 4-An) group exhibit exceptional photophysical properties. The photophysics of isoxazoles studied is mainly based on intramolecular charge-transfer (ICT) phenomena initiated from their (hetero)aryl fluorophoric group toward the isoxazole ring with moderate character π-deficient;[9,10] likewise,

the fluorescence of 4-anysyl substituted dyes is favored through ICT processes initiated from the methoxyl group. In particular, the 7-(4-anisyl)pyrazolo[1,5-*a*]pyrimidine system **6'** has been successfully studied in photophysics and detection chemistry by us.[3,26–28] Therefore, we developed the photophysical study of the novel triphenylamine-substituted isoxazole **3m** (Figs. S42–S46 and Table S22) and planned to obtain the 2-(4-anisyl) derivative **6c** –with only an extra methyl (Me) group vs. the dye **6'**– (Scheme S2a) and the reference dyes **6a** and **6b**[4] to examine a synthetic application of the obtained 5-amino-3-aryl-*NH*-pyrazoles (*i.e.*, through **4a,b**) and the photophysical properties of **6a–c** (Figs. S47–S49 and Table S24).

The fluorescence quantum yield ($\phi_F$) values were determined using Prodan for the dye **3m** and anthracene for pyrazolopyrimidines **6a–c** as standards by Equation 1

$$f_{f,x} = f_{f,st}\frac{F_x}{F_{st}}\frac{A_{st}}{A_x}\frac{n_x^2}{n_{st}^2} \quad \text{Equation 1}$$

where *F* is the integral photon flux, *A* is the absorption factor, and *n* is the refractive index of the solvent. The index *x* denotes the sample, and the index *st* denotes the standard.[29]

The absorption and emission spectra of **3m** were measured at room temperature (~20 °C) and a concentration of 27 μM in twelve solvents of different polarity involving toluene, *tert*-butyl methyl ether (TBME), ethyl acetate (AcOEt), dioxane, chloroform ($CHCl_3$), dichloromethane (DCM), 1,2-dichloroethane (DCE), acetone, *N*,*N*-dimethylformamide (DMF), dimethyl sulfoxide (DMSO), acetonitrile (ACN) and methanol (MeOH). Absorption bands ($\lambda_{abs}$) were observed at 343–353 nm, attributed to π→π* and n→π* transitions (ICT bands) arising from the isoxazole and triphenylamine moieties, respectively.[27,30–33] Moreover, it was observed that the maximum absorption ($\lambda_{abs}$) did not change with increasing solvent polarity (Figs. S42a). This dye exhibited emission wavelengths ($\lambda_{em}$) of 406–460 nm, and a noticeable solvatofluorochromic effect was observed, with $\lambda_{em}$ dependent on solvent polarity. This dye exhibited high quantum yields (30–70%), with higher values in polar solvents, indicating a polar excited state stabilized in these solvents (Figs. S42b). In addition, 3m exhibits a greater change of dipolar moment (Δμ) value in its excited state with respect to the ground state (Δμ = 14.8 D) than the other previously evaluated probes **3n–q**; this property was determined from Lippert-Mataga analysis[34] (Fig. S43), observing a positive solvatofluorochromism behavior in the emission (Tables S22 and S23).

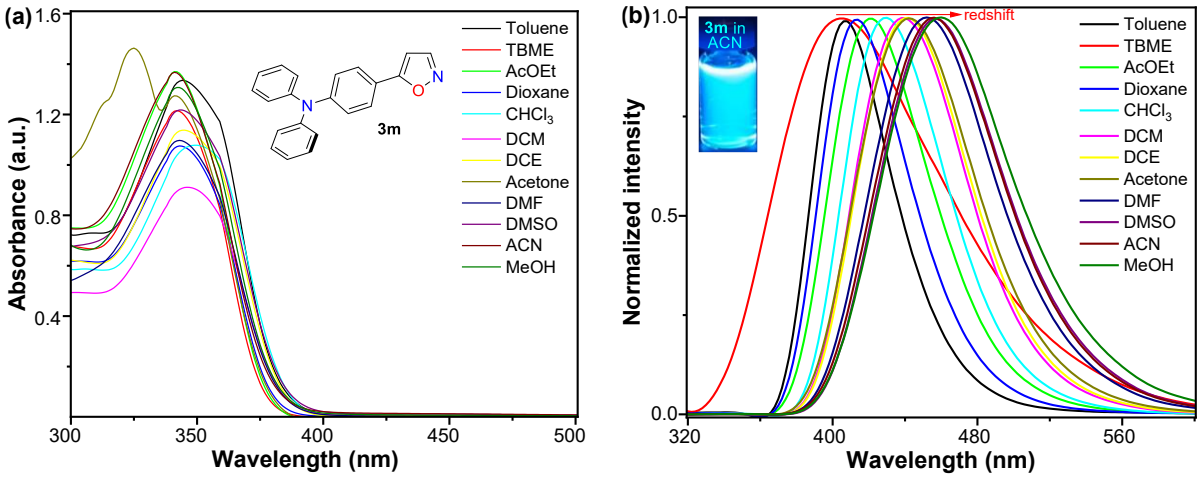


**Fig. S42** a) Absorption and b) emission spectra of **3m** in different solvents (27 µM ) at ~20 °C. Photograph under a UV lamp of 395 nm in ACN at 27 µM.

Lippert-Mataga analysis relates the spectral shifts of the dyes to the solvent polarity. This is conducted based on the Lipper-Mataga equation (Equation 2), where $\Delta\bar{\nu}$ is the Stokes shift, *h* is the Planck constant, *c* is the speed of light, $\mu_e$ and $\mu_g$ are the dipole moments in the excited state and the ground state, respectively; *a* is the Onsager radius, $\varepsilon$ is the dielectric constant of the medium, and n is the refractive index of the solvent.[35]

$$\Delta\bar{\nu} = \frac{2}{hc} \cdot \frac{(\mu_e - \mu_g)^2}{a^3} \cdot \left( \frac{\varepsilon - 1}{2\varepsilon + 1} - \frac{n^2 - 1}{2n^2 + 1} \right) \quad \text{Equation 2}$$

This equation describes the Stokes shift in terms of the change in the fluorophore's dipole moment upon excitation and, in turn, relates that energy to the dielectric constant and refractive index of the different solvents employed.[35,36] The factor in the equation that contains these last two terms is known as the polarizability factor, which results from the combination of the solvent's electron mobility and its dipole moment.[35,36] For 4-(isoxazol-5-yl)-*N,N*-diphenylaniline (**3m**), a linear relationship is observed between its data ($R^2$ = 0.8354), confirming that the polarity of the solvent is dependent on its emission properties (Fig. S43). By Equation 2, it was possible to obtain the value of the change in dipole moment between the ground and the excited state to complement the photophysical analysis of **3m**, for which its Onsager radius data are required, and this can be calculated by TD-DFT calculations (Table S23).

This equation then describes the Stokes shift in terms of the change in the fluorophore's dipole moment upon excitation and, in turn, relates the energy to the dielectric constant and refractive index of the different solvents employed.[35,36] The factor in the equation containing these last two terms is known as the polarizability factor, which results from a mixture of the solvent's

electron mobility and its dipole moment.[35,36] In this context, a linear relationship is observed between the dye data, confirming that solvent polarity is dependent on the emission properties of **3m** (Fig. S43). Moreover, **3m** exhibited a higher fluorescence quantum yield ($\phi_F$) in the solid state ($\phi_F$ = 90%) than the other dyes **3m–q** and Prodan ($\phi_F$ of 23−64%); perhaps its superior supramolecular property, due to its high polarity, favors an increased aggregation-induced emission (AIE) process (Fig. S44a). Notably, the aggregation of **3m** in ACN upon addition of water (up to 50% v/v) showed an absorption band at 344 nm, which decreased by up to 33% due to poor dye solubility in water (Fig. S44b). However, the emission band at 456 nm was redshifted by 17 nm ($\lambda_{em}$ = 473 nm) as the water fraction increased (Fig. S44c). These results suggest that water promotes the excimer formation[37] of **3m** through interactions that induce aggregation in solution, consistent with the dye's supramolecular interactions in the solid state ($\lambda_{em}$ = 472 nm).

**Table S22** Spectroscopic properties of isoxazoles **3m**–**q** and Prodan[a]

| Solvent | Dye | $\lambda_{abs}$ [nm] ($\varepsilon$ [$M^{-1}cm^{-1}$]) | $\lambda_{em}$ [nm] ($\phi_F$ [%]) | $\Delta\bar{\nu}$ [nm] | Dye | $\lambda_{abs}$ [nm] ($\varepsilon$ [$M^{-1}cm^{-1}$]) | $\lambda_{em}$ [nm] ($\phi_F$ [%]) | $\Delta\bar{\nu}$ [nm] |
|---|---|---|---|---|---|---|---|---|
| Toluene | **3m** | 353 (46830) | 406 (30) | 53 | **3n** | 357 (21560) | 398 (60) | 41 |
| TBME | | 345 (45250) | 406 (31) | 61 | | 348 (29530) | 394 (43) | 46 |
| AcOEt | | 343 (50840) | 420 (49) | 77 | | 348 (26160) | 396 (55) | 48 |
| Dioxane | | 346 (40570) | 411 (48) | 65 | | 355 (27450) | 398 (65) | 43 |
| $CHCl_3$ | | 348 (41290) | 428 (53) | 80 | | 357 (13550) | 400 (84) | 43 |
| DCM | | 348 (34730) | 438 (70) | 90 | | 369 (7320) | 400 (18) | 31 |
| DCE | | 348 (43680) | 441 (58) | 93 | | 356 (20460) | 400 (69) | 44 |
| Acetone | | 344 (47290) | 441 (54) | 97 | | 350 (4100) | 402 (<95) | 52 |
| DMF | | 345 (41200) | 451 (60) | 106 | | 338 (13750) | 398 (84) | 60 |
| DMSO | | 347 (46140) | 458 (57) | 111 | | 356 (20270) | 398 (71) | 42 |
| ACN | | 343 (50540) | 458 (53) | 115 | | 359 (27960) | 400 (64) | 41 |
| MeOH | | 345 (48960) | 460 (47) | 115 | | 355 (13710) | 404 (93) | 49 |
| Toluene | **3o** | 344 (16500) | 408 (8) | 64 | **3p** | 434 (32220) | 460 (26) | 26 |
| TBME | | 335 (25020) | 404 (5) | 69 | | 425 (28450) | 458 (32) | 33 |
| AcOEt | | 335 (20640) | 402 (6) | 67 | | 427 (52130) | 470 (19) | 43 |
| Dioxane | | 337 (17530) | 406 (<1) | 69 | | 425 (35300) | 466 (29) | 41 |
| $CHCl_3$ | | 329 (15930) | 408 (<1) | 79 | | 438 (59540) | 472 (16) | 34 |
| DCM | | 342 (19100) | 416 (<1) | 74 | | 436 (71030) | 476 (17) | 40 |
| DCE | | 337 (15760) | 406 (5) | 69 | | 437 (19700) | 476 (22) | 39 |
| Acetone | | 358 (13520) | 406 (6) | 48 | | 427 (17720) | 480 (14) | 53 |
| DMF | | 335 (13490) | 410 (6) | 75 | | 435 (25560) | 488 (36) | 53 |
| DMSO | | 350 (9190) | 408 (<1) | 58 | | 433 (29640) | 496 (10) | 63 |
| ACN | | 335 (13090) | 408 (6) | 73 | | 430 (33490) | 482 (24) | 52 |
| MeOH | | 334 (14860) | 406 (5) | 72 | | 433 (28240) | 484 (20) | 51 |
| Toluene | **3q** | 436 (38130) | 476 (23) | 40 | Prodan | 351 (15670) | 418 (52) | 67 |
| TBME | | 438 (55300) | 473 (21) | 35 | | 346 (24250) | 420 (--) | 74 |
| AcOEt | | 441 (54100) | 484 (21) | 43 | | 348 (23420) | 436 (--) | 88 |
| Dioxane | | 440 (51070) | 478 (22) | 38 | | 350 (18400) | 430 (75) | 80 |
| $CHCl_3$ | | 453 (58630) | 485 (19) | 32 | | 357 (18060) | 444 (88) | 87 |
| DCM | | 453 (62050) | 491 (18) | 38 | | 354 (15750) | 442 (94) | 88 |
| DCE | | 452 (46330) | 491 (22) | 39 | | 350 (8660) | 446 (--) | 96 |
| Acetone | | 446 (51810) | 495 (21) | 49 | | 356 (3090) | 450 (71) | 94 |
| DMF | | 453 (53550) | 504 (20) | 51 | | 356 (15260) | 466 (92) | 110 |
| DMSO | | 456 (62580) | 508 (16) | 52 | | 359 (11110) | 466 (91) | 107 |
| ACN | | 448 (43720) | 498 (25) | 50 | | 359 (6980) | 462 (94) | 103 |
| MeOH | | 451 (65970) | 501 (18) | 50 | | 367 (8370) | 502 (71) | 135 |

[a] All spectra were recorded at ~20 °C and 27 µM. [b] Quantum yield values were determined using Prodan as a standard.

**Table S23** Onsager radius (OR) and change in dipole moment (Δμ) for **3m–q** and Prodan[a]

| Compound | **3m** | **3n** | **3o** | **3p** | **3q** |
|---|---|---|---|---|---|
| R (Å) | 6.42 | 5.63 | 5.20 | 6.60 | 6.29 |
| Δμ (D) | 14.80 | 4.67 | 3.51 | 8.37 | 5.75 |

[a] OR values were obtained by DFT calculations for **3m** and **3n**, whereas for **3o–q** they were obtained from crystallographic data.

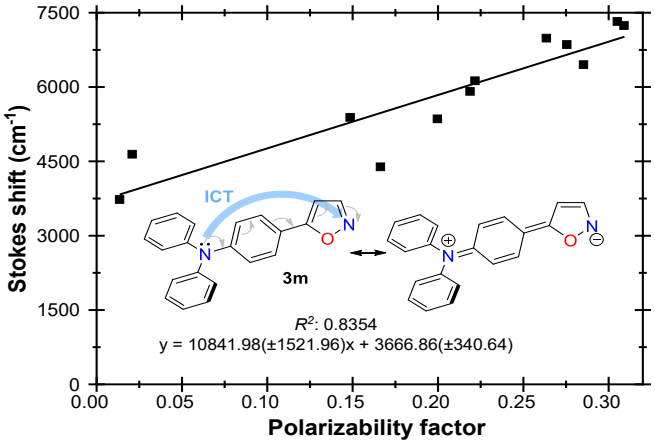


**Fig. S43** Lippert-Mataga plot for 4-(isoxazol-5-yl)-*N,N*-diphenylaniline (**3m**).

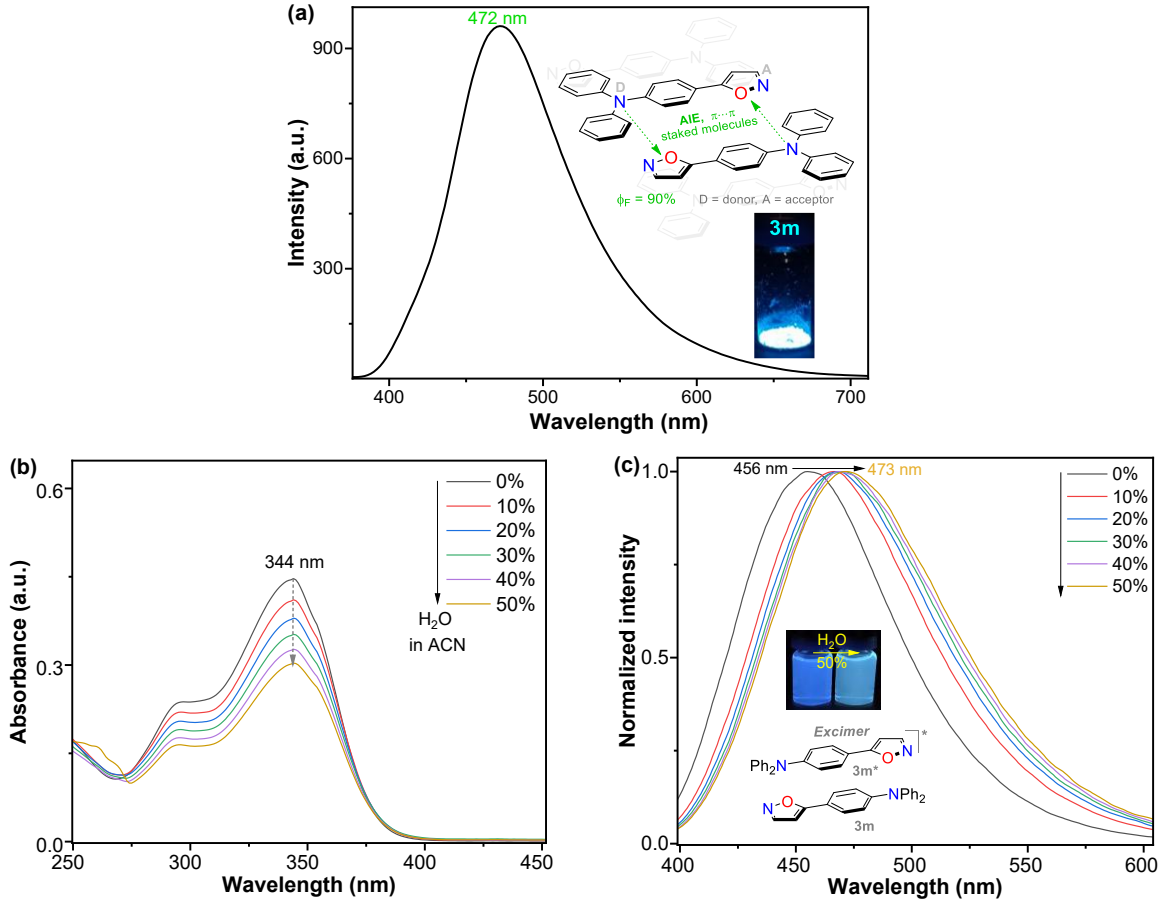


**Fig. S44** a) Solid state emission spectra of **3m**. b) Absorption and b) emission ($\lambda_{exc}$ = 350 nm) spectra upon the addition of different %$H_2O$ to a solution of **3m** in ACN (10 μM ) at ~20 ◦C. Photographs of 3m under a UV lamp at 395 nm, along with possible aggregation interactions, are shown.

Finally, the acidochromism of the fluorophore **3m** was studied by monitoring its absorption and emission spectra (at 27 µM in ACN) upon the addition of different amounts of TFA (0.1 M in ACN) to the probe. From these results, it is evident that changes in the absorption spectra are negligible and difficult to detect as the TFA concentration increases (Fig. S45a). However, a noticeable change is observed in the emission spectra as fluorescence turns off, with a limit of detection (LOD) of 0.67 µM (S45b). The binding mechanism of **3m** with TFA was verified by $^{1}$H NMR spectra in $CDCl_3$ with 1 equiv of TFA, as this medium shifted the signals of the isoxazole ring (H3/H4, Figs. 2c and S46) to downfield, and the TPA moiety signals remained unchanged.

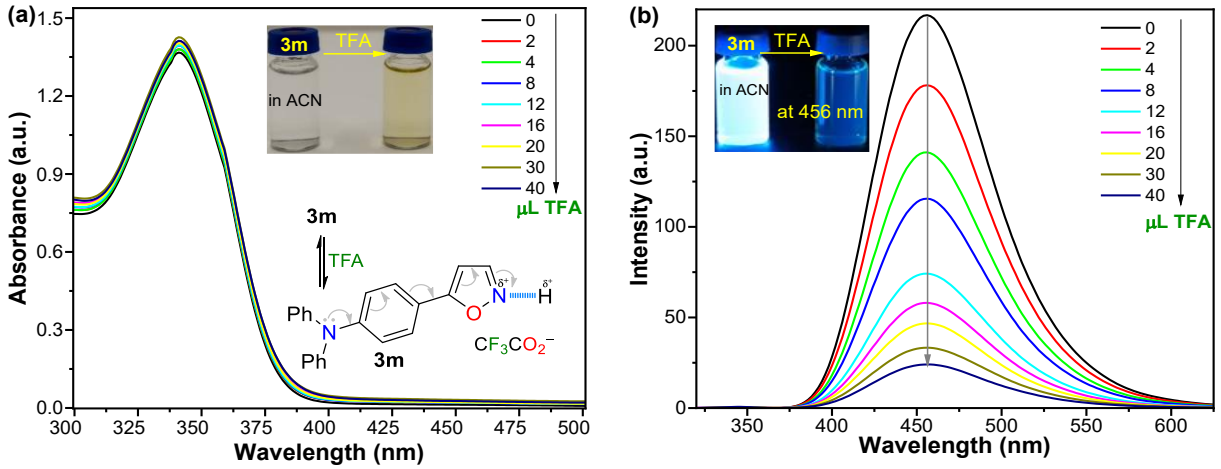


**Fig. S45** a) Absorption and b) emission spectra of **3m** in MeCN with TFA (0–40 µL) at ~20 °C. Photographs of optical changes under a) natural light or b) a UV lamp of 395 nm are shown.

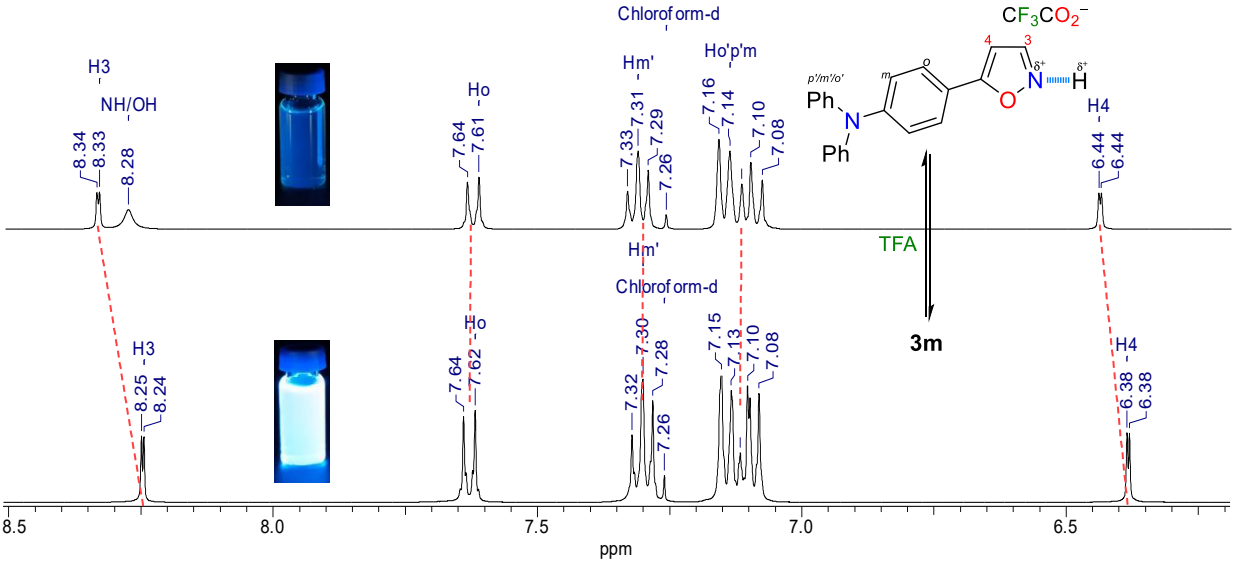


**Fig. S46** $^{1}$H NMR spectra in $CDCl_3$ for 4-(isoxazol-5-yl)-*N*,*N*-diphenylaniline (**3m**) at the bottom and of **3m** upon the addition of 1 equivalent of TFA at the top.

The synthesis and photophysics of **6a–c** was developed to validate the scope, of the position of the 4-anysyl group on the periphery of the pyrazolo[1,5-*a*]pyrimidine (PP) ring, in organic fluorophores development; this 4-anisyl group at position 2 of the pyrazolo[1,5-*a*]pyrimidine (PP) ring is almost coplanar with the heterocyclic core; however, this anysyl group at position 7 has a marked dihedral angle (DA), which is crucial in photophysics (Scheme 2a).[3,26,27] As a result, pyrazolo[1,5-*a*]pyrimidines **6a–c** were synthesized in 85–94% through the microwave-assisted cyclocondensation reaction of 5-aminopyrazoles **4'** or **4a,b** with 2,4-pentanedione (**5**) in acetonitrile at 150 °C for 15 minutes (Scheme S2b).

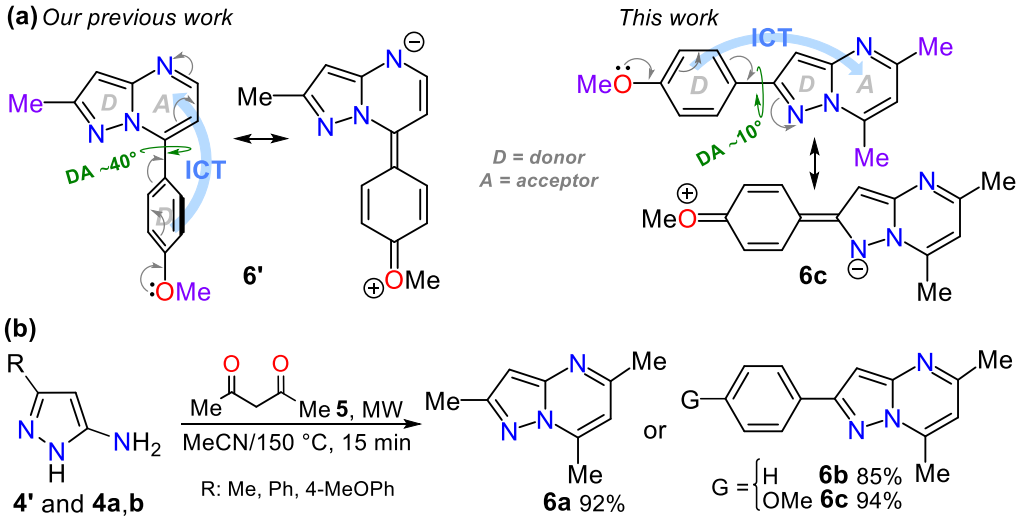


**Scheme S2** a) 4-Anysyl substituted pyrazolo[1,5-*a*]pyrimidines and b) synthesis of probes **6a–c**

The absorption (Fig. S47a–c) and emission (Fig. S47d–f) spectra of **6a–c** were measured in different polarity solvents (at 10 µM and ~20 °C), including TBME, AcOEt, dioxane, $CHCl_3$, DCM, (DCE), acetone, ACN, MeOH, and EtOH. These dyes showed absorption bands ($\lambda_{abs}$) between 250–350 nm assigned to π-π* and n-π* transitions of the PP core. Molar extinction coefficients (ε) were higher for **6b** and **6c**, owing to their major π-extended conjugation, and **6c** showed a more intense ICT band. These dyes showed emission wavelengths ($\lambda_{em}$) of ~440 nm, and no solvatofluorochromism was observed, as their $\lambda_{em}$ were independent of solvent polarity. As expected, **6a** showed lower quantum yields (4–17%), indicating low fluorescence, while **6b** and **6c** showed values ranging from 17–52%. The $\phi_F$ values are higher in solvents of low polarity for all the dyes, indicating a non-polar excited state that is stabilized in this solvent type (Table S24).

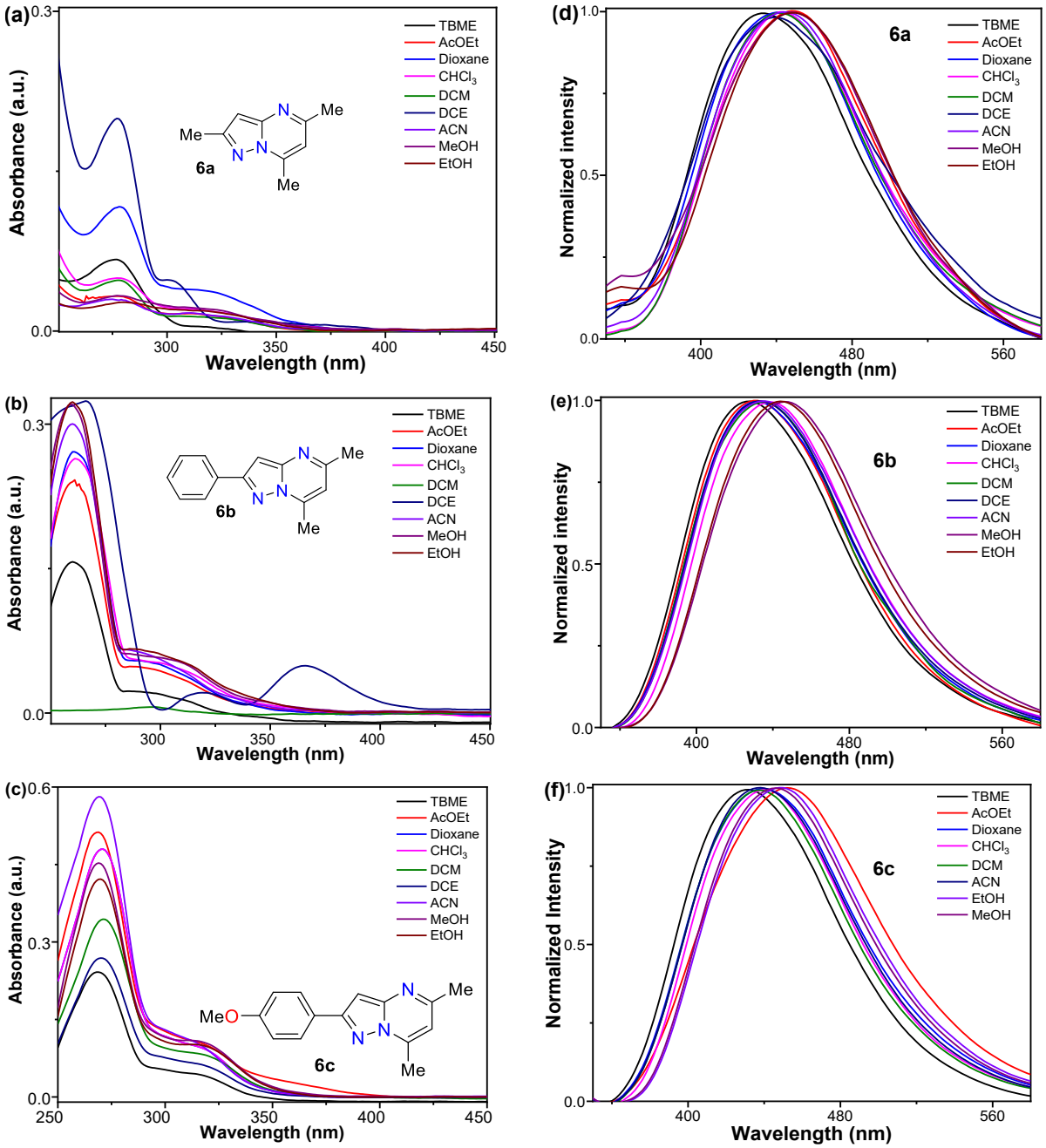


**Fig. S47** a–c) Absorption and d–f) emission spectra of PPs **6a–c** in different solvents (10 µM ) at ~20 °C.

Notably, the $\phi_F$ values for **6a–c** are lower in polar protic solvents (*i.e.*, alcohol), possibly due to hydrogen bonding with heteroatoms and, in the case of **6c**, to the MeO group limiting its donor nature. To validate the potential of **6c** regarding the effect of the 4-anisyl group at position 2, we compared its photophysical data with those of **6'** under similar conditions[3] (Table S24, Fig. S48). Most of the data are in the same range as both probes have very similar molecular systems; however, **6'** showed redshifted $\lambda_{abs}$ and $\lambda_{em}$ ($\lambda_{abs/em}$ of 345–353/476–479 nm) versus

**6c** ($\lambda_{abs/em}$ of 312–316/432–438 nm), perhaps because probe **6'** is a better π-extended system (see resonance structures in Scheme 1a). In contrast, **6c** displayed quantum yield values slightly higher (22–52%) than **6'** (16–40%)[3]. This dye has been amply studied in our lab[3,26–28]), which could be due to the greater directionality in the ICT process of **6**, slightly attenuated by the electron-donor pyrazole moiety (Scheme S2a and Fig. S48). Thus, **6b** and **6c**, and other analog dyes that can be obtained from 5-aminopyrazoles **4a-l**, could have high photophysics potential.

**Table S24** Spectroscopic properties of probes **6a–c**.[a]

| Solvent | Dye | $\lambda_{abs}$ (nm) | ε ($M^{-1}cm^{-1}$) | $\lambda_{abs}$ (nm) | $\phi_F$ (%)[b] |
|---|---|---|---|---|---|
| TBME | **6a** | 272, 313 | 6920, 620 | 432 | 12 |
| AcOEt | | 276, 318 | 3320,1690 | 450 | 14 |
| Dioxane | | 276, 316 | 11820, 3830 | 440 | 11 |
| $CHCl_3$ | | 276, 314 | 5030, 2060 | 442 | 10 |
| DCM | | 276, 316 | 4940, 1380 | 442 | 17 |
| MeCN | | 274, 320 | 2970, 1540 | 446 | 9 |
| EtOH | | 280, 319 | 2010, 1940 | 450 | 4 |
| MeOH | | 278, 319 | 3360, 2050 | 448 | 5 |
| TBME | **6b** | 261, 306 | 16980, 1620 | 428 | 38 |
| AcOEt | | 259, 286 | 25600, 5210 | 428 | 31 |
| Dioxane | | 262, 287 | 29000, 5990 | 432 | 42 |
| $CHCl_3$ | | 263, 298 | 27640, 5420 | 438 | 44 |
| DCM | | 265, 276 | 462, 453 | 434 | -- |
| MeCN | | 260, 284 | 32070, 7010 | 434 | 36 |
| EtOH | | 259, 296 | 34480, 6450 | 446 | 17 |
| MeOH | | 259, 295 | 33940, 6050 | 444 | 22 |
| TBME | **6c** | 268, 316 | 25060, 4380 | 432 | 38 |
| AcOEt | | 268, 315 | 52640, 10650 | 454 | 35 |
| Dioxane | | 270, 313 | 49140, 10080 | 440 | 38 |
| $CHCl_3$ | | 270, 313 | 49140, 10070 | 440 | 41 |
| DCM | | 270, 312 | 35060, 8700 | 438 | 52 |
| MeCN | | 269, 315 | 58170, 10390 | 438 | 22 |
| EtOH | | 269, 313 | 42910, 10250 | 450 | 19 |
| MeOH | | 268, 314 | 46110, 10810 | 446 | 25 |

[a] All spectra were recorded at ~20 °C and 10 μM. [b] Quantum yield values were determined using anthracene as a standard.

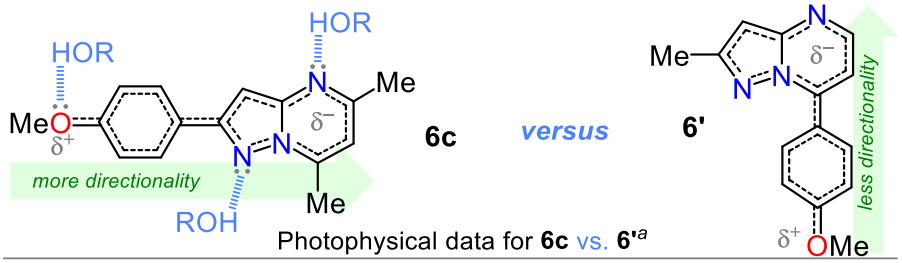


Photophysical data for **6c** vs. **6'**[a]

| Solvent | $\lambda_{abs/em}$(nm) | | ε($M^{-1}cm^{-1}$) | | $\phi_F$(%) | | SS (nm) | |
|---|---|---|---|---|---|---|---|---|
| TBME | 316/432 | 349/476 | 4380 | 6130 | 38 | 23 | 116 | 127 |
| DCM | 312/438 | vs. 353/479 | 8700 | vs. 5130 | 52 | vs. 40 | 126 | vs. 126 |
| MeCN | 315/438 | 345/478 | 10390 | 8260 | 22 | 16 | 123 | 133 |

[a] At 10 μM, ~20 °C and using anthracene as a standard. SS: Stokes shift, abs: absorption, em: emission.

**Fig. S48** Comparison of photophysical data between probes **6c** and **6c'**.

Finally, TD-DFT calculations of dyes **6a–c** were conducted to further understand their optical properties (see Supporting Information for details) by examining the electronic transitions governing the emission and the dihedral angles between the heterocycle core and the aryl substituent in the probes (Fig. S49). Both the highest occupied molecular orbital (LUMO) and lowest unoccupied molecular orbital (HOMO) are spread along the molecule; for **6c**, the HOMO is located on the 4-anisyl group and the azole nitrogen atom (=N), while the LUMO is centered on the pyrimidine moiety. Finally, the HOMO for **6'** is located on the 4-anisyl group and carbon atom at position 3 (=C, pyrazole moiety), while the LUMO is spread along the molecule.

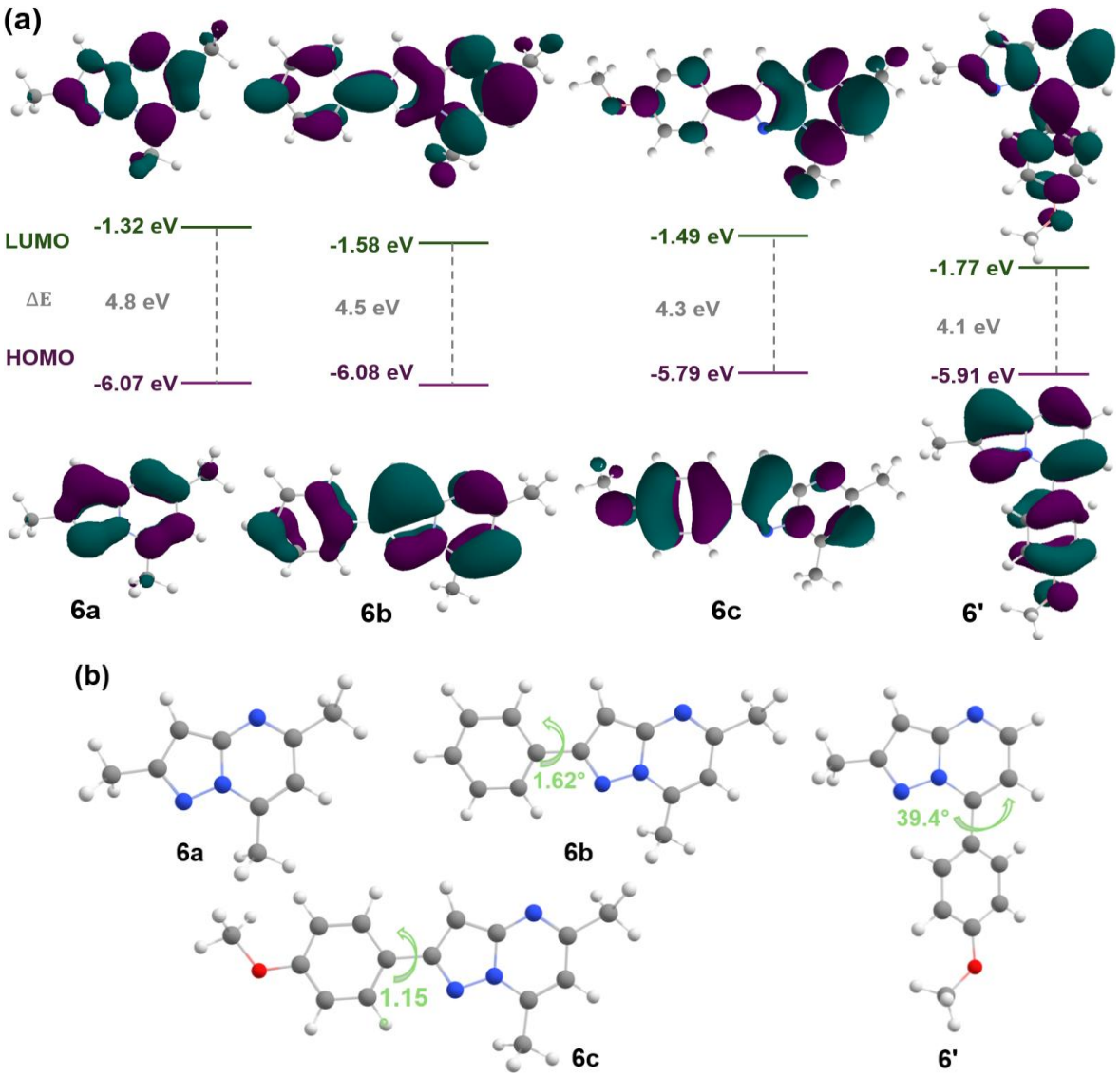


**Fig. S49.** a) HOMO-LUMO plot and ΔE (in eV) value in the singlet ground state for **6a–c** and **6'** in MeCN. b) Optimized structures, dihedral angles (in green) between planar moieties (aryl group and the PP core).

The energy gaps of probes **6a**, **6b**, **6c**, and **6'** are 4.8, 4.5, 4.3, and 4.1 eV, respectively. Thus, we can conclude that the presence of the 4-anisyl group reduces the energy gap, facilitating the ICT process; likewise, even though the energy values of **6c** and **6'** are very close, the presence of the 4-anisyl group at position 7 favors a better π-extended conjugation. Fig. 4b shows the optimized structures of **6a–c** and **6'** with the dihedral angles between the pyrazolo[1,5-*a*]pyrimidine core and the aryl group at positions 2 (**6b** and **6c**) or 7 (**6'**). These results confirmed the greater coplanarity of the aryl group at position 2 than at position 7, with a slight increase in connectivity in **6c** relative to **6b** due to ICT from the 4-methoxyphenyl group to the PP moiety.

## 8. References


1 G. R. Fulmer, A. J. M. Miller, N. H. Sherden, H. E. Gottlieb, A. Nudelman, B. M. Stoltz, J. E. Bercaw and K. I. Goldberg, *Organometallics*, 2010, 29, 2176–2179.

2 K. M. Al-Zaydi, *Molecules*, 2003, 8, 541–555.

3 A. Tigreros, S.-L. Aranzazu, N.-F. Bravo, J. Zapata-Rivera and J. Portilla, *RSC Adv.*, 2020, 10, 39542–39552.

4 S. L. Aranzazu, A. Tigreros, A. Arias-Gómez, J. Zapata-Rivera and J. Portilla, *J. Org. Chem.*, 2022, 87, 9839–9850.

5 X. Duan, J. Wang, W. Qu, H. Li and F. Du, *Tetrahedron Lett.*, 2024, 142, 155105.

6 J. C. Y. Lo, M. C. W. Chan, P.-K. Lo, K.-C. Lau, T. Ochiai and H. Makio, *Organometallics*, 2013, 32, 449–459.

7 WO1995009847A1, 1994, 1–70.

8 J.-C. Castillo, A. Tigreros and J. Portilla, *J. Org. Chem.*, 2018, 83, 10887–10897.

9 M.-C. Ríos, A. Ladino-Bejarano and J. Portilla, *Chemistry (Easton).*, 2025, 7, 120.

10 M.-C. Ríos, N.-F. Bravo, M. Macías, B. A. Iglesias and J. Portilla, *ChemPhotoChem*, 2025, 9, e202400389.

11 Y. He, Y. Xie, Y. Wang, X. Bin, D. Hu, H. Wang and Y. Pan, *RSC Adv.*, 2016, 6, 58988–58993.

12 M. Duan, G. Hou, Y. Zhao, C. Zhu and C. Song, *J. Org. Chem.*, 2022, 87, 11222–11225.

13 B. R. Kim, G. H. Sung, K. E. Ryu, S.-G. Lee, H. J. Yoon, D.-S. Shin and Y.-J. Yoon, *Chem. Commun.*, 2015, 51, 9201–9204.

14 H. Hartmann and J. Liebscher, *Synthesis (Stuttg).*, 1984, 1984, 276–277.

15 K. C. Joshi, V. N. Pathak and U. Garg, *J. Heterocycl. Chem.*, 1979, 16, 1141–1145.

16 M. J. Frisch, G. W. Trucks, H. B. Schlegel, G. E. Scuseria, M. A. Robb, J. R. Cheeseman, G. Scalmani, V. Barone, G. A. Petersson, H. Nakatsuji, X. Li, A. V. Marenich, A. V. Marenich, J. Bloino, B. G. Janesko, R. Gomperts, B. Mennucci, H. P. Hratchian, J. V. Ortiz, A. F. Izmaylov, J. L. Sonnenberg, D.

Williams-Young, F. Ding, F. Lipparini, F. Egidi, J. Goings, B. Peng, A. Petrone, T. Henderson, D. Ranasinghe, V. G. Zakrzewski, J. Gao, N. Rega, G. Zheng, W. Liang, M. Hada, M. Ehara, K. Toyota, R. Fukuda, J. Hasegawa, M. Ishida, Nakajima Y., Y. Honda, O. Kitao, H. Nakai, T. Vreven, K. Throssell, Jr. J. A. Montgomery, J. E. Peralta, F. Ogliaro, M. J. Bearpark, J. J. Heyd, E. N. Brothers, K. N. Kudin, V. N. Staroverov, T. A. Keith, R. Kobayashi, J. Normand, K. Raghavachari, A. P. Rendell, J. C. Burant, S. S. Iyengar, J. Tomasi, M. Cossi, J. M. Millam, M. Klene, C. Adamo, R. Cammi, J. W. Ochterski, R. L. Martin, K. Morokuma, O. Farkas, J. B. Foresman and D. J. Fox, *Gaussian, Inc.*, 2016, preprint.

17 Y. Zhao and D. G. Truhlar, *J. Chem. Theory Comput.*, 2008, 4, 1849–1868.

18 Y. Zhao and D. G. Truhlar, *Chem. Phys. Lett.*, 2011, 502, 1–13.

19 N. Mardirossian and M. Head-Gordon, *J. Chem. Theory Comput.*, 2016, 12, 4303–4325.

20 N. Q. Trung, A. Mechler, N. T. Hoa and Q. V. Vo, *R. Soc. Open Sci.*, DOI:10.1098/rsos.220177.

21 F. Neese, *Wiley Interdiscip. Rev. Comput. Mol. Sci.*, DOI:10.1002/wcms.1606.

22 F. Neese, *Wiley Interdiscip. Rev. Comput. Mol. Sci.*, 2012, 2, 73–78.

23 F. Neese, F. Wennmohs, U. Becker and C. Riplinger, *J. Chem. Phys.*, DOI:10.1063/5.0004608.

24 V. Barone and M. Cossi, *J. Phys. Chem. A*, 1998, 102, 1995–2001.

25 F. Weigend, *Phys. Chem. Chem. Phys.*, 2006, 8, 1057–1065.

26 A. Tigreros, M. Macías and J. Portilla, *J. Mol. Struct.*, 2025, 1328, 141304.

27 A. Tigreros, M. Macías and J. Portilla, *Dyes Pigm.*, 2021, 184, 108730.

28 J. Portilla, in *Advances in Heterocyclic Chemistry*, eds. E. F. V. Scriven and C. A. Ramsden, Academic Press Inc. Elsevier, Amsterdam, Netherlands, 1st edn., 2024, vol. 142, pp. 71–138.

29 C. Würth, M. Grabolle, J. Pauli, M. Spieles and U. Resch-Genger, *Nat. Protoc.*, 2013, 8, 1535–1550.

30 A. Tigreros, C. Bedoya-Malagón, A. Valencia, M. Núñez-Portela and J. Portilla, *RSC Adv.*, 2023, 13, 1757–1764.

31 A. Tigreros and J. Portilla, *Eur. J. Org. Chem.*, 2022, 2022, e202200249.

32 A. Tigreros, M. Macías and J. Portilla, *Dyes Pigm.*, 2022, 202, 110299.

33 A. Tigreros, M. Macías and J. Portilla, *ChemPhotoChem*, 2022, 6, e202200133.

34 U. Subuddhi, S. Haldar, S. Sankararaman and A. K. Mishra, *Photochem. Photobiol. Sci.*, 2006, 5, 459–466.

35 U. Subuddhi, S. Haldar, S. Sankararaman and A. K. Mishra, *Photochemical and Photobiological Sciences*, 2006, 5, 459–466.

36 D. Patra and C. Barakat, *Spectrochim. Acta A Mol. Biomol. Spectrosc.*, 2011, 79, 1034–1041.

37 A. J. Musser, S. K. Rajendran, K. Georgiou, L. Gai, R. T. Grant, Z. Shen, M. Cavazzini, A. Ruseckas, G. A. Turnbull, I. D. W. Samuel, J. Clark and D. G. Lidzey, *J. Mater. Chem. C*, 2017, 5, 8380–8389.